DESIGN AND ANALYSIS OF FIXED LOAD CRUSHABLE COLUMN TYPE ENERGY ABSORBING MECHANISM FOR A HELICOPTER SEAT

A THESIS SUBMITTED TO
THE GRADUATE SCHOOL OF NATURAL AND APPLIED SCIENCES
OF
MIDDLE EAST TECHNICAL UNIVERSITY

BY

GÜLCE ÖZTÜRK

IN PARTIAL FULFILLMENT OF THE REQUIREMENTS
FOR
THE DEGREE OF MASTER OF SCIENCE
IN
AEROSPACE ENGINEERING

AUGUST 2018

DESIGN AND ANALYSIS OF FIXED LOAD CRUSHABLE COLUMN TYPE ENERGY ABSORBING MECHANISM FOR A HELICOPTER SEAT

submitted by **GÜLCE ÖZTÜRK** in partial fulfillment of the requirements for the degree of **Master of Science in Aerospace Engineering Department, Middle East Technical University** by,

Prof. Dr. Halil Kalıpçılar _____
Dean, Graduate School of **Natural and Applied Sciences**

Prof. Dr. Ozan Tekinalp _____
Head of Department, **Aerospace Engineering**

Prof. Dr. Altan Kayran _____
Supervisor, **Aerospace Engineering Dept., METU**

Examining Committee Members:

Assoc. Prof. Dr. Melin Şahin _____
Aerospace Engineering Dept., METU

Prof. Dr. Altan Kayran _____
Aerospace Engineering Dept., METU

Assoc. Prof. Dr. Ercan Gürses _____
Aerospace Engineering Dept., METU

Asst. Prof. Dr. Gökhan O. Özgen _____
Mechanical Engineering Dept., METU

Assoc. Prof. Dr. Barış Sabuncuoğlu _____
Mechanical Engineering Dept., Hacettepe University

Date: 29.08.2018

I hereby declare that all information in this document has been obtained and presented in accordance with academic rules and ethical conduct. I also declare that, as required by these rules and conduct, I have fully cited and referenced all material and results that are not original to this work.

Name, Last Name: GÜLCE ÖZTÜRK

Signature:

ABSTRACT

DESIGN AND ANALYSIS OF FIXED LOAD CRUSHABLE COLUMN TYPE ENERGY ABSORBING MECHANISM FOR A HELICOPTER SEAT

ÖZTÜRK, Gülce

M.S., Department of Aerospace Engineering

Supervisor: Prof. Dr. Altan Kayran

August 2018, 98 pages

Crashworthiness is the survivability of occupants inside a vehicle during a crash. In helicopters, crashworthiness is ensured by three subsystems; the landing gear, floor structure and the seats. Because of the critical role of the seats in helicopter crashworthiness evaluation, dynamic performance of the seat has to be studied in depth. There are different regulations in which requirements of survivable loads and crash conditions are defined. In this respect, a seat that is used in helicopter should be certified by complying applicable regulations and should satisfy the safety of the occupants during a crash. In order to comply with the regulations, a seat must absorb some portion of the crash energy and reduce the load that comes to the occupant. In this thesis, a crushable absorber system is designed to analyze the dynamic behavior and performance of the helicopter seat. The mechanism of the absorption system makes use of the crash energy to plastically deform the aluminum material of the seat legs. The designed helicopter seat is analyzed using the explicit finite element method to evaluate how the seat energy absorbing mechanism works. Dynamic simulations are performed in ABAQUS by crashing the seat to a fixed rigid wall. To simulate the plastic deformation, true stress-strain curve of the aluminum material of the seat leg has been used. Time response results are filtered to calculate the meaningful g loads which incur damage to the occupants. Analyses are done with and without the absorption mechanism in order to see the effectiveness of the mechanism on the human survivability by comparing the g loads on the seat bucket

with the acceptable loads given by European Aviation Safety Agency (EASA). Simulation results are compared and energy absorption mechanism has been showed to be effective for reducing the impact loads that comes to the occupant during crash.

Keywords: Crash, Energy absorption, Helicopter Seat, Explicit finite element analysis

ÖZ

HELİKOPTER KOLTUĞU İÇİN SABİT YÜKLÜ EZİLEBİLİR KOLON TİPİ ENERJİ SÖNÜMLEME MEKANİZMASININ TASARIMI VE ANALİZİ

ÖZTÜRK, Gülce
Yüksek Lisans, Havacılık ve Uzay Mühendisliği Bölümü
Tez Yöneticisi: Prof. Dr. Altan Kayran

Ağustos 2018, 98 sayfa

Çarpma dayanıklılığı çarpma anında araç içerisinde bulunan yolcuların hayatta kalabilmesidir. Helikopterlerde çarpma dayanıklılığı iniş takımı, zemin yapısalı ve koltuklar olmak üzere üç alt sistem ile sağlanır. Koltuğun çarpma dayanıklılığındaki bu rolü sebebiyle, koltuğun dinamik performansı derinlemesine çalışılmalıdır. Yaşanabilir yüklerin ve çarpışma koşullarının tanımlandığı farklı düzenlemeler ve gereksinimler vardır. Helikopterlerde kullanılacak koltukların, ilgili otoritenin tanımladığı bu gereksinimler bazında lisanslandırılması ve çarpma anında yolcu güvenliğini sağlaması gerekmektedir. Koltuğun çarpma dayanıklılığını sağlaması ve lisanslandırılması için çarpmadan gelen enerjinin büyük çoğunluğunu sönümleyerek yolcuya gelen yük miktarını azaltması gerekmektedir. Bu tezde, helikopter koltuğunun dinamik davranışını ve performansını analiz etmek için bir sönümleme mekanizması tasarlanmıştır. Sönümleme mekanizması, çarpışma enerjisini koltuk ayaklarının alüminyum malzemesini plastik olarak deforme etmek için kullanır. Tasarlanan helikopter koltuğu, sönümleme mekanizmasının nasıl çalıştığını değerlendirmek için açık sonlu elemanlar yöntemi kullanılarak analiz edilir.

Dinamik simülasyon ABAQUS programında koltuğu sabit ve katı bir duvara çarptırarak gerçekleştirilir. Plastik deformasyonu simüle etmek için, oturma ayağının alüminyum malzemesinin gerçek gerilme-gerinme eğrisi kullanılmıştır.

Yolculara zarar vermeyecek anlamlı g yüklerini hesaplamak için analiz sonuçları filtrelenmiştir.

EASA tarafından verilen kabul edilebilir yükler ile koltuk üzerindeki g yükleri karşılaştırarak, mekanizmanın insan üzerindeki etkinliğini görebilmek için analizler koltuk üzerinde enerji sönümleme mekanizması varken ve yokken tekrarlanmıştır. Simülasyon sonuçları karşılaştırılmış ve enerji sönümleme mekanizmasının çarpışma sırasında yolcuya gelen darbe yüklerini azaltmak için etkili olduğu görülmüştür.

Anahtar Kelimeler: Çarpma, Enerji sönümleme, Helikopter koltukları, Açık sonlu eleman analizi

To my family

ACKNOWLEDGMENTS

This thesis was conducted under the supervision of Prof. Dr. Altan Kayran. I would like to express my sincere appreciation for the support, encouragement, guidance and insight he has provided throughout the thesis.

This work was partially supported by Turkish Aerospace. For this reason, I would like to thank to my company the Turkish Aerospace.

Special thanks to my close friend Barkan Ulubalcı for his support, guidance and motivation throughout this work. I would not have been able to achieve without his help and patience.

I would like to thank my dear friends Kevser Yüceer, Başak Okumuş, Dilan Özdil and Eren Kozan, for being always there for me to support and for the encourage they provide throughout this study.

I also would like to express my thanks to my oldest friends Gözde Keleş and Cansu Emir for always being with me with all their love and support.

In addition, I would like to thank my friend, my brother from another mother and my confidant Alperen Demirdöğen for his efforts to increase my motivation on this thesis study.

Finally, I would like to thank my family, my father Sedat Öztürk, my mother Güler Öztürk and my dear brothers Osman Fuat and Özkan Mert Öztürk for always being there for me. They always support me, motivate me and encouraged me to complete this thesis study.

TABLE OF CONTENTS

ABSTRACT……vi
ÖZ……. vii
ACKNOWLEDGEMENTS…….....ix
TABLE OF CONTENTS……..…x
LIST OF TABLES……...……xi
LIST OF FIGURES……..…… xii
LIST OF ABBREVIATIONS…….……..xiii
LIST OF SYMBOLS…….……xiv

CHAPTERS

1 INTRODUCTION 1
1.1 Motivation of the Thesis Study 2
1.2 Crashworthiness 2
1.3 Objective of the Thesis 3
1.4 Scope of the Thesis 4
2 LITERATURE REVIEW AND THEORETICAL BACKGROUND 7
2.1 Literature Review 7
2.2 Energy Absorption System 17
2.2.1 Design Criteria and Crash Physics 17
2.2.2 System Concepts 22
2.3 Seat Regulations in Aviation 23
2.3.1 Civil Regulations 23
2.3.2 Military Regulations 26
3 METHODOLOGY 33
3.1 Helicopter Seat Design 33
3.2 Finite Element Modeling 39
3.3 Low-pass Digital Filtering 40
4 CRASH SIMULATION AND RESULTS 45
4.1 ABAQUS Model Creation 45
4.1.1 Mesh Definition and Refinement 50
4.1.2 Materials Used in Seat Assembly 55
4.1.3 Load and Boundary Conditions 57
4.1.4 Finite Element Analyses 60
4.2 Results 61
4.2.1 Acceleration Results 61
4.2.2 Energy Results 79
4.2.3 Stress Results 81
4.2.4 Effect of Occupant Weight on the Acceleration Results 85
4.2.5 Effect of Material on Acceleration Results 88
5 CONCLUSION 91
5.1 General Conclusions 91

5.2 Recommendations for Future Works 95
REFERENCES 96

TABLES

Table 1: Frequency Response Classes [22] 41
Table 2: Units of measure 45
Table 3: Mesh size parameters 52
Table 4: Material properties used in analysis model 57
Table 5: Standing body dimensions of Air Force Pilots [25] 86

FIGURES

Figure 1: Meshed seat geometry [10] 9
Figure 2: Comparison of test and simulation results [10] 10
Figure 3: MD-500 helicopter deployable energy absorber [12] 12
Figure 4: FE model for frontal analysis [15] 14
Figure 5: Deformed shape of frontal analysis [15] 15
Figure 6: Schemes of human body 17
Figure 7: H/C energy management system [16] 18
Figure 8: Displacement, velocity & acceleration relations during a crash event 20
Figure 9: Military helicopter cabin seats deceleration graph [17] 21
Figure 10: Civil helicopter cabin seats deceleration graph [7] 21
Figure 11: Two types of crushable column energy absorbers [8] 23
Figure 12: Seat/restraint system dynamic test 1 [7] 24
Figure 13: Seat/restraint system dynamic test 2 [7] 25
Figure 14: Seat/restraint system dynamic test 1 [17] 27
Figure 15: Seat/restraint system dynamic test 2 [17] 28
Figure 16: Floor warpage requirement [17] 29
Figure 17: Maximum acceptable vertical pulse acceleration and duration values [17] 30
Figure 18: Seat model-1 34
Figure 19: Seat model-2 34
Figure 20: Front view dimensions of the seat model-2 36
Figure 21: Isometric view dimensions of the seat model-2 37
Figure 22: Damping system of the seat model-2 38
Figure 23: Detail view of the damping system of the seat model-2 38
Figure 24: Butterworth data filtering sample [5] 40
Figure 25: Reference points created on the seat model 47
Figure 26: Joint locations in the seat design 48
Figure 27: Contact surfaces in the seat design 49
Figure 28: Detailed view of contact surfaces in the seat legs 49
Figure 29: Coarse and fine meshed seat model-2 geometry 51
Figure 30: Local meshing of upper damping part of the seat model-2 53
Figure 31: Local meshing of lower leg part of the seat model-2 53
Figure 32: Seat field output location 54
Figure 33: Filtered spatial acceleration time histories of different mesh sizes 54
Figure 34: True stress-strain diagram of AL 2024 [23] 56
Figure 35: Parts and materials of the seat model-2 57
Figure 36: Reference point of rigid wall 58
Figure 37: Initial velocity given to whole seat body 59
Figure 38: Reference point of concentrated mass 60
Figure 39: Seat field output location 62
Figure 40: Time histories of decelerations of fighter airplane [24] 62
Figure 41: Time history of deceleration of fighter airplane seat pan [24] 63
Figure 42: Finite element mesh at the beginning moment of the crash event (Time=0.00 second) 63
Figure 43: Distance between the damping part and the leg protrusion (Time=0.00 sec) 64
Figure 44: Distance between the damping part and the leg protrusion (Time=0.0009 sec) 64

Figure 45: Distance between the damping part and the leg protrusion (Time=0.0011 sec)..... 65
Figure 46: Detailed view of the plastic deformation..... 65
Figure 47: Rolling and flattening a tube 66
Figure 48: MIL-S-85510 test conditions [17] 67
Figure 49: Accelerometer and load cell positions on Hybrid III test dummy..... 68
Figure 50: Acceleration time history of test fixture 69
Figure 51: Acceleration time history of seat pan 69
Figure 52: Seat Field Output Location..... 70
Figure 53: Velocity time history of the seat model-1 71
Figure 54: Velocity time history of the seat model-2 71
Figure 55: Unfiltered spatial acceleration time history of the seat model-1 72
Figure 56: Filtered spatial acceleration time history of the seat model-1 72
Figure 57: Unfiltered spatial acceleration time history of the seat model-2 73
Figure 58: Filtered spatial acceleration time history of the seat model-2 73
Figure 59: Comparison of the spatial acceleration time histories of the seat model-1 and the seat model-2 75
Figure 60: Maximum acceptable vertical pulse acceleration and duration values [17] 77
Figure 61: Duration of filtered spatial acceleration exposure of the seat model-2 77
Figure 62: Kinetic energy time histories of the seat model-1 the seat model-2..... 80
Figure 63: Internal energy time histories of the seat model-1 and the seat model-2 . 80
Figure 64: Plastic dissipation time histories of the seat model-1 and the seat model-2 81
Figure 65: Initial state of the seat model-2 at time=0.00 sec, Unit: MPa 82
Figure 66: State of the seat model-2 at time=0.0007 sec, Unit: MPa 82
Figure 67: State of the seat model-2 at time=0.0008 sec, Unit: MPa 83
Figure 68: State of the seat model-2 at time=0.0009 sec, Unit: MPa 83
Figure 69: State of the seat model-2 at time=0.0012 sec, Unit: MPa 84
Figure 70: State of the seat model-2 at time=0.0015 sec, Unit: MPa 84
Figure 71: Final state of the seat model-at time=0.02 sec, Unit: MPa..... 85
Figure 72: Filtered spatial acceleration time history of the seat model-2 simulated with 77 kg occupant weight..... 87
Figure 73: Filtered spatial acceleration time history of the seat model-2 simulated with 107 kg occupant weight..... 87
Figure 74: Upper damping part of the seat model-2 88
Figure 75: Filtered spatial acceleration time history of the seat model-2 simulated with steel upper damping part 89
Figure 76: Filtered spatial acceleration time history of the seat model-2 simulated with aluminum upper damping part 89

LIST OF ABBREVIATIONS

AEA	Advanced Energy Absorber
ATD	Anthropomorphic Test Dummy
AvCIR	Aviation Crash Injury Research
CFR	Code of Federal Regulations
DEA	Deployable Energy Absorber
EASA	European Aviation Safety Agency
FAA	Federal Aviation Administration
FAR	Federal Aviation Regulation
FE	Finite element
FEA	Finite element analysis
FEM	Finite element method
FLEA	Fixed Load Energy Absorbers
FPEA	Fixed Profile Energy Absorbers
LandIR	Landing and Impact Research Facility
NASA	National Aeronautics and Space Administration
N/A	Not Applicable
RP	Reference Point
SAE	Society of Automotive Engineers
VLEA	Variable Load Energy Absorbers
VPEA	Variable Profile Energy Absorbers

LIST OF SYMBOLS

a	Acceleration
Econt	Contact Energy
Eint	Internal Energy
Ekin	Kinetic Energy
Et	Total Energy
G	Gravitational Constant
Gm	Maximum Deceleration
m	Mass
ΔS	Displacement
t_m	Time to G_m
Wext	External Work
V	Velocity

CHAPTER 1

INTRODUCTION

Air transportation takes the place of other transportations since it is time efficient. In 2012, the number of people traveling on airplanes reached 2,957 million, which was 4.7% more than the previous year, which is equivalent to 42% of the world's population [1]. In response to this growing demand, regulations did also grow in order to make sure that the air travel is safe for the passengers.

There are emergency landing dynamic conditions and requirements in which survivable loads and crash conditions are defined for rotorcraft in order to reduce the g loads that come to the occupants to the acceptable levels. The focus about the dynamic conditions is mainly on the energy absorbing mechanisms of the seats.

To verify the capability of the energy absorbing system, the dynamic behavior of the seat is generally predicted by simulation. Analysis of complex systems by numerical simulation is more efficient than the actual full-scale testing in the aspects of time and cost. Repetition of test is inevitable in case of failure, which means even more time and money lost. This is why "Certification by analysis" is very popular in the industry. LS-DYNA [2], DYTRAN [3], PAMCRASH [4] and ABAQUS [5] are very useful finite element codes in order to simulate the behavior of systems under dynamic conditions.

In this thesis study, finite element analyses of a rotorcraft seat are performed and simulation results are compared with the aviation regulation seat requirements. The aim is to see the effect of seat energy absorption mechanism design on crash loads. In addition, a comparison is also done between the finite element analysis results and actual test results in order to see that the analysis gives reliable results in terms of crash reaction and seat behaviors.

1.1 Motivation of the Thesis Study

Crashworthy seat design mainly depends on the verification of the energy absorption system solution. Full scale crash test is the expensive and time-consuming method for the confirmation of the system design. Finite element modeling, on the other hand, is repeatable and less expensive compared to the actual tests. The time effectiveness gives the advantage of analyzing complex systems and understanding the rationale of the crashworthiness.

Different types of absorption systems have been used in helicopter seat designs from early 1960's to today. By repetitively working on the crash simulation results, most effective crashworthy design can be adapted to the aircraft seat. At the end, best possible design solution can be designed for the crash protection of occupants.

1.2 Crashworthiness

Crashworthiness concept is generally defined as the vehicle's ability upon the protection of the occupant from an impact. In the rotorcraft industry, the crashworthiness has a clear definition such that the exact limits of the protection level are declared with the set of requirements. In this aspect, rotorcraft manufacturers aim to design structural parts and equipment, which have an important role on the energy absorption, to plastically deform and reduce crash energy by sustaining a sufficient survival space for occupants. Controlling the crash deceleration pulse to decrease up to the survivable limit of human tolerance is the most challenging design consideration.

The energy absorption concept is valid for whole aircraft starting from the fuselage and up to the occupant inside the cabin. The progression of the absorption is starts at the landing gears, followed by the floor structure and ending with the seats. In this order, it is seen that every system on the absorption row affects the other. If the fuselage is big and absorbs most of the crash energy, the remaining crash energy for the seat to reduce is lower comparing to the seat inside an aircraft that has a smaller fuselage. For example, for the airplanes, since the fuselage section is big and thick, the seat requirements written in the airplane regulations are lower than the helicopter seat regulations.

The crash requirements given in the applicable regulations are written for the insurance of the occupant safety. These requirements state the maximum g load and its time interval that an occupant should receive, which mainly defines the design criteria of the seats. The base of these requirements is the human body resistance. The survivability of the human depends on the loads that come to the lumbar and pelvis area from the crash. So, the starting point of a crashworthy design is the human tolerance.

To develop an effective, crashworthy seat, designers should know how to protect the occupant inside the aircraft. To know how to protect, they should also know the resistance of the human body. In this aspect, head/neck/lumbar acceleration tests have been conducted with military volunteers in the 1970s. To derive the injury criteria, researchers documented the biomedical data from cadaver tests. The Society of Automotive Engineers (SAE) has published specific documents about the biomedical injury data [6].
Human body injury criterion guides the regulations, which are given in Chapter 2.3, in the aspect of designating the test criteria. For a crashworthy seat design, defined conditions should be satisfied.

1.3 Objective of the Thesis

In this thesis study the main objective is to design a crushable absorber system which dissipates energy based on the plastic deformation of the components of the helicopter seat. Following the seat design with the absorption system, the helicopter seat is analyzed to study the dynamic behavior and performance of the helicopter seat with the absorption system. The seating system is composed of the main seat structure (seat bucket), seat legs and the damping mechanism. The mechanism of the absorption system makes use of the crash energy to plastically deform the aluminum material of the seat legs. The conditions defined by civil helicopter regulation, CS 29 [7], are implemented using the explicit finite element (FE) software ABAQUS in order to simulate how the seat energy absorbing mechanism works. Detailed FE

model for the seating system with the structural loading is set up in ABAQUS. Explicit finite element analyses are done with and without the absorption mechanism in order to see the effectiveness of the mechanism on the human survivability by comparing the g loads on the seat bucket with the acceptable loads of the human body tolerances. It should be noted that present study only covers the seat part of the three-level absorption system which is composed of the landing gear, the floor and the seat.

1.4 Scope of the Thesis

In this thesis study, there are 5 main chapters as following:

1) Introduction
2) Literature Review and Theoretical Background
3) Methodology
4) Crash Simulation and Results
5) Conclusion

- In the first chapter, introduction part, purpose and the advantages of the finite element analyses and crash simulations are mentioned. Furthermore, crashworthiness and energy absorption concept are defined.
- In the second chapter, literature review is presented. Similar studies about energy absorption mechanisms and their analyses are shown. In addition to literature review, theoretical background of crashworthiness analyses is expressed in this chapter with the crash energy absorption system design criteria and their mechanism concepts. Lastly the regulations, giving the helicopter seat design requirements, are summarized.
- In the third chapter, seat design details are given including the energy absorption system solution, which is uniquely designed for this thesis study. Moreover, finite element modeling is mentioned with a general overview.
- In Chapter 4, a finite element model of the designed seat is created. Material properties, loads and boundary conditions are defined. Afterwards, finite element analyses are carried and results are given.

- In Chapter 5, the thesis is summarized and the results are discussed. In addition, the future work that can be carried on based on the work applied in this thesis is given as recommendations.

CHAPTER 2

LITERATURE REVIEW AND THEORETICAL BACKGROUND

2.1 Literature Review

The main objective of crashworthiness is reliable design solutions that will reduce the crash load up to survivable levels for human body. There are different design solutions implemented on rotorcraft seats as energy absorber mechanisms. Desjardins [8] elaborated on the details of energy absorber concepts in his paper. He states that energy absorber systems are divided into different design concepts in the aspects of different human weight tolerances and stroke distances as follows:

- Fixed Load Energy Absorbers (FLEA)
- Variable Load Energy Absorbers (VLEA)
- Fixed Profile Energy Absorbers (FPEA)
- Variable Profile Energy Absorbers (VPEA)
- Advanced Energy Absorber (AEA)

FLEA mechanisms are designed for a specific occupant weight by targeting an average population. 50th percentile occupant represents the average population and seats are approved according to the 50th percentile occupant weight. In this concept, occupants lighter than the average weight receive a higher impact load and heavier occupants, on the other hand, receive a lower deceleration. As a result, the lighter occupants experience higher crash loads. VLEA mechanisms are developed to adjust the limit load according to the occupant weight. VLEA concepts allow to modify the

system manually according to the human weight before boarding. This is an important feature from the initiation of the system and the crash load magnitude points of view. If the occupant is lightweight, it is hard to initiate the system since the occupant cannot provide the necessary load at the start of the crash event. VLEA allows to protect for different weight occupants. FPEA mechanism protection concept is independent of the occupant weight. FPEA mechanisms are not designed according to the variable load concept. Instead of the variable load, FPEA uses a load-displacement profile which varies with stroke. VPEA mechanisms are the combination of VLEA and FPEA concepts. VPEA mechanisms also use the load-displacement profile that changes with the stroke, but limit loads of the system can be adjusted manually according to the occupant weight. AEA concept also includes the occupant weight adjustment but it differs from others in a way that the weight adjustment is not manually done but it automatically sets the appropriate limit load for the occupant's weight.

In the present study, fixed load energy absorber (FLEA) is used. The methods to demonstrate the effectiveness and success degree of the energy absorption concept are test and analysis. Numerical simulation is more efficient than the actual test because repetition of the test is inevitable in case of a failure, which means even more time and money loss.

Bhonge [9] argued in his study that dynamic testing for the seat certification is expensive and methods such as finite element analysis reduce the cost and give chance to change the design parameters repetitively and understand the effect of each parameter on the design. In Bhonge's study a dynamic finite element analysis (DFEA) model of the passenger seat is developed and challenges in the simulation are revealed. Direct impact effects on the seat structure are evaluated from different points of view such as comfort, crashworthiness and manufacturing. Moreover, validation of the FE model is also made by comparing the DFEA results with the actual test results, and it is concluded that computer models are useful and less expensive tools for crash analysis.

Simitcioglu and Dogan [10] also stated that using computer aided dynamic finite element techniques instead of actual tests provides cost and time saving. They supported their argument with an analysis by comparing the analysis results and the actual test results. To make a comparison they first created an analysis model in LS-DYNA. To use in the analysis model, they generated a seat model as shown in Figure 1 which is similar to the actual one used in the tests. The FE occupant model FTSS 50 percentile Hybrid II ATD is chosen to represent the human body in the analyses. Figure 2 shows the comparison of the test and simulation results taken from the study of Simitcioglu and Dogan. Their paper concludes that simulation and test results are very similar, and LS-DYNA is a reliable simulation code in order to see the dynamic behavior of the seat in a crash event. At the end of the paper, they state that FEM may be used reliably instead of actual tests as a repeatable and less expensive alternative.

Figure 1: Meshed seat geometry [10]

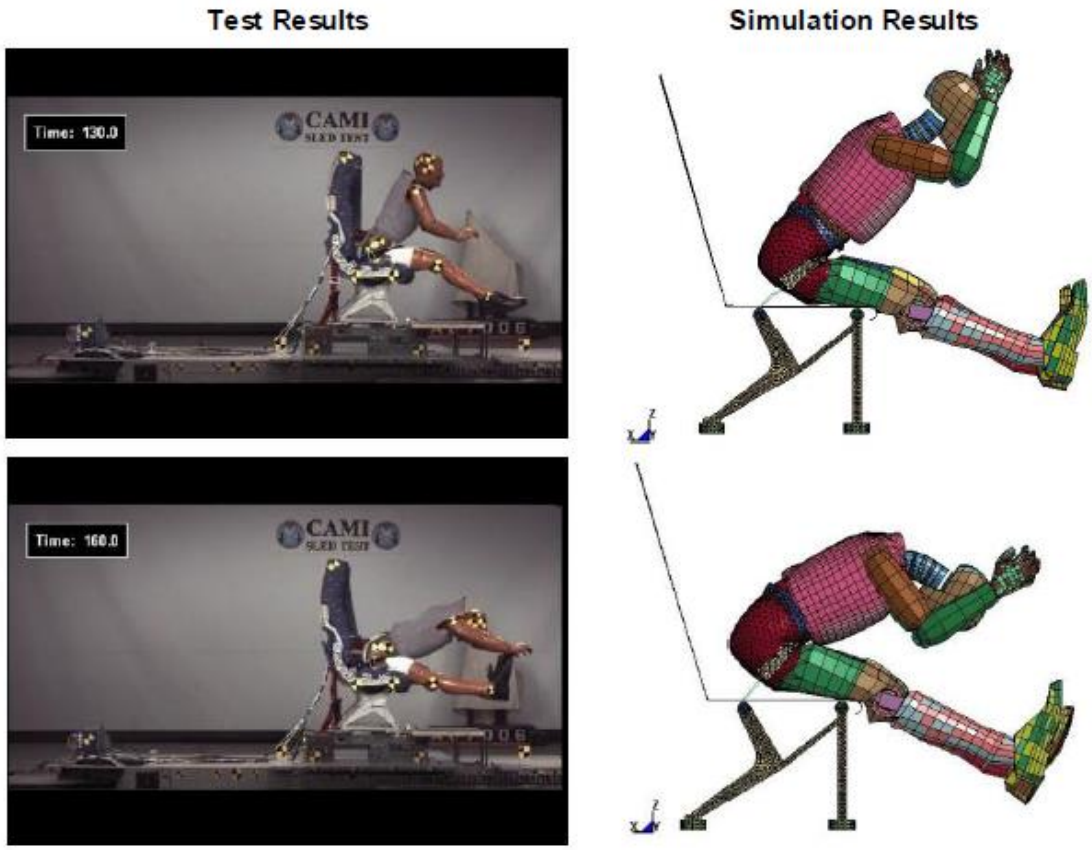

Figure 2: Comparison of test and simulation results [10]

Another validation study of finite element analysis of an aircraft seat is done by Dhole [11]. In his thesis, Dhole stated that to reduce the cost of a crashworthy seat production, one should predict the dynamic behavior of seating system using computer modeling techniques. He claimed in his study that to understand crashworthiness area computer simulations are widely used. In his thesis, simulation results of a finite element model of an aircraft passenger seat which is generated with LS-DYNA explicit finite element code is compared with actual dynamic tests that are conducted at the sled facility of Civil Aero Medical Institute. Dhole used data channels for head acceleration, chest acceleration, pelvis acceleration, lumbar force and moment, belt forces and floor reaction forces. Comparisons of the forces and the accelerations show that the simulation dummy followed the same kinematics with the test dummy. At the end of Dhole's study, he concluded that since the results with test

data showed a good correlation and established a confidence in finite element methodology, computer simulations can be helpful in product development process.

Today, rotorcrafts are used not only in military applications, but also in other applications like search and rescue or cargo transfer. In order to make these applications safely, the pre-cautions should be taken. The most important pre-caution for a rotorcraft is to make it crashworthy in order to protect occupant inside in case of a crash.

Governments are supporting researches associated with improvements in rotorcraft crashworthiness. Day by day, new innovative design solutions are implemented on this specific subject. However, although design stage is very important, the other important issue is to validate the design. Validation process is generally means testing the absorber system and see if it works with compatible to its intended design purpose. However, full-crash testing is not always a good idea because of its cost and waste. It only makes sense to proceed a full-scale test with a reliable design solution and to name a design "reliable" there should be a background knowledge about the system working mechanism. At this stage, finite element analysis steps in. This is why computer aided system validation is very popular in the industry.

Annett [12] is also one of the researchers aiming to prove a computer aided simulation that is created for an energy absorber validation. The object of his study is the validation of a system integrated LS-DYNA® finite element model. In this aspect, a full-scale crash test, which was conducted in December 2009 at NASA Langley's Landing and Impact Research facility (LandIR), results of an MD-500 helicopter is used and generated test data is used for validation of a system integrated LS-DYNA® finite element model.

The object of the validation is the energy absorber of the MD-500 helicopter. The absorber is a composite honeycomb Deployable Energy Absorber (DEA) that is fitted to helicopter fuselage as seen in Figure 3.

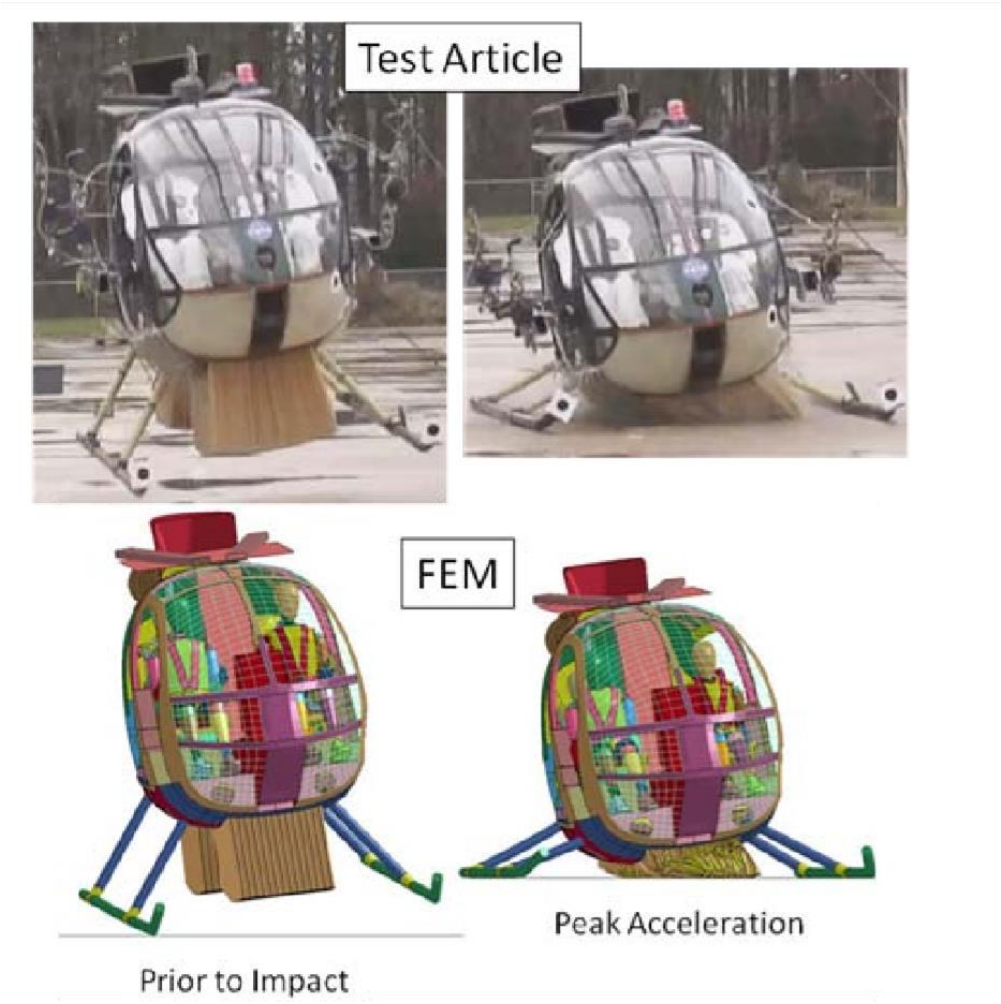

Figure 3: MD-500 helicopter deployable energy absorber [12]

The objectives of the test were to evaluate the performance of the DEA concept under realistic crash conditions and to generate test data for validation of a system integrated LS-DYNA® finite element model. After the test, parameters are defined within the system integrated finite element model were determined. After preparing the LS-DYNA analysis model, simulation is performed and test results and simulation results are compared. The test impact orientation and deformation at peak load for test and analysis is as shown in Figure 3. At the end of this comparison, Annett [12] states in his study that the global deformation pattern of the energy absorber is similar to the deformation observed in the high-speed video of actual test. Primarily folding on the right side and crushing on the left side behaviors are same in

test and analysis. At the end, he concluded that good agreement for strains and CG accelerations was seen between test and analysis.

The crash analysis is very popular in not only the aviation industry but also in the automobile industry. Nowadays, product development in the car industry heavily relies on numerical simulations as stated in the study of Peherstorfer and his friends [13]. It is stated in the study that analysis is used to explore the influence of design parameters on the weight, costs or functional properties of new car models and engineers spend a considerable amount of time on analyzing these influences by examining the simulations. In their study, Peherstorfer and his friends propose using machine learning methods to semi-automatically analyze the arising finite element data and they combine clustering and nonlinear dimensionality reduction to show that the method is able to automatically detect parameter dependent structure instabilities in the time-dependent behavior of beams. Peherstorfer and his friends concludes that using the nonlinear procedures, the number of relevant parameters to be investigated can be reduced.

Pawlus and his friends [14] also argue in their study that vehicle crash tests are complex and complicated experiments it is advisable to establish their mathematical models. Study contains an overview of the kinematic and dynamic relationships of a vehicle in a collision. The purpose of the study is to simulate how the crash looks like and to show what are the main parameters describing the collision without performing any real test. Pawlus and his friends perform a crash analysis of a standard Ford Fiesta 1.1L 1987 model, for which they have an experiment results report to compare with their analysis results. It is shown in the study that how the velocity changes and what are the changes in acceleration of a car during a crash. In addition, the maximum occupant deceleration is estimated, which is one of the main tasks in the area of crashworthiness study. At the end, it is concluded by Pawlus and his friends that the approximation of the data is not quite exact but accuracy of the approximation is very good and close to the experiment results. So, it can be said that the real-world experiments are difficult to conduct since there are needed appropriate facilities, measuring devices, data acquisition process, qualified staff and a car. Therefore, preparing a mathematical model of a collision and analyze it instead of a real experiment is more preferable.

Another example of using finite element analysis model for crash analysis popularity in the field is the study of Kim, Park and Song [15]. They perform a crash analysis of upper body and sub-frame of an electric car, and establish the basic crash describe equation and FE discretized equation according to the basic principle of the dynamic non-linear finite element method.

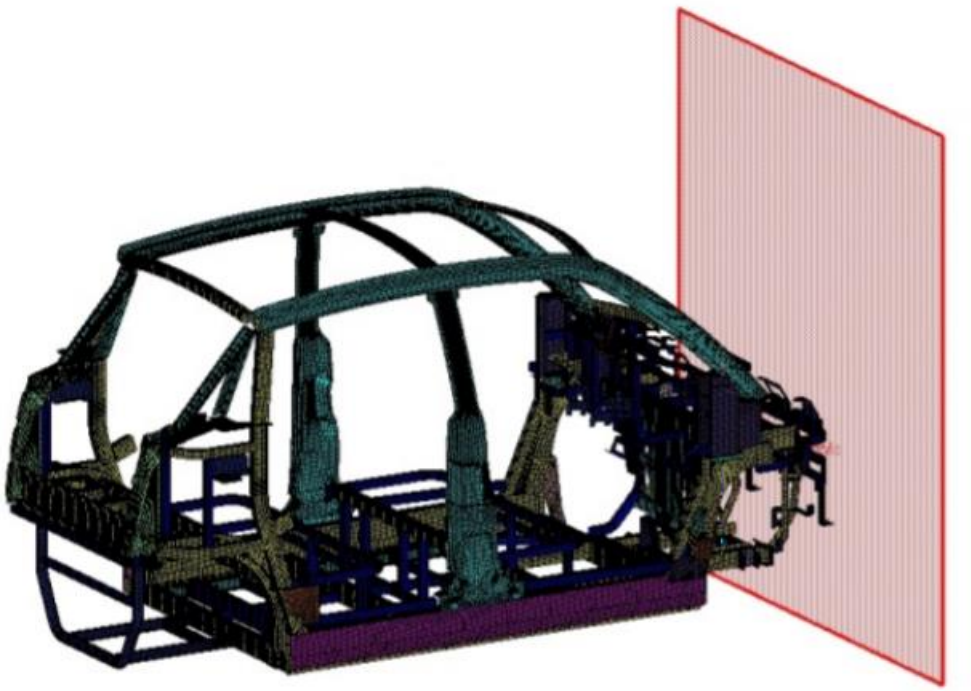

Figure 4: FE model for frontal analysis [15]

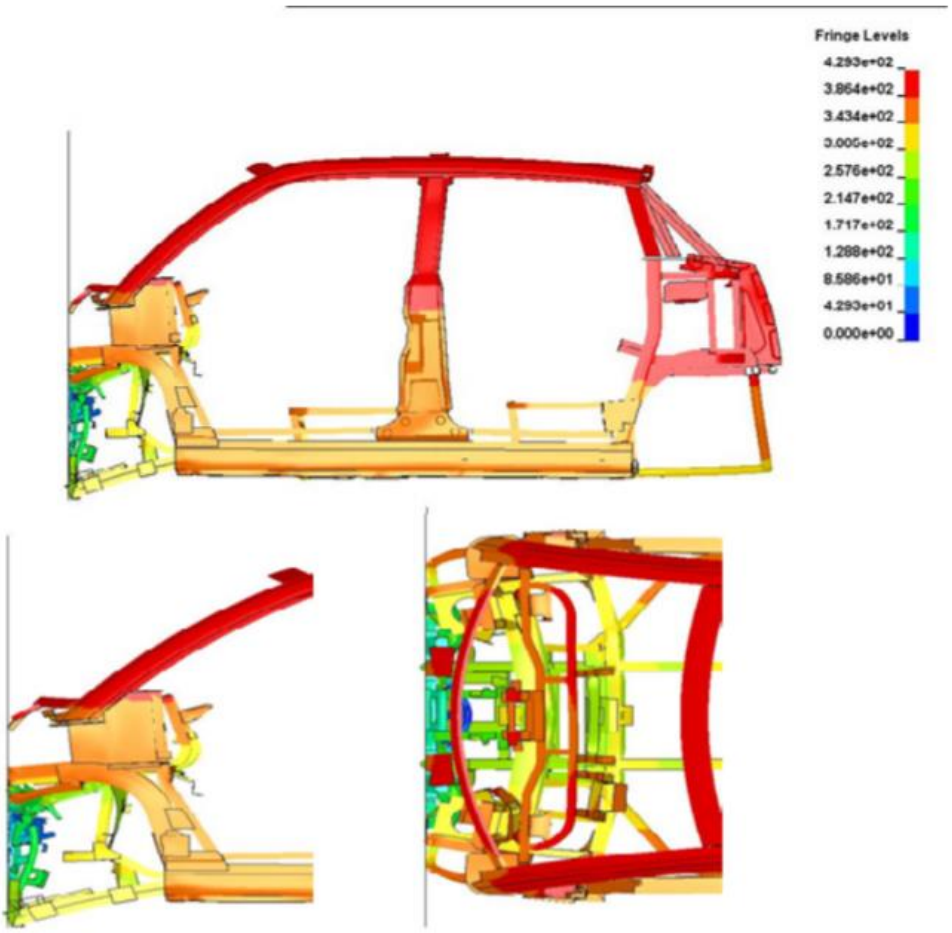

Figure 5: Deformed shape of frontal analysis [15]

Figure 4 and Figure 5 taken from Kim, Park and Song study [15], show finite element model and deformed shape of the electric car subjected to analysis respectively. LS-DYNA software is used as finite element processor and crash analysis through the electrical vehicle for the upper body, and sub-frame of the mechanical characteristics compared to the simulation by electrical vehicle for the upper body and the sub-frame of the collision trends and deflection for the basic data presented. It is stated in the study that, the advantage of the explicit FE method is that due to the nature of the computational approach, extremely small time steps coupled with an iterative solving method.

In this study, a helicopter seat is designed with an energy absorbing mechanism to reduce the load that the occupant receives in the event of a crash. The designed helicopter seat is analyzed using the explicit finite element method to evaluate how the seat energy absorbing mechanism works. Crushable column method is used in the seat damping system design and the crash conditions are defined by the civil helicopter regulation, CS 29 [7]. Detailed FE model for the seating system with the structural loading is set up in ABAQUS [5]. Test conditions are implemented using the explicit finite element (FE) code in ABAQUS in order to simulate how the seat energy absorbing mechanism works. The seating system is composed of the main seat structure (seat bucket), seat legs and the damping mechanism. Analyses are performed with and without the absorption mechanism in order to see the effectiveness of the mechanism on the human survivability by comparing the g loads on the seat bucket with the acceptable loads of the human body tolerance.

2.2 Energy Absorption System

2.2.1 Design Criteria and Crash Physics

Energy absorption system concept came up during the 1960's by the result of the crash injury researches of Aviation Crash Injury Research (AvCIR) foundation, which is a nonprofit organization established to investigate the cause of crash injuries [6]. Foundation concluded that, occupants could survive from a crash only if the loads coming from the vertical direction is limited. By defining a load control in the vertical direction, spinal injury risk is minimized and only human tolerable loads are transferred to the occupant located on the seat.

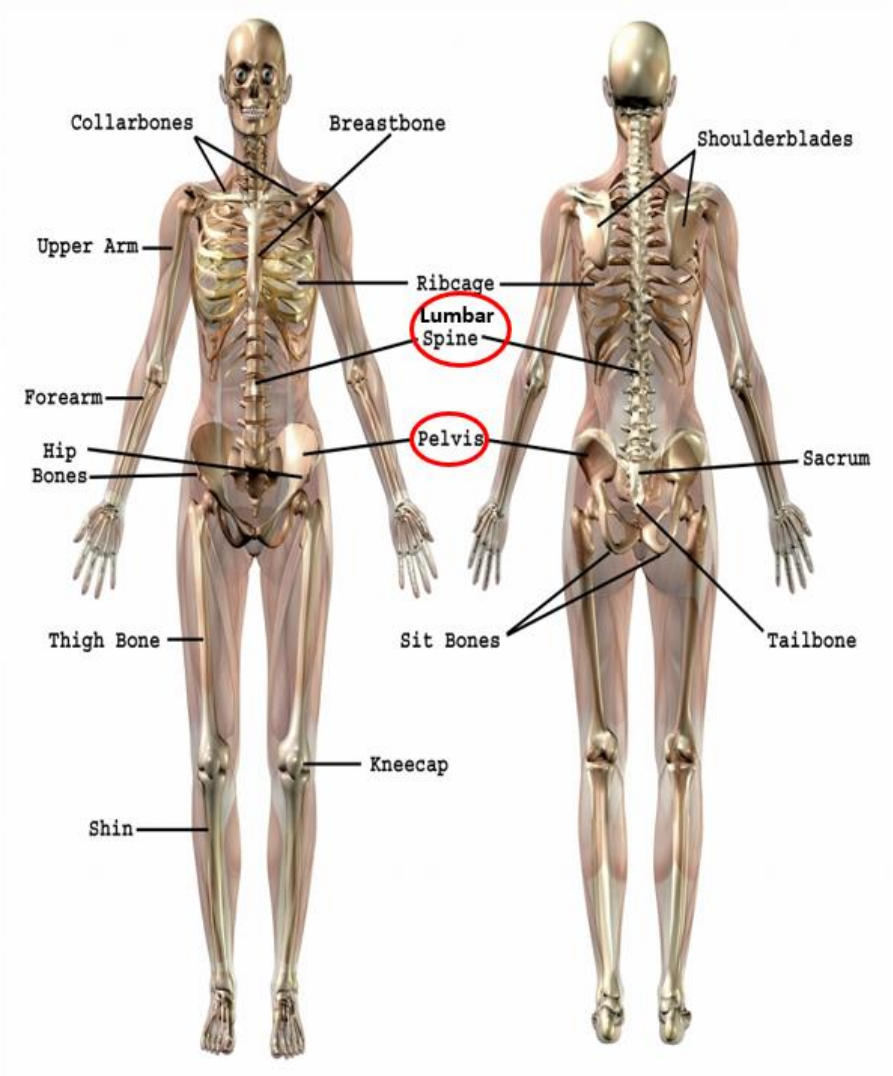

Figure 6: Schemes of human body

Crashworthiness means the vehicle's ability upon the protection of the occupant from an impact by means of load-limiting devices. Load-limiting energy absorber systems control the crash deceleration pulse to decrease up to the survivable limit of human tolerance.

The energy absorption concept is valid for whole rotorcraft starting from the fuselage and up to the occupant inside the cabin. The progression of the absorption is starts at the landing gears, followed by the floor structure and ending with the seats as shown in Figure 7.

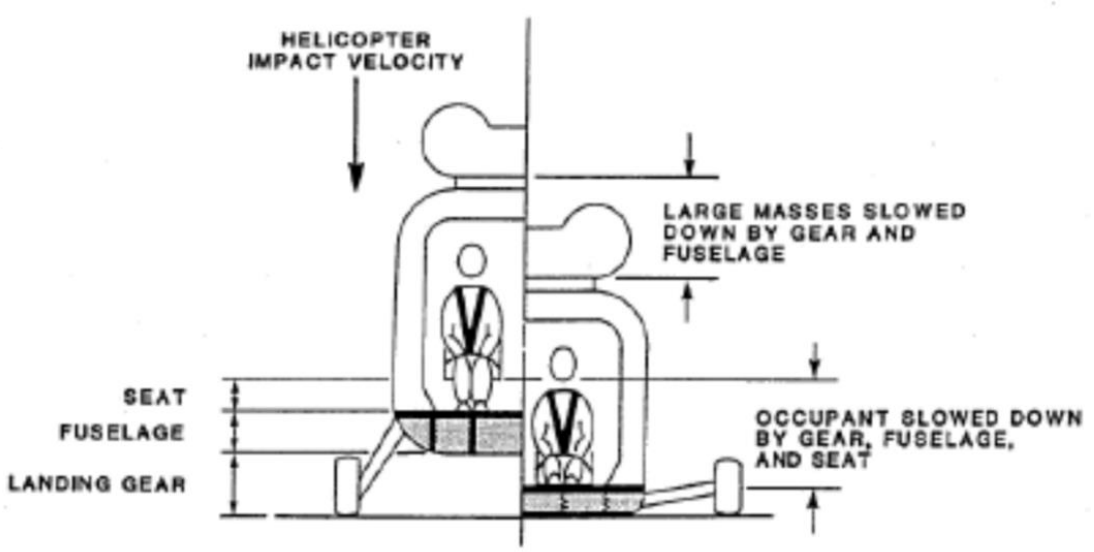

Figure 7: H/C energy management system [16]

The survivability of human from a crash depends on the loads that come to the lumbar and pelvis area, shown in Figure 6, from the seat bucket. As shown in Figure 7, crash energy is damped with landing gear and the rotorcraft fuselage before the seat. In order to control the crash loads coming to the seat, the energy absorption concepts are defined within the seat design. The concepts are worked with the energy conservation concept.

Conservation of energy principle states that the energy of interacting bodies remains constant. As objects move around over time, the energy associated with them may change forms, around kinetic, gravitational, potential and heat, but the total energy remains same.

$$E_t(t) = \sum E(t) = constant \quad (1)$$

where $E_t(t)$ is the total energy stored in the system.

During a crash event, while the elastic share is released and transforms to kinetic energy, plastic part is the measurement of the energy absorption ability of the energy absorbing mechanism.

At all times, the sum of potential and kinetic energy is constant. Friction slows down the mechanisms and dissipates the energy gradually. For these mechanisms, as energy cannot be generated or destroyed, all types of energy must meet the energy conservation principle.

$$E_t(t) = E_{int}(t) + E_{kin}(t) - W_{ext}(t) + E_{cont}(t) \quad (2)$$

where $E_t(t)$ is the total energy stored in the system, $E_{int}(t)$ is the internal energy, $E_{kin}(t)$ is the kinetic energy, $W_{ext}(t)$ is the external work and $E_{cont}(t)$ is the contact energy.

Contact energy is also defined as the friction energy. Change in the kinetic energy defines work which is done during the crash.

$$\Delta E_{kin} = \frac{1}{2} m V_2^2 - \frac{1}{2} m V_1^2 \quad (3)$$

Acceleration or deceleration during crash events usually define complex functions. In order to represent these functions some simple general pulses such as rectangular, triangular pulses and their different forms are used in the field. In this study, symmetrical triangular pulse is used since this type of pulse is generally used for simulating the crash of structure.

For triangular symmetric pulse, acceleration, velocity and displacement relations during a typical crash event is given in Figure 8.

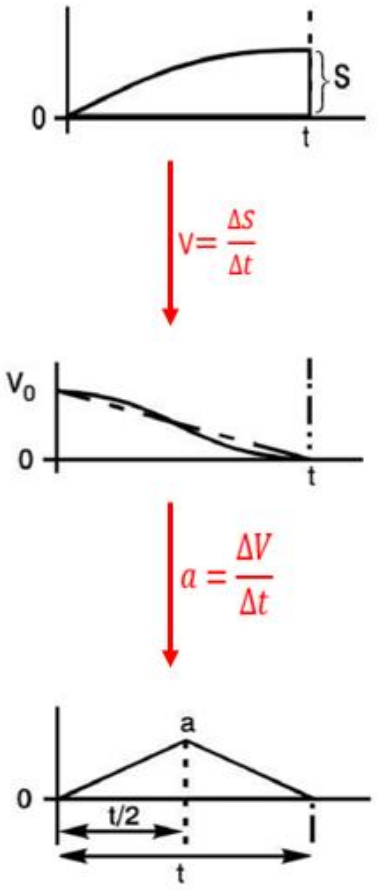

Figure 8: Displacement, velocity & acceleration relations during a crash event

For the prediction of the occupant safety, there is a triangle in the applicable regulation, depending on the helicopter application category as civil or military, that shows the g load and its time interval, which mainly defines the test conditions. While for civil applications CS 29 [7] is taken as reference, for military applications, MIL-S-85510 [17] standard is taken as reference for this thesis study. Details of these regulation are given in Section 2.3.

The triangles defining the test conditions give the idealized crash pulse drawn in the vertical axis as shown in Figure 9 and Figure 10.

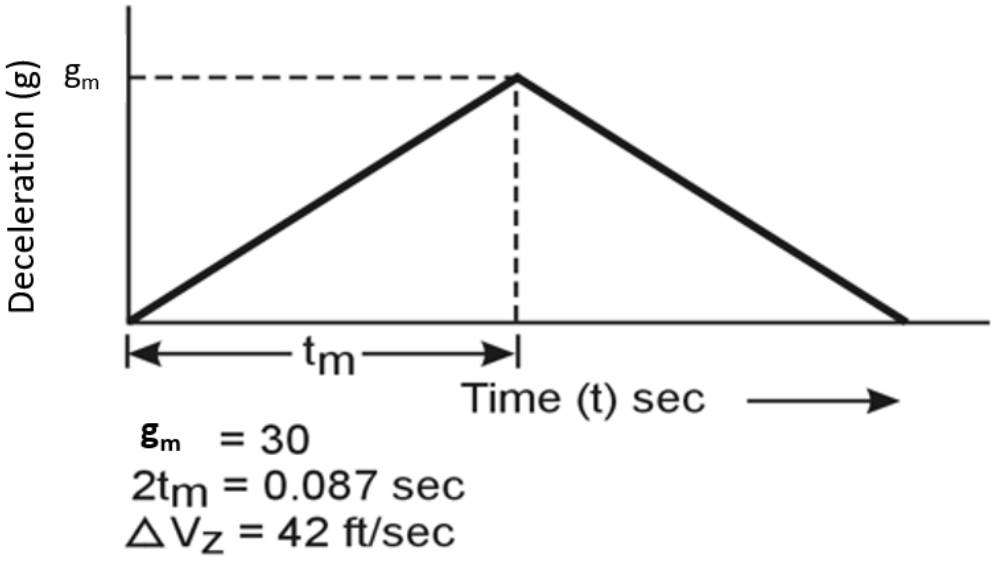

Figure 9: Military helicopter cabin seats deceleration graph [17]

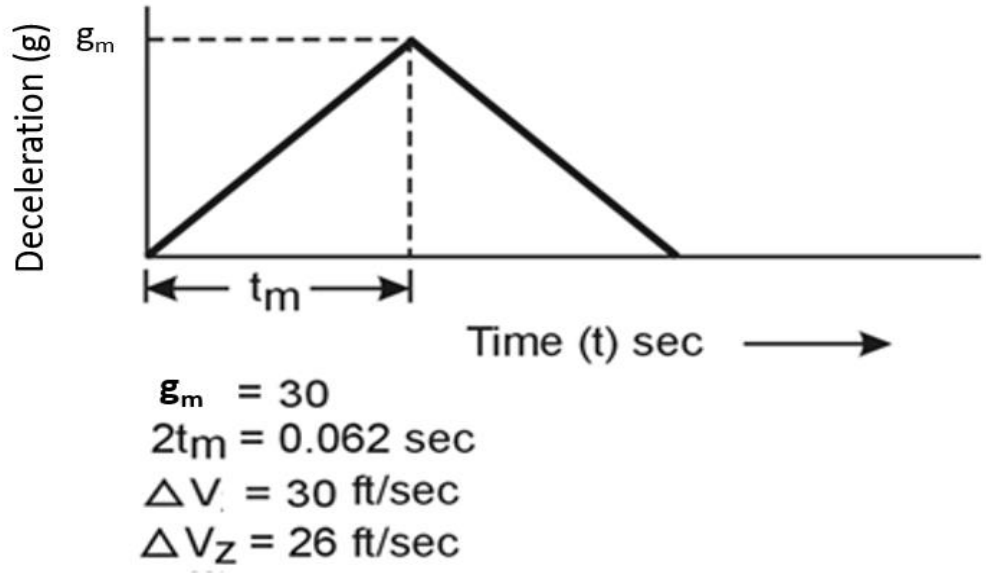

Figure 10: Civil helicopter cabin seats deceleration graph [7]

Parameters given in Figure 9and Figure 10 are defined as:

g = Gravitational constant (9.81 m/ sec^2)

g_m=Maximum deceleration, g

t_m=time to g_m, sec.

In the civil helicopter cabin seat deceleration graph, triangle says that peak floor deceleration must occur in not more than 0.031 seconds after the impact and deceleration must reach a minimum of 30 g.

2.2.2 System Concepts

Energy absorbing system logic is to plastically deform and reduce the crash energy by sustaining a sufficient survival space for occupants. There are a lots of absorption mechanism used in the field. Some of them are listed below:

- Crushable Column
- Rolling Torus
- Inversion Tube
- Cutting or Slitting
- Tube and Die
- Rolling/Flattening a Tube
- Strap, Rod, or Wire Bender
- Wire-Through-Platen
- Deformable Links

These concepts are also divided into different design concepts in the aspects of different human weight tolerances and stroke distances.

Figure 11 shows two different type of crushable column example and their effect on load behavior. The load-deflection characteristics were produced by crushing the column. The one that is used in this study is very similar to the “Crushable Column” Method. The Fixed Load Energy Absorber (FLEA) mechanism is used in this design. FLEA mechanism is used for a specific occupant weight by targeting an average population. 50th percentile occupant represents the average population and seats are approved according to these 50th percentile occupant weights. By this concept, occupants lighter than average weight receive a higher impact load and heavier occupants, on the other hand, receive a lower deceleration. As a result, the lighter occupants experience higher crash loads.

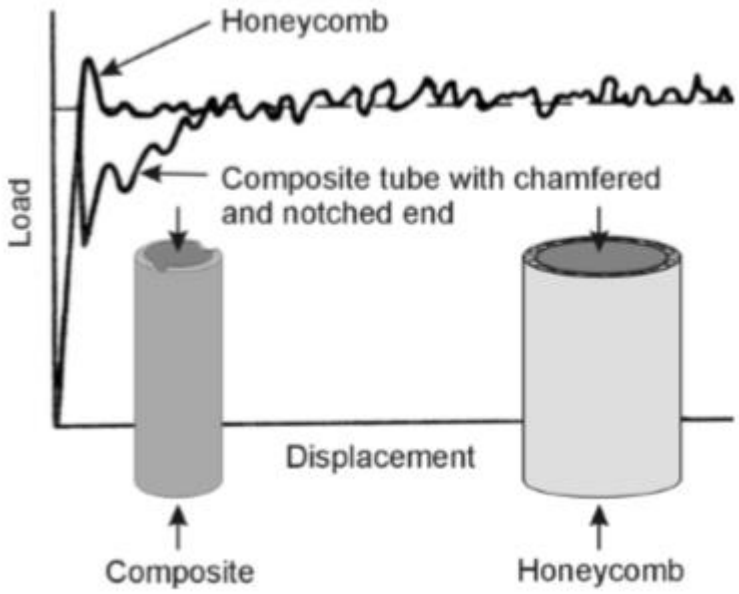

Figure 11: Two types of crushable column energy absorbers [8]

2.3 Seat Regulations in Aviation

From the day of "government" and "society" figures come into existence, all activities depend on some rules and regulations that a government specify in order to protect the population safety and rights. If a person wants to drive a car, a license should be provided from the authority stating that the person has the ability and qualified training to drive the car. In the same manner, if an aircraft will flight, it must be certified by the authority and get the certification of the related category. Certification rules are defined aiming the safe flights for not only the occupant inside the aircraft but also the people on the ground. Certification rules are written in the regulations defined by the authority.

2.3.1 Civil Regulations

The Federal Aviation Regulations, or FARs, are rules described for the aviation activities by the Federal Aviation Administration (FAA) in the United States. European Aviation Safety Agency (EASA) also follow same rules for the aviation safety.

Regulations are divided into chapters according to the aircraft category. Rotorcraft chapters are given below:

- CFR 14 → Chapter I → Subchapter C → Part 27—AIRWORTHINESS STANDARDS: NORMAL CATEGORY ROTORCRAFT [7]
- CFR 14 → Chapter I → Subchapter C → Part 29—AIRWORTHINESS STANDARDS: TRANSPORT CATEGORY ROTORCRAFT [7]

2.3.1.1 Dynamic Test Conditions

A minimum of two dynamic tests are required to assess the performance of a rotorcraft seat, restraints, and the related interior system. CS 29.562 defines test conditions as [7]:

1. The rotorcraft's longitudinal axis is canted upward 60°, with respect to the impact velocity vector, and the rotorcraft's lateral axis is perpendicular to a vertical plane containing the impact velocity vector and the rotorcraft's longitudinal axis, as seen in Figure 12.
    - Peak floor deceleration must occur in not more than 0.031 seconds after impact and must reach a minimum of 30 g.

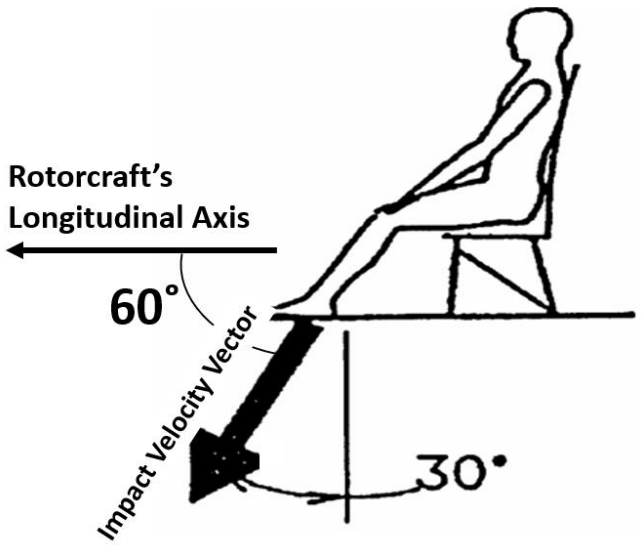

Figure 12: Seat/restraint system dynamic test 1 [7]

2. The rotorcraft's longitudinal axis is yawed 10°, either right or left of the impact velocity vector (whichever would cause the greatest load on the shoulder harness), the rotorcraft's lateral axis is contained in a horizontal plane containing the impact velocity vector, and the rotorcraft's vertical axis is perpendicular to a horizontal plane containing the impact velocity vector as seen in Figure 13.

    - Peak floor deceleration must occur in not more than 0.071 seconds after impact and must reach a minimum of 18.4 g.

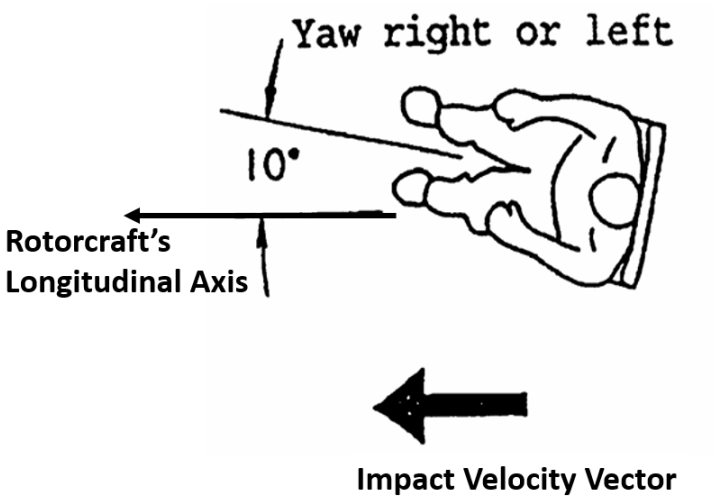

Figure 13: Seat/restraint system dynamic test 2 [7]

Tests also require that the floor is deformed by at least 10° in pitch and 10° in roll in order to simulate the actual crash case.

2.3.1.2 Occupant Injury Criteria

The most important aim of the regulation is to ensure the safety of the occupant inside a helicopter. The survivability of human from a crash depends on the loads that come to the lumbar and pelvis area as stated before in Section 2.2.1 Design Criteria. For this reason, regulation defines the limitations for the loads come to the occupant at different locations CS 29.562 [7]. These requirements, given below, have

to be satisfied at the end of the dynamic tests in order to state that the dynamic test was performed successfully.

1. If the test dummy's head contacts with any structure inside the helicopter, impact should not exceed the Head Injury Criteria of 1000. HIC is calculated by:

$$\boldsymbol{HIC = (t_2 - t_1)\left[\frac{1}{(t_2-t_1)}\int_{t_1}^{t_2} a(t)dt\right]^{2.5}} \quad (4)$$

   where

   - a(t) is the resultant acceleration at the center of gravity of the head and expressed as a multiple of g
   - t_2-t_1 is the time duration of major head impact and expressed in seconds. Time duration should not exceed 0.05 seconds.

2. Tension loads in the individual shoulder harness straps should not exceed 7784 N. If dual straps are used, the total harness strap loads should not exceed 8896 N.
3. Compressive load measured between the pelvis and the lumbar column of the test dummy should not exceed 6674 N.
4. The safety belt and shoulder harness straps must remain on the test dummy's pelvis and shoulder during the impact.

2.3.2 Military Regulations

There are different military regulations in the field that are used as design guides by manufacturers. Design guides are different in the aspect of usage for military applications. For crew seats, for example, the crash requirements are higher. For troop seats on the other hand, the crash requirements are lower than the crew seat requirements.

Some of these regulations are given below:

- MIL-S-85510 [17]
- NATO-STANAG-3950 [18]

These specifications established the design requirements for crashworthy seats in military helicopters. STANAG 3950 defines the rules for crew seats located in the cockpit. MIL-S-85510 standard defines requirement of seats that are used by troops/passengers sitting in the cabin compartment of the helicopter.
This study is focused on the passenger compartment area. For that reason, MIL-S-85510 is used for the comparison.

2.3.2.1 Dynamic Test Conditions

A minimum of two dynamic tests are required to assess the performance of a rotorcraft. The seat should not loss the structural integrity during and after the impact.
MIL-S-85510 defines test conditions as follows [17]:

1. The rotorcraft's longitudinal axis is canted upward 60°, with respect to the impact velocity vector, and the rotorcraft's lateral axis is perpendicular to a vertical plane containing the impact velocity vector and the rotorcraft's longitudinal axis, as seen in Figure 14.

    - Peak floor deceleration must occur in not more than 0.087 seconds after impact and must reach a minimum of 37 g.

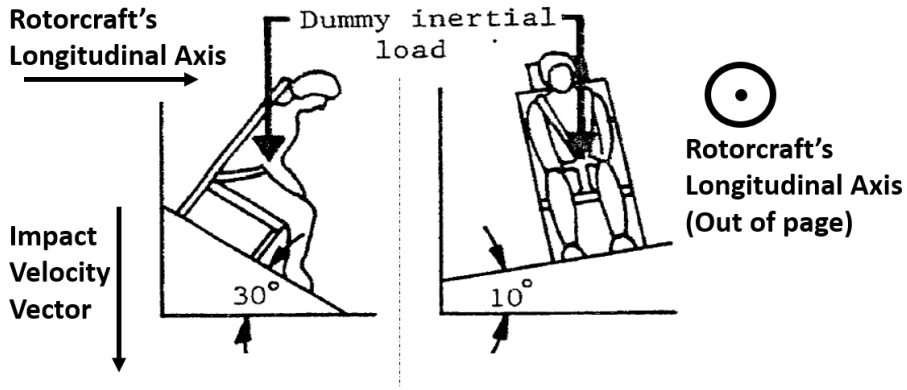

Figure 14: Seat/restraint system dynamic test 1 [17]

2. The rotorcraft's longitudinal axis is yawed 30°, either right or left of the impact velocity vector (whichever would cause the greatest load on the

shoulder harness), the rotorcraft's lateral axis is contained in a horizontal plane containing the impact velocity vector, and the rotorcraft's vertical axis is perpendicular to a horizontal plane containing the impact velocity vector as seen in Figure 15.

- Peak floor deceleration must occur in not more than 0.127 seconds after impact and must reach a minimum of 27 g.

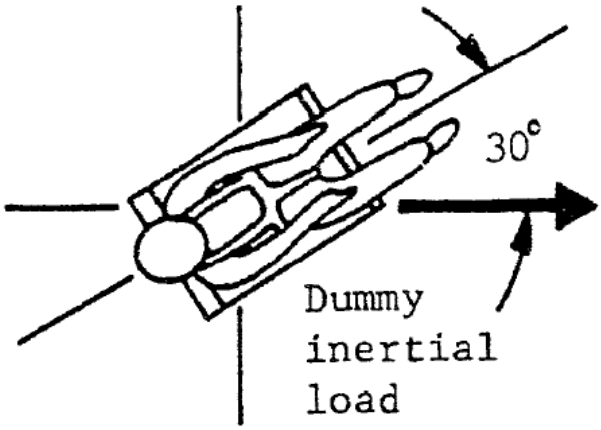

Figure 15: Seat/restraint system dynamic test 2 [17]

Tests also require that the floor is deformed by at least 10° in pitch and 10° in roll, as seen in Figure 16 in order to simulate the actual crash case.

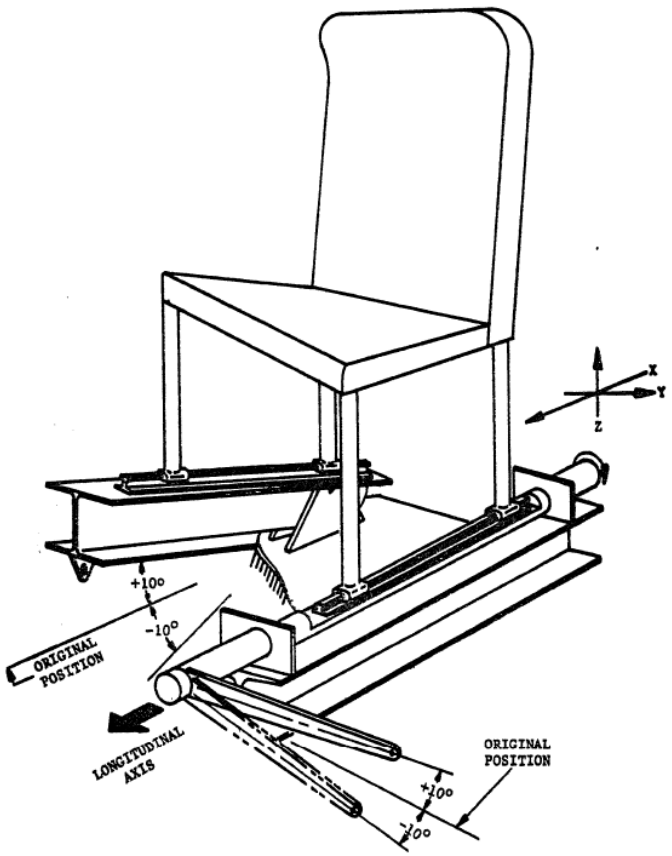

Figure 16: Floor warpage requirement [17]

2.3.2.2 Occupant Injury Criteria

The most important aim of the both civil and military seat regulations is to ensure the safety of the occupant inside a helicopter. The survivability of human from a crash depends on the loads that come to the lumbar and pelvis area as stated before in Section 2.2.1 Design Criteria. Figure 17 gives the maximum acceptable vertical pulse acceleration and duration values specified in MIL-S-85510 [17]. It should be noted that magnitude of the acceleration is not the only parameter which is effective on the injury that is incurred on the occupant during an impact event. The duration of the sustained acceleration is also very important in assessing the injury incurred. In this respect, very high accelerations can be tolerated if the duration of the sustained acceleration is very short. For instance, according to Figure 17, if one seat design gives a result of 60 g in 0.003 seconds, then it said to be successful for occupant survivability. On the other hand, if a seat gives a result of 40 g in 0.006 seconds, it is in the area of injury and said to be failed.

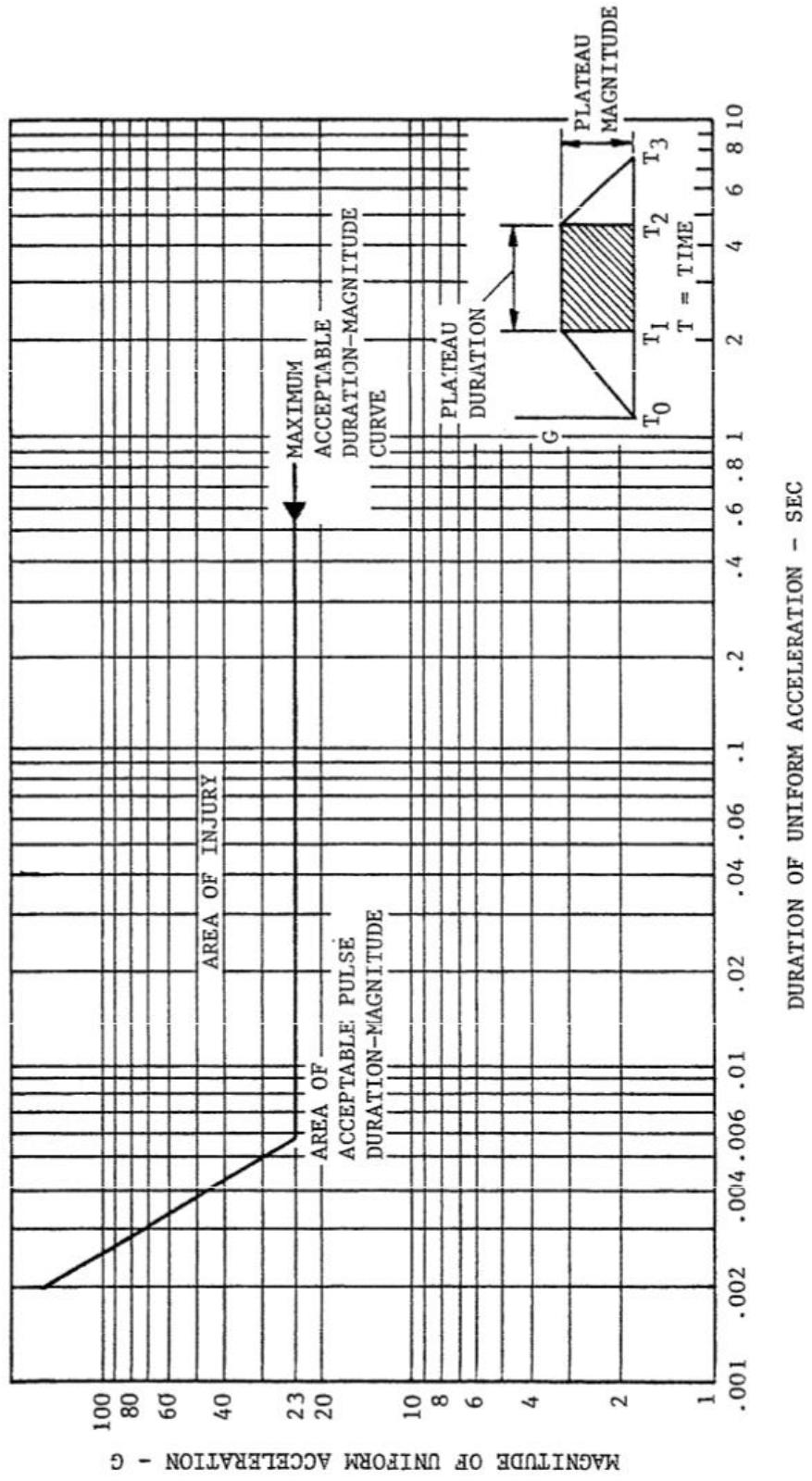

Figure 17: Maximum acceptable vertical pulse acceleration and duration values [17]

In this study, the simulation mainly focuses on occupants' safety and rotorcraft seat structures. For this purpose, civil seat specification, CS 29, requirements are taken as reference and crash loads defined in this specification is applied to designed seats. Only downward test definition is implemented on the crash analysis among the test definitions listed above. By implementing this test condition on crash, one can;

i. Evaluate the structural integrity of the seat and
ii. Track data on seat bucket displacement, velocity, and acceleration time histories [19].

The seat shall prevent the occupants from experiencing vertical decelerations in excess of human tolerance during crash pulses and not experience structural failure. Energy shall be absorbed in the vertical axis by load-limiting devices. The seat having energy-absorption mechanism shall minimize occupant submarining and dynamic overshoot.

In this study two different seat models having different energy absorber concepts are subjected to the finite element analysis with the civil specification requirements mentioned above. In addition, in order to compare the results, both seat models are analyzed also with removing the energy absorber mechanism completely.

CHAPTER 3

METHODOLOGY

3.1 Helicopter Seat Design

In this thesis study, a seat model having energy absorber system subjected to the finite element analysis with the civil specification requirements as mentioned in previous chapter. In addition, in order to compare the results, the seat model is analyzed also with removing the energy absorber mechanism completely. To summarize, simulation is performed with 2 seat models:

- Seat Model-1: Seat model without energy absorber
- Seat Model-2: Seat model having an absorber system

Seat model-1 is composed of 3 parts which are 2 legs and a seat bucket as shown in Figure 18. Seat model-2, on the other hand, is designed such that it includes a seat bucket, two legs and a lower damping part and an upper damping part on each leg. Seat model-2, shown in Figure 19, has a type of load-limiting devices which is based on the crushable column concept as mentioned before.

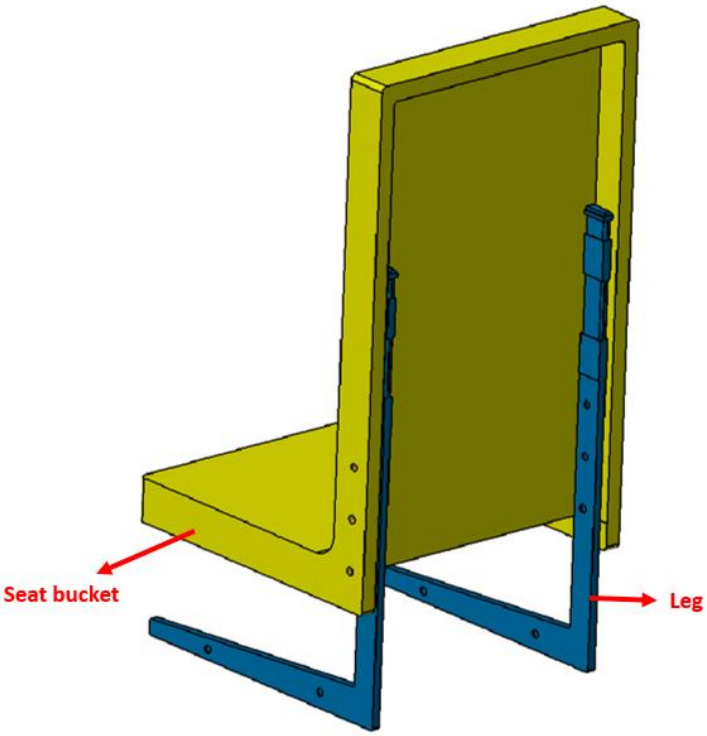

Figure 18: Seat model-1

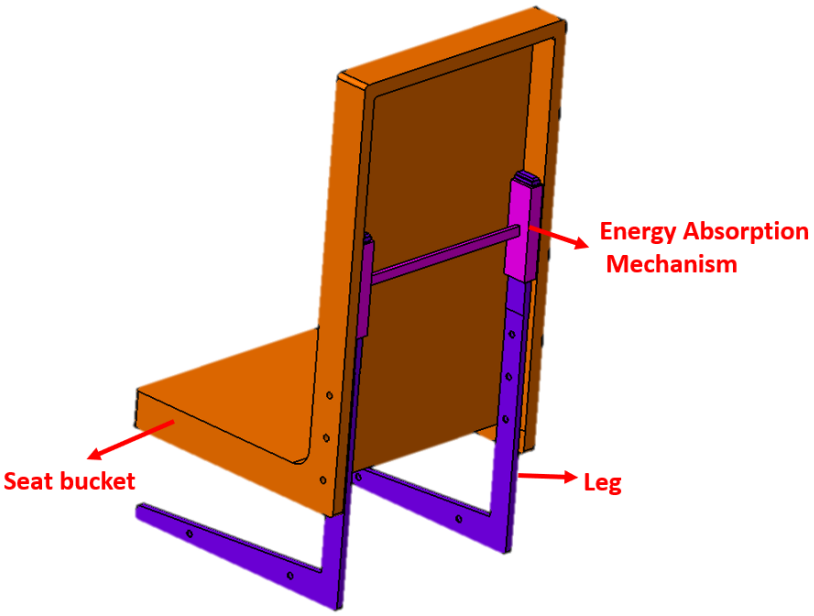

Figure 19: Seat model-2

For the purpose of the study seat models are designed by using CATIA V5 [20]. The seat model-1 is designed such that there is no damping mechanism in the seat design to limit the crash load and only the seat bucket and the legs are included in the design. Bucket and legs are connected from 6 joint locations and seat structure is installed to the floor from 4 joint locations from the legs, as can be seen on Figure 18.

The seat Model-2, on the other hand, is designed such that seat structure includes a load limiter system besides a seat bucket and two legs. Bucket and legs are connected from 6 joint locations and seat structure is installed to the floor from 4 joint locations from the legs as same conceptual design with seat model-1. Energy absorption mechanism, on the other hand, stands with tight contact with aluminum legs. The energy absorber mechanism of the seat model-2 works with a plastic deformation of the aluminum legs, which means damping and load reduction is made by interaction forces. In the crash moment, the protrusion on the upper steel damping part of the seat leg accelerates and with its velocity, lower damping part is deformed and crushed. By this way, the crash pulses are reduced.

The plastic deformation is the most important mechanism for the success of the absorbing system of the seat model such that it has to be effective in the load reduction that the occupant receives.

The dimensions of the seat model-2 are given in Figure 20 and Figure 21 below.

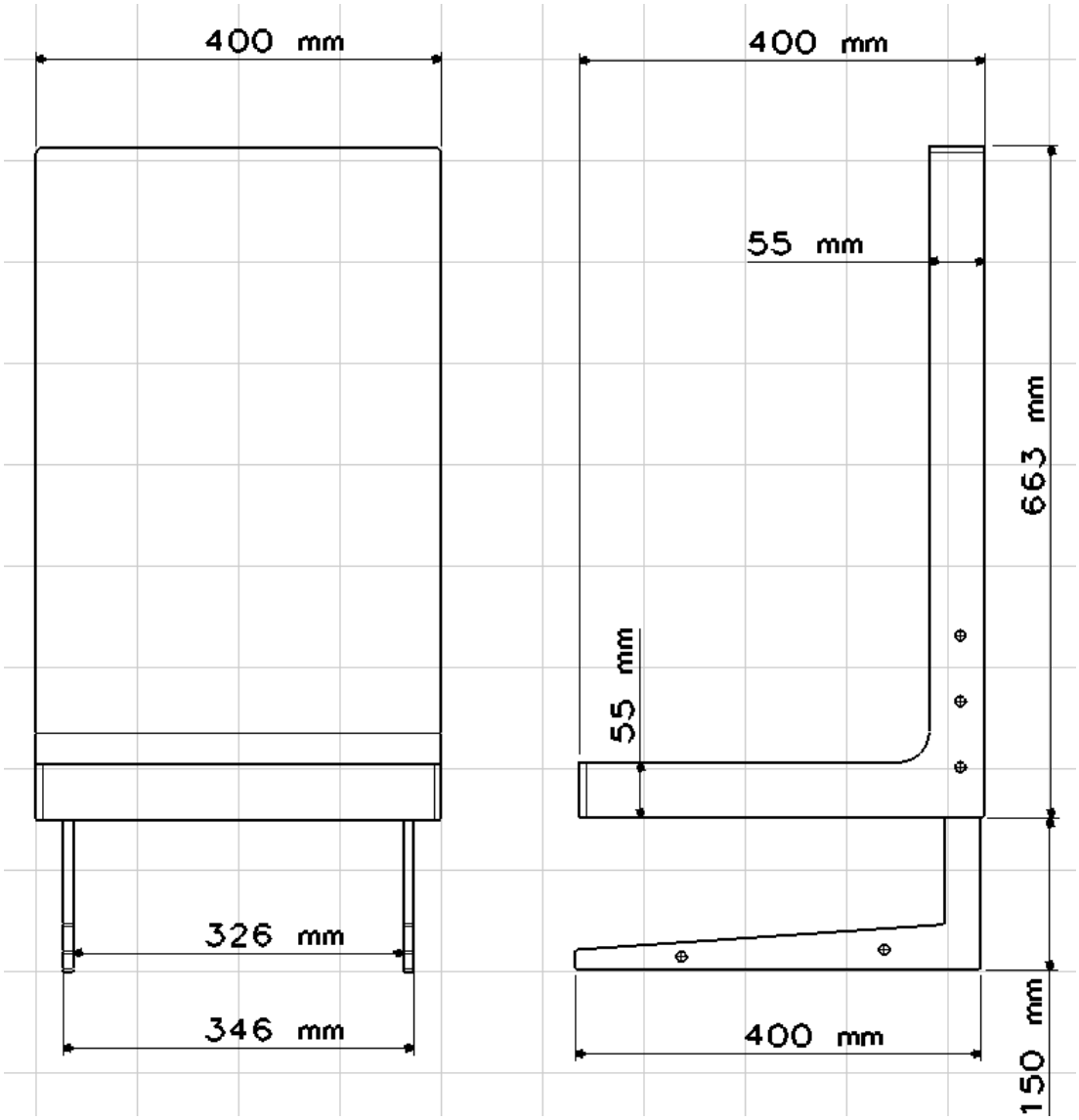

Figure 20: Front view dimensions of the seat model-2

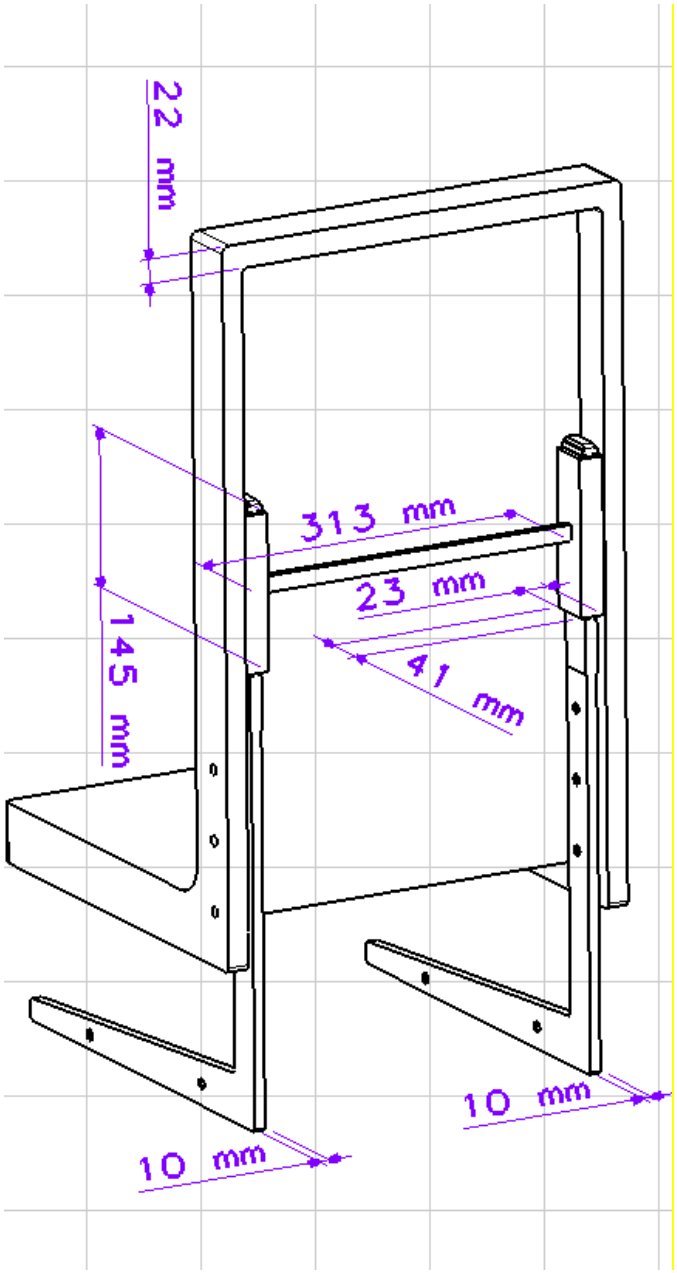

Figure 21: Isometric view dimensions of the seat model-2

The details of the seat model-2 and damping mechanism design are given in Figure 22 and Figure 23. In the crushable absorber system, lower aluminum leg part of the seat leg is plastically deformed by the steel upper damping part of the seat structure. At the crash moment, upper damping part accelerates and, with its velocity, plastically deforms the lower part. By this way, energy is absorbed in the vertical axis by load-limiting, energy absorber device.

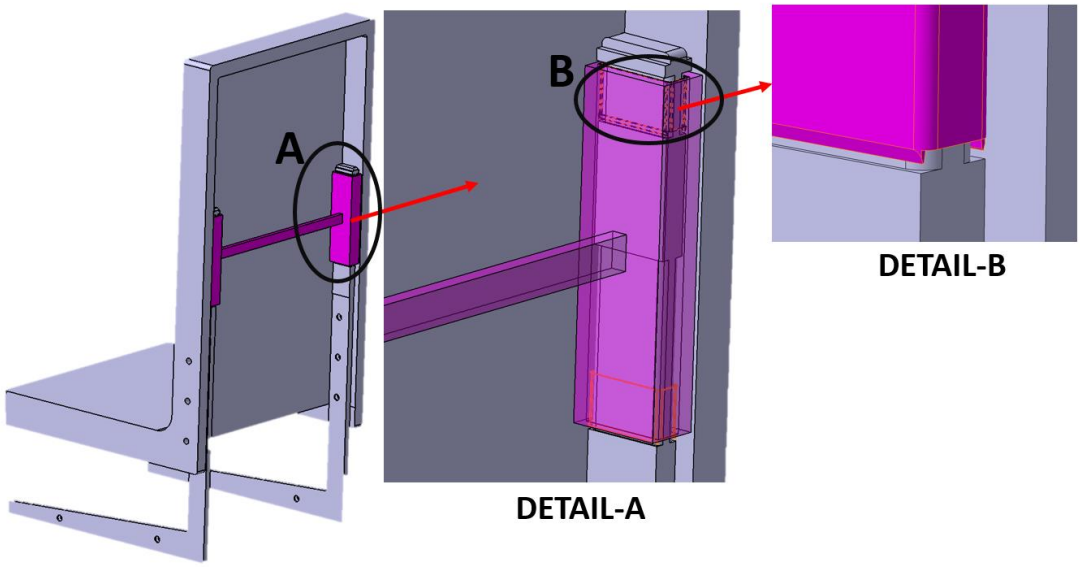

Figure 22: Damping system of the seat model-2

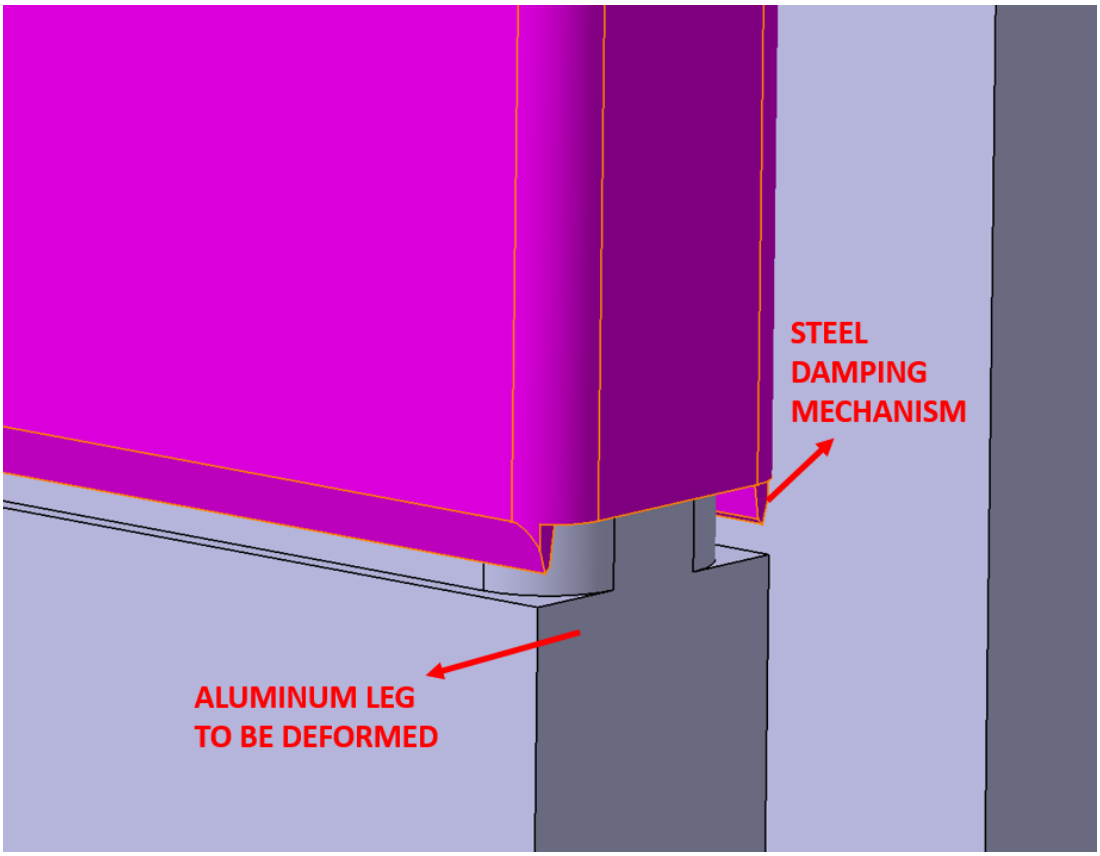

Figure 23: Detail view of the damping system of the seat model-2

3.2 Finite Element Modeling

Finite element model of the crash event is generated such that it simulates the crash test as close as possible. For this specific crash simulation analysis ABAQUS Explicit software is used for both seat models.

ABAQUS is a general-purpose finite element program capable of simulating complex problems. The code's origins lie in highly nonlinear, transient dynamic finite element analysis using explicit time integration.

"Nonlinear" means at least one of the following complications:

- Changing boundary conditions (such as contact between parts that changes over time)
- Large deformations (for example the crumpling of sheet metal parts)
- Nonlinear materials that do not exhibit ideally elastic behavior (for example thermoplastic polymers)

The ability of ABAQUS/Explicit to effectively handle severely nonlinear behavior such as contact makes it very attractive for the simulation and it is generally used to simulate brief transient dynamic events such as ballistic impact or automotive crashworthiness.

In this study, helicopter seat crash analysis is performed by using ABAQUS Explicit. The finite element modeling procedure starts with a generation of computer aided design model of the seat. After importing the three-dimensional seat design into ABAQUS, modeling is started for the analysis. Modeling of the crash analysis is divided into six steps as follows:

1. Definition of materials and their properties like density, young modulus, Poisson’s ratio and, true stress true strain curve for plastic deformation;
2. Meshing of the structure components and inspecting the mesh quality in terms of askewness, warping, mesh size and aspect ratio;
3. Defining the simulation time period and, if used, mass scaling factors;
4. Defining output characteristics;
5. Defining constraints;
6. Defining initial forces, velocities and boundary conditions;

Detailed model creation is given in Section 4.1 of Chapter 4 ABAQUS Model Creation.

3.3 Low-pass Digital Filtering

In the acceleration time-histories for a particular node, generally high frequency content is seen. For this reason, acceleration signals are usually filtered using a low-pass digital filter. Current practice in crash analysis is to use Butterworth digital low-pass filter which is applied forward and backward in time to avoid phase shifts in time [21]. Figure 24 shows an example of how the filter affects the data [5].

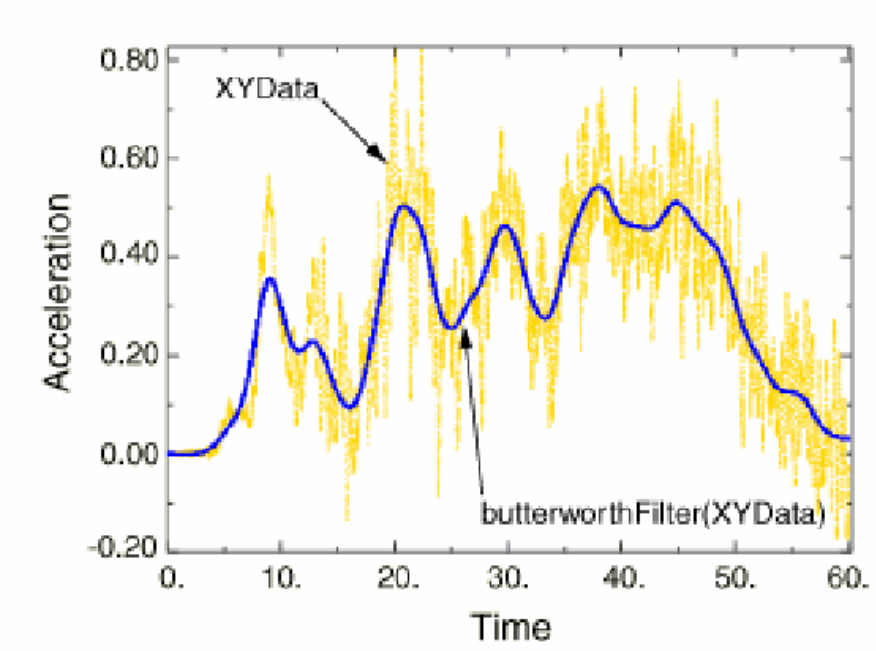

Figure 24: Butterworth data filtering sample [5]

In crash analysis, generally data filtering is done according to Channel Frequency Class (CFC) defined by the SAE J211-1 specification [22]. In this specification, SAE has defined a set of Channel Frequency Classes (CFC) for impacts of vehicles, which originally were designed for automobile impacts. These CFC's are 60, 180, 600, and 1000. Table 1 gives the frequency classes by showing which channel frequency class should be used for specific test measurements.

Table 1: Frequency Response Classes [22]

Typical Test Measurements	Channel Frequency Class (CFC)
Vehicle structural accelerations for use in:	
Total vehicle comparison	60[1]
Collision simulation input	60
Component analysis	600
Integration for velocity or displacement	180
Barrier face force	60
Belt restraint system loads	60
Anthropomorphic Test Device	
Head accelerations (linear and angular)	1000
Neck	
Forces	1000[2][3]
Moments	600[2][3]
Thorax	
Spine accelerations	180
Rib accelerations	1000[2]
Sternum accelerations	1000[2]
Deflections	600[2][4]
Lumbar	
Forces	1000[5]
Moments	1000[5]
Pelvis	
Accelerations	1000[5]
Forces	1000[5]
Moments	1000
Femur/Knee/Tibia/Ankle	
Forces	600
Moments	600[2]
Displacements	180[2]
Sled acceleration	60
Steering column loads	600
Headform acceleration	1000

1. When overall acceleration of the frame or body in a given direction is desired and a higher frequency response class is used, readability of the data may be improved by averaging outputs of two or more transducers at different locations.
2. References are listed in Appendix A, Section A.4.
3. These classifications are needed to calculate head impact forces based on neck forces and head accelerations when using the Hybrid III crash test dummy.
4. See SAE Paper 930100.
5. No rationale for this classification. By default, class 1000 was chosen.

To understand Table 1, it can be exemplified as follows: If the crash results are read from an anthropomorphic test device, for head acceleration, CFC 1000 should be use. It means that in ABAQUS, after getting the head acceleration graph, one should apply the Butterworth filtering in "operate on X-Y data" section in the program and enter the "1000" channel frequency class as the filtering value. Then ABAQUS runs the necessary formulation in the background to give the filtered head acceleration data as a graph.

It is important to choose the correct CFC for the filtering of the analysis results. An event that occurs in a millisecond should not be filtered with the same low-pass filter frequency as an event that occurs in 100 milliseconds. For extremely short duration impacts, the SAE CFC 1000 can be too low, likewise for long pulse durations the CFC of 60 can be too high to extract the underlying fundamental pulse shape.

In this study, the acceleration output is taken from the seat pan. There is no "seat pan acceleration" in Table 1, however there is "sled acceleration". In crash tests, sled is used to crash the seat to a fixed rigid wall. In this analysis, there is no sled, but seat directly strikes to the fixed rigid wall. In this respect, sled acceleration is taken as reference for the seat pan acceleration and output data is filtered with CFC 60.

Appendix C of SAE J211/1 presents a general algorithm that can be used for CFC 60 and CFC 180. Following equations are used to calculate the filtering data.

$$Y[t] = a_0X[t] + a_1X[t-1] + a_2X[t-2] + b_1Y[t-1] + b_2Y[t-2] \quad (5)$$

where, X[t] is the input data stream, Y[t] is the filtered output data stream and a_0, a_1, b_1 and b_2 are constants depending on the CFC class and given by,

$$w_d = 2 * II * CFC * 2.0775 \quad (6)$$

$$w_a = \frac{\sin\left(w_d\frac{T}{2}\right)}{\cos\left(w_d\frac{T}{2}\right)} \quad (7)$$

$$a_0 = \frac{w_a^2}{1.0+\sqrt{2}w_a+w_a^2} \quad (8)$$

$$a_1 = 2a_0 \tag{9}$$

$$a_2 = a_0 \tag{10}$$

$$b_1 = -\frac{2\left(w_a^2-1\right)}{1+\sqrt{2}w_a+w_a^2} \tag{11}$$

$$b_2 = \frac{-1+\sqrt{2}w_a-w_a^2}{1+\sqrt{2}w_a+w_a^2} \tag{12}$$

where T is the sample period in seconds.

In this thesis study, filtering is done with CFC 60 according to SAE J211-1 specification [22]. The SAE CFC 60 low-pass digital filter is applied to the raw acceleration data. The SAE specifies the resulting filter as a 4-pole filter. The formula (6) given above, which is taken from Appendix C of the SAE digital filter specification, states that the filter frequency equals 2.0775 times the CFC. So, the frequency input in the formula for the SAE CFC 60 low-pass filter must be 60 times 2.0775 =124.65 Hz.

CHAPTER 4

CRASH SIMULATION AND RESULTS

4.1 ABAQUS Model Creation

While preparing the ABAQUS finite element analysis model, CATIA V5 software is used for the seat modelling and geometry is imported to ABAQUS as a step file. While importing the geometries, all seat related bodies are imported as 3D deformable solid bodies. In the finite element analyses conducted, the measure units of the model are given in Table 2.

Table 2: Units of measure

Measure	Unit
Length	mm
Time	s
Velocity	mm/s
Acceleration	mm/s^2
Force	N
Weight	ton
Energy	N.mm
Stress	MPa

The finite element modeling procedure starts with the generation of the CAD model of the seat system. Then, the one should clean up the geometry and prepare it for meshing. Cleaning the geometry means that the complex geometries and sharp edges are removed from the model in order to simplify the finite element model and to reduce the analysis time. The next step is determining the connections of the seat

parts. After determining the connections, FE mesh is created and the model quality is checked in terms of askewness, warping, mesh size and aspect ratio. Mesh definition and mesh refinement details are explained in the 4.1.1 Mesh Definition chapter.

After the part meshing is completed, the seat assembly is created in ABAQUS. Since step file is used and imported directly to ABAQUS from the CATIA assembly, all parts are assembled in correct places as defined in the CATIA step file.

ABAQUS assembly module also contains the Reference Point (RP) assignments. A reference point is useful for creating a point in analysis model where a vertex is not available; for example, at the center of a hole. In contrast to a vertex a reference point is ignored by the mesh module when the mesh is generated.

When a rigid body constraint is created, a reference point on the assembly must be referred in the interaction module. A rigid body constraint constrains the motion of regions of the assembly to the motion of a reference point. One can create a reference point at the desired location and use a rigid body constraint to attach a part instance to the reference point. In addition to constraints, loads and boundary conditions can also be applied to a reference point.

In this thesis study analyses, reference points are used to attach seat pan and seat leg from their fastener holes and also used to give occupant load and to read acceleration data from it. Figure 25 shows the reference points created on the seat assembly. In the figure, white arrows show the reference point created for the fastener constraint definitions. Red circle shows the reference points created for the occupant load assignment and acceleration data output assignment.

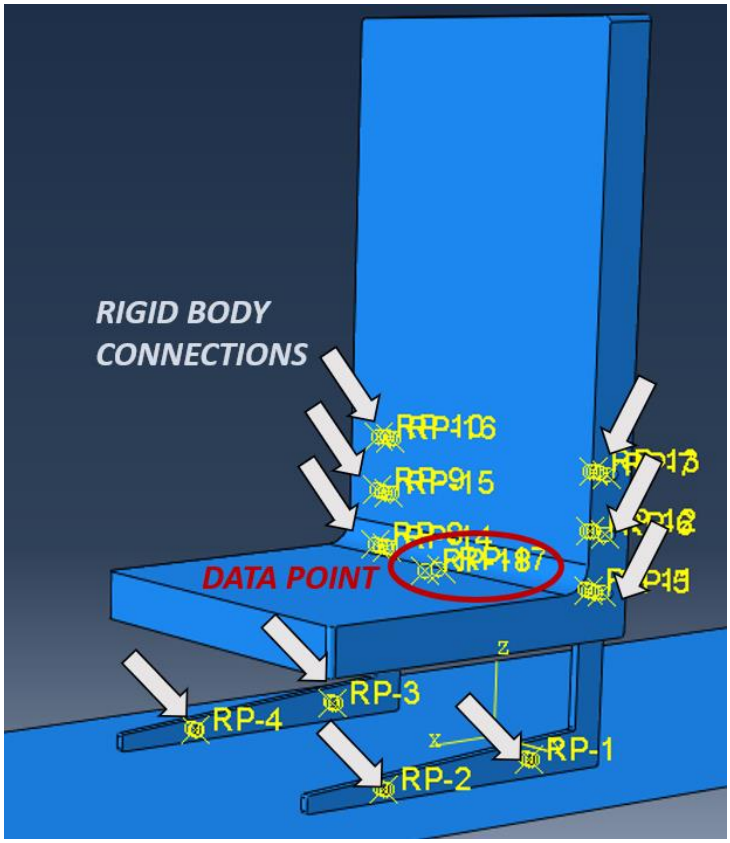

Figure 25: Reference points created on the seat model

Figure 26 shows the joint locations in the seat design. For all the holes and bolted joints, shown in Figure 26, a RP is created to be used as the force transfer point between different parts. These RPs are used in the constraint definitions and all constraints are defined using the coupling method. Coupling method is used to bind the holes to each other in order to compute the load transfer between the holes and the joint locations.

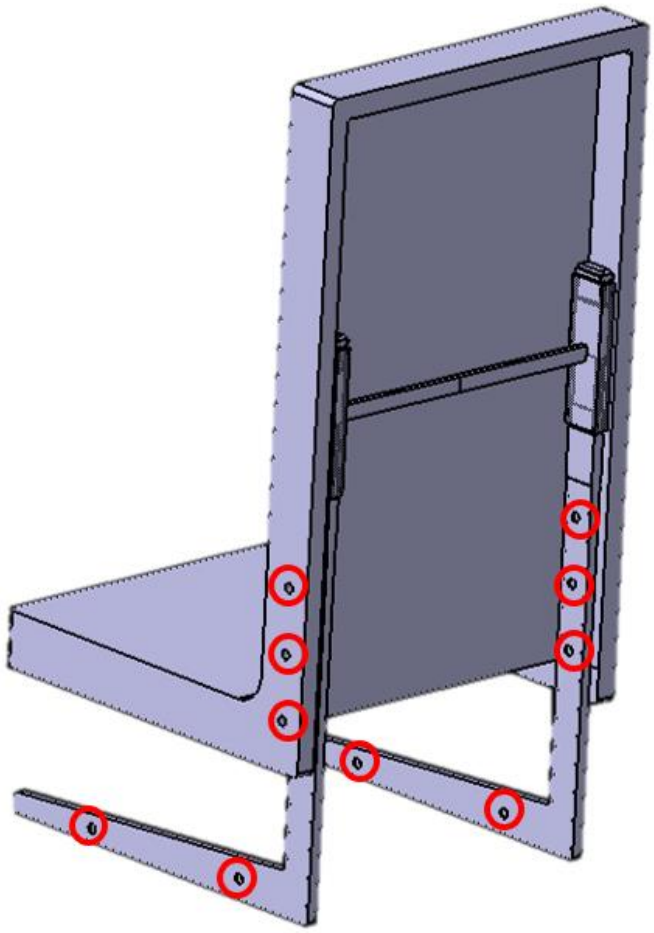

Figure 26: Joint locations in the seat design

Since the seat model-2 is used to simulate the material deformation between parts of the seat, an interaction should be generated to define the contact points. This is done by using the general explicit interaction feature in ABAQUS. Figure 27 and Figure 28 show the contact surfaces of the seat. Seat leg footplate surface gets in contact with the rigid wall during the impact. Moreover, damping mechanism support parts gets in contact with themselves with the effect of crash impact. Figure 28 shows the location of the contact surfaces of damping mechanism support parts.

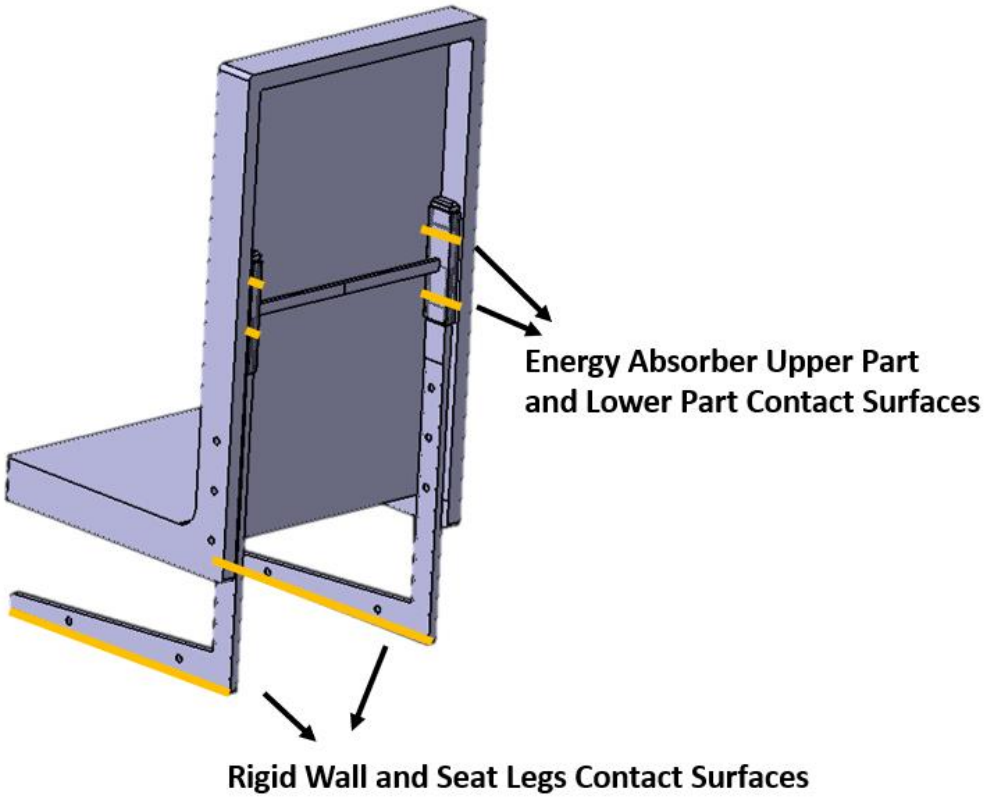

Figure 27: Contact surfaces in the seat design

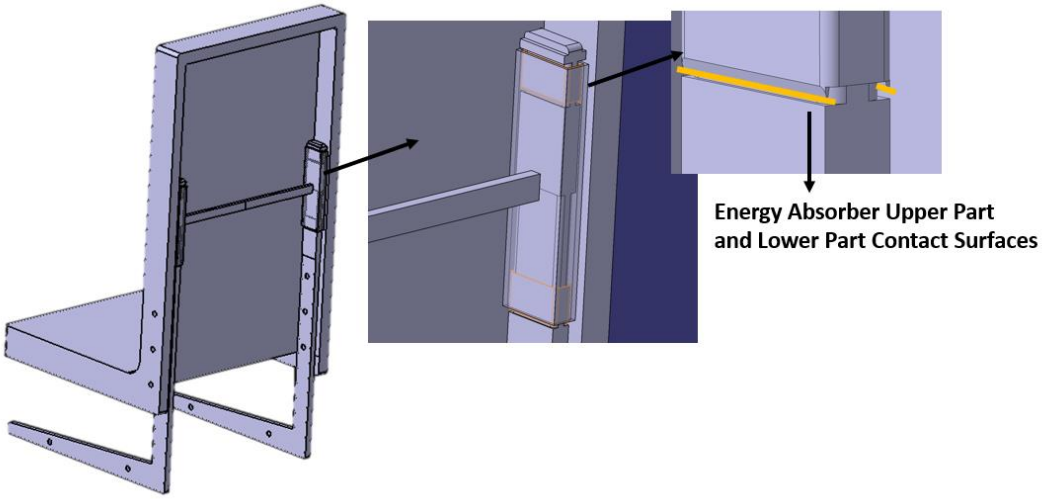

Figure 28: Detailed view of contact surfaces in the seat legs

Explicit interaction feature creates an interaction surface relation when two or more mesh surfaces get into contact in a specific time step.

For the interaction properties, both tangential penalty and normal behavior is used to simulate the material flow for the plastic deformation and the normal load transfer for the frictional contact. For tangential penalty, friction coefficient is added. For aluminum material, friction coefficient is 0.3 and for steel material it is 0.15.

4.1.1 Mesh Definition and Refinement

The accuracy which will be obtained from any finite element analysis model is directly concerning the finite element mesh that is used. The finite element mesh is employed to subdivide the model that will be subjected to analysis into smaller domains called elements, over that a set of equations area solved. As these elements are made smaller and smaller, as the mesh is refined, the computed solution will approach the true solution. However, it is very important to find the optimum element size in finite element analyses because small mesh sizes in the explicit analyses significantly increases the time of the computation.

In order to find an optimum element size, finite element analysis may be started with a preliminary mesh. Early in the analysis process, it makes sense to start with a mesh that is as coarse as possible, which means a mesh with very large elements. A coarse mesh will require less computational resources to solve and, while it may give a very inaccurate solution, it can still be used as a rough verification.

After running the analysis and computing the solution on the coarse mesh, the process of mesh refinement begins. Mesh refinement is the process of resolving the analysis model with successively finer and finer meshes, comparing the results between these different meshes. By comparing the results, it is possible to judge the convergence of the solution with respect to mesh refinement. After comparing a minimum of three successive solutions, an asymptotic behavior of the solution starts to emerge, and the changes in the solution between meshes become smaller. Eventually, these changes will be small enough and the solution starts to converge.

In this thesis study, as mesh refinement strategy, reducing the element size is used. In this method, element size is reduced gradually and, by controlling the results,

optimum mesh size is determined. Optimum mesh size occurs at where the solution starts to converge and the changes in the results are minimized, which means there is no change in the solution behavior even the mesh size gets smaller. It is important to find the optimum mesh size in this kind of finite element analyses because smaller mesh sizes in the explicit analyses significantly increases the time of the computation.

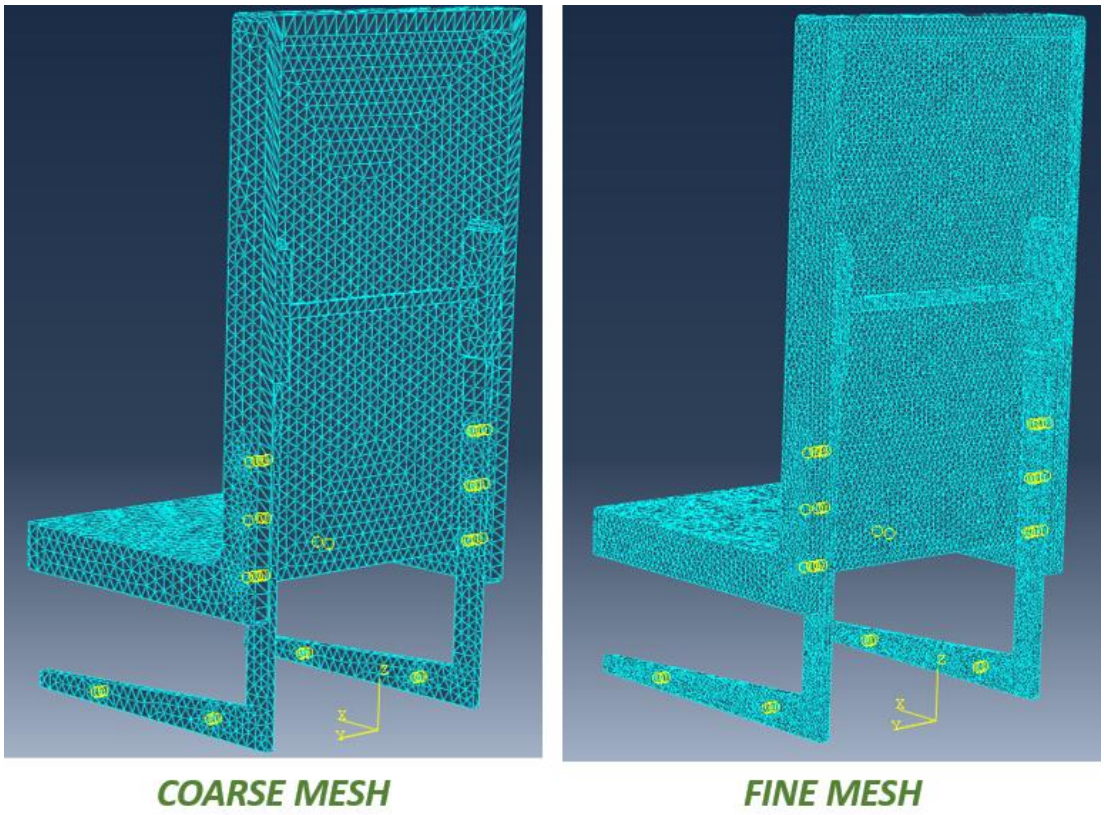

Figure 29: Coarse and fine meshed seat model-2 geometry

The two examples to generated meshes of the seat model-2 are given in the Figure 29 above. In this figure, an example for coarse mesh and an example of fine mesh is shown. For the coarse mesh definition, the approximate element size is given as 15 mm. As defining the mesh properties curvature control and minimum size control is selected. For curvature control, maximum deviation factor is used as 0.1, which is the default value of the ABAQUS program. For minimum size control, on the other hand, the absolute value is given as 4 mm. These values are the first trial of the mesh

refinement procedure. After that computation, the values are changed by reducing the mesh size in order to see how the result change and to see whether if solution converges or not.

The given mesh size parameters through the mesh refinement procedure are defined in Table 3.

Table 3: Mesh size parameters

	Global Element Size	Local Element Number
Trial-1 (Coarse Mesh)	15	N/A
Trial-2	12	N/A
Trial-3	10	N/A
Trial-4 (Fine Mesh)	7	25

The different mesh element sizes given above is used in the analyses as trials by means of mesh refinement. Besides the mesh size, the mesh properties are the same for all trials. For the mesh of the seat models that will be going through an explicit crash analysis, 3D explicit, C3D10M 10 node modified quadratic tetrahedron element type is used.

In the fine mesh trial, besides meshing by size, meshing by number is also used for local meshing. Local meshing is used for the upper sharp-edged steel damping part and the lower aluminum leg part that contacts with the upper part since the plastic deformation is performed in this specific area in the seat model-2. Figure 30 shows the locally meshed damping part. As it can be seen in Figure 30, local meshing is done by reducing the element size by increasing the mesh number for specific sharp edges of the damping mechanism and the protrusions of the legs.

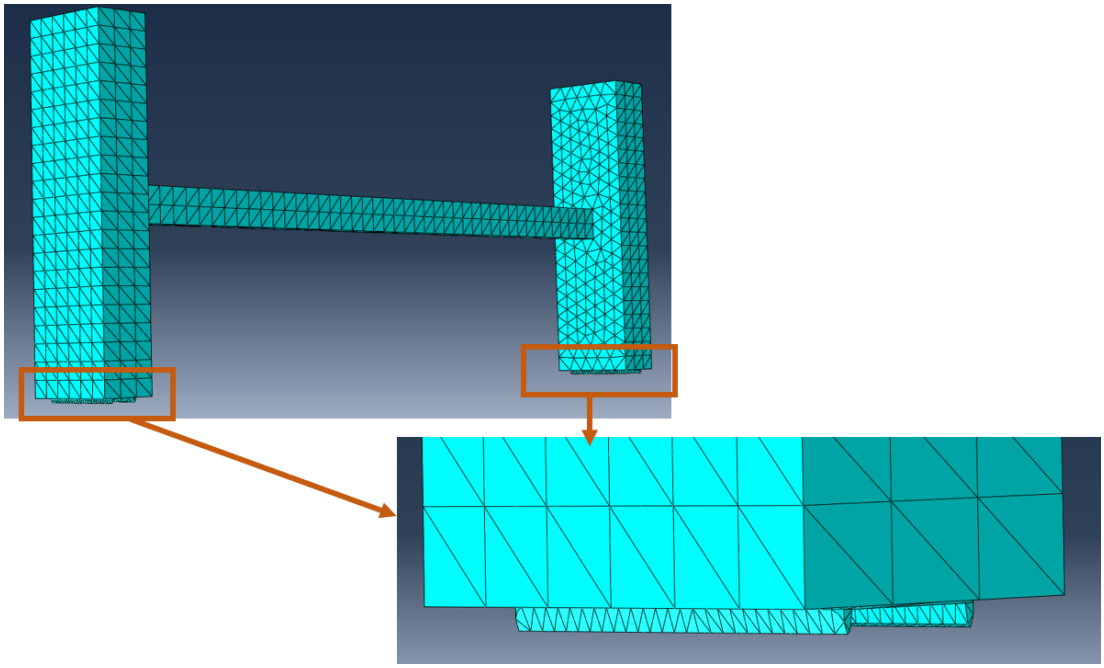

Figure 30: Local meshing of upper damping part of the seat model-2

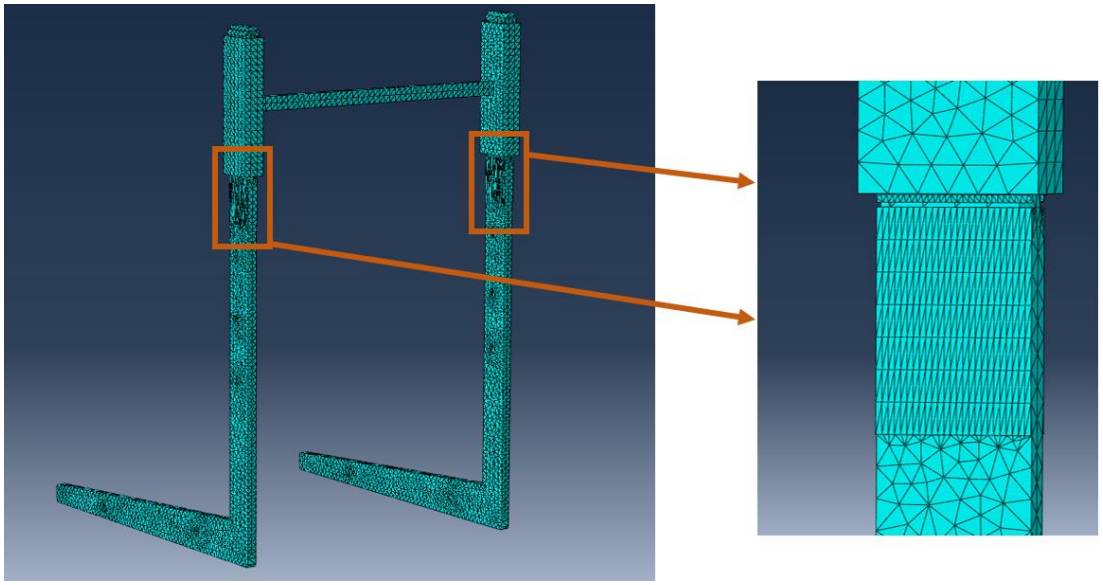

Figure 31: Local meshing of lower leg part of the seat model-2

At the end of each computation, results are recorded to be compared with the next computation results. Figure 33 shows the acceleration time histories of different mesh sizes. In the aim of comparison between the seat verification requirements and the simulation results, field output is used to collect acceleration, displacement and velocity values. The node location where the displacement field output is tracked is shown in Figure 32. This node is at the location where the occupant's pelvis is and

the loads are transferred to the lumbar area which is also a critical location of the occupant. To compare the results and to see the convergence, peak acceleration value will be taken as reference since it is the most important value in the seat crashworthiness concept as defined in the regulations, which are mentioned before in the 2.3 Seat Regulations in Aviation chapter.

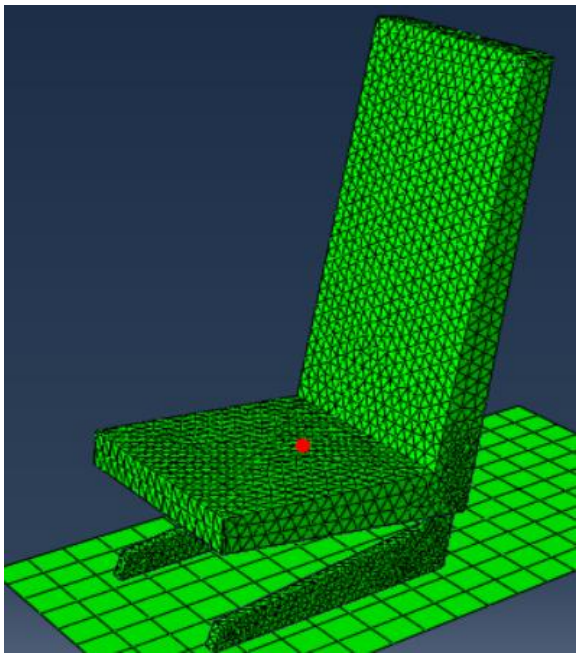

Figure 32: Seat field output location

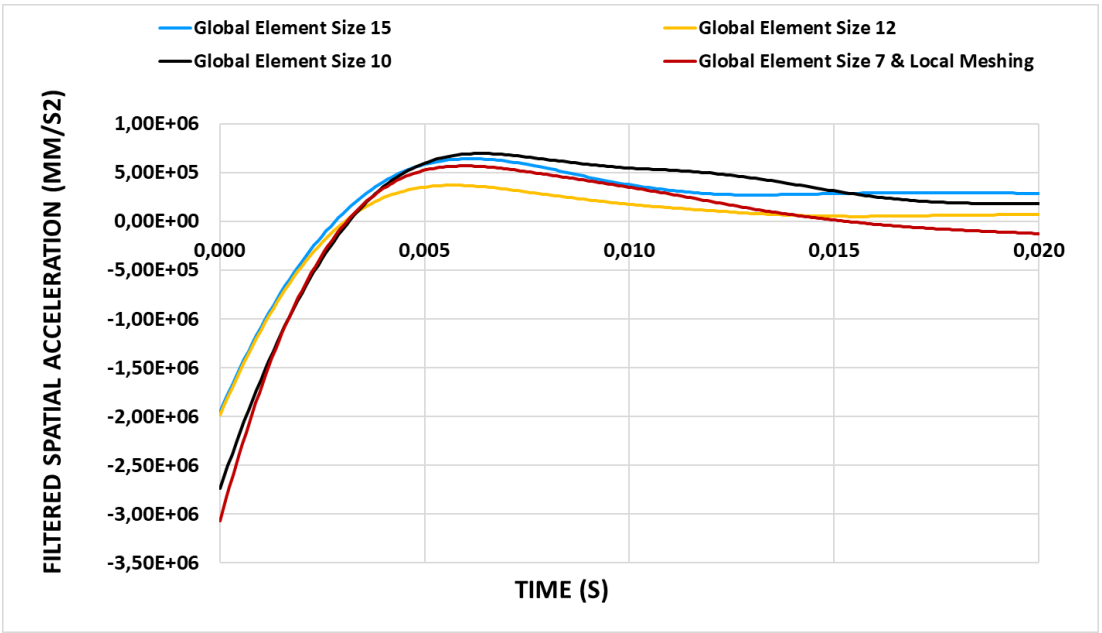

Figure 33: Filtered spatial acceleration time histories of different mesh sizes

Filtered spatial acceleration time histories given in Figure 32 show that peak values for four different mesh sizes are very close to each other. However, the local meshing in the plastic deformation zone is expected to give more reliable results. So, it is concluded that, for this crash analysis study, the approximate global element size can be specified as 7 mm and local meshing can be done near the plastic deformation region on the upper steel damping part and lower aluminum leg part.

4.1.2 Materials Used in Seat Assembly

For the crash analysis, materials and their characteristics should be defined as analysis parameters. These parameters include stress-strain relation, density, elastic modulus, Poisson's ratio and the frictional coefficient. Elastic modulus and Poisson's ratio define the elastic properties of the material. Data points on stress-strain curve, on the other hand, define the plastic properties of the material.

The material used for the seat leg structure is AL 2024. The true stress strain diagram of aluminum material is shown on Figure 34. Stress-strain values are added to plastic region in ABAQUS material definition page as x-y data of Figure 34.

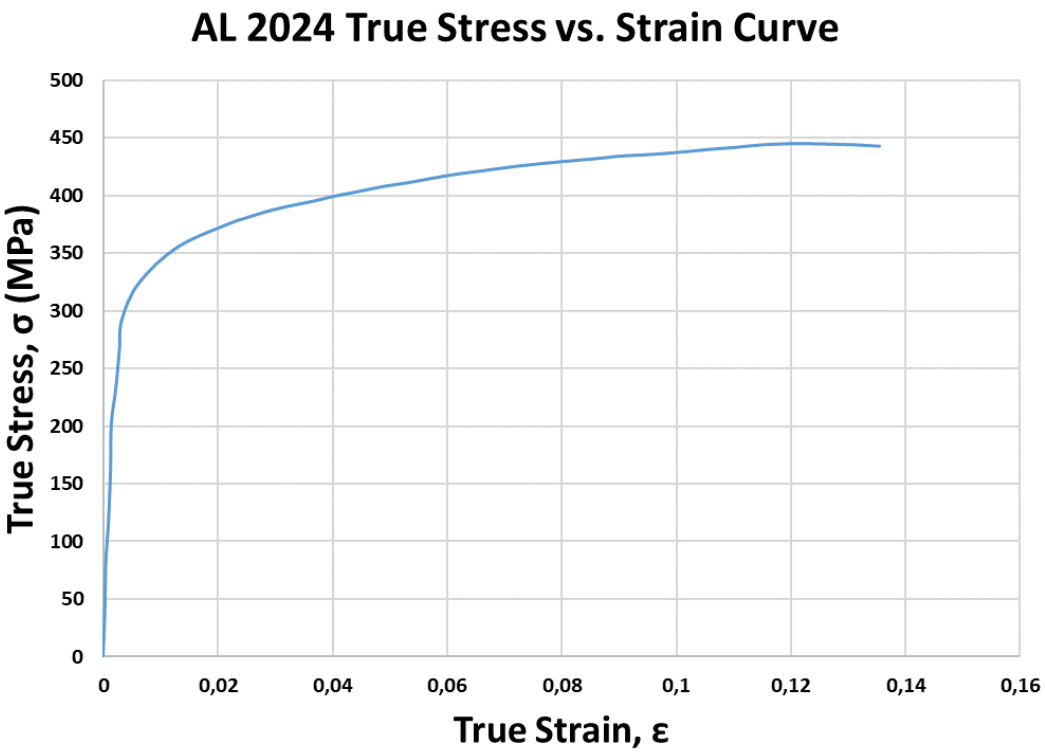

Figure 34: True stress-strain diagram of AL 2024 [23]

For the damping mechanism, in order to deform the aluminum legs more effectively, steel material is used. To simulate the seat bucket, a user defined material is defined with the same elastic behavior as Al 2024 but with different density to adjust the total weight of the seat according to the weight of the real rotorcraft seat. Generally, in civil rotorcraft seats, different composite materials, such as Kevlar are used for the seat bucket. The main reason for the usage of composite material is the weight advantage. For rotorcraft design, weight is an important parameter. For this reason, seat manufacturers aim to design a light weight crashworthy seat. However, in this study, wood material is defined for seat bucket instead of composite in order to ease the analysis. Wood material, which is defined as isotropic in the analysis, eases the analysis with less complex structure by reducing the analysis time.

Figure 35 shows the main parts of the helicopter seat and materials used. Table 4 shows the material properties that are used in simulation model.

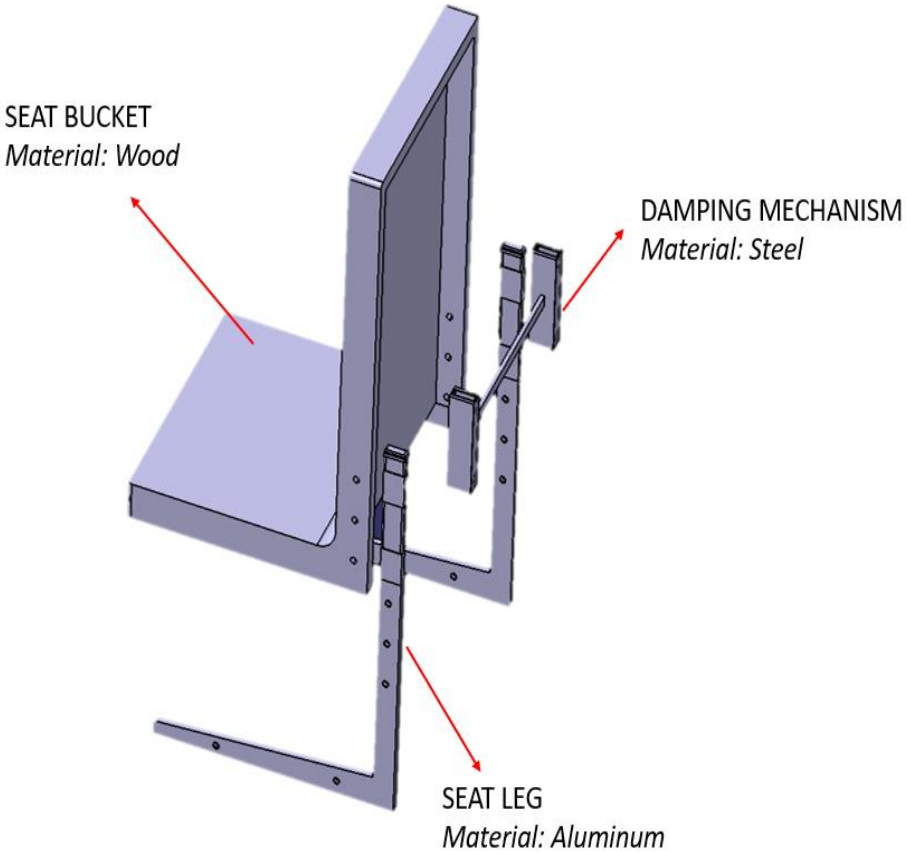

Figure 35: Parts and materials of the seat model-2

Table 4: Material properties used in analysis model

	Density (ton/mm^3)	Young's Modulus (N/mm^2)	Poisson's Ratio
Wood	7 e-10	12600	0.036
Aluminum	2.7 e-9	71000	0.3
Steel	8.7 e-9	210000	0.28

4.1.3 Load and Boundary Conditions

To simulate the crash event, 2D discrete rigid planar shell geometry is used to represent the rigid wall shown in Figure 36. The boundary condition is used to define the fixed non-deformable rigid wall. While modeling the wall, a single reference

point (RP) is created at the corner of the surface in order to define the rigid wall boundary condition as shown in Figure 36.

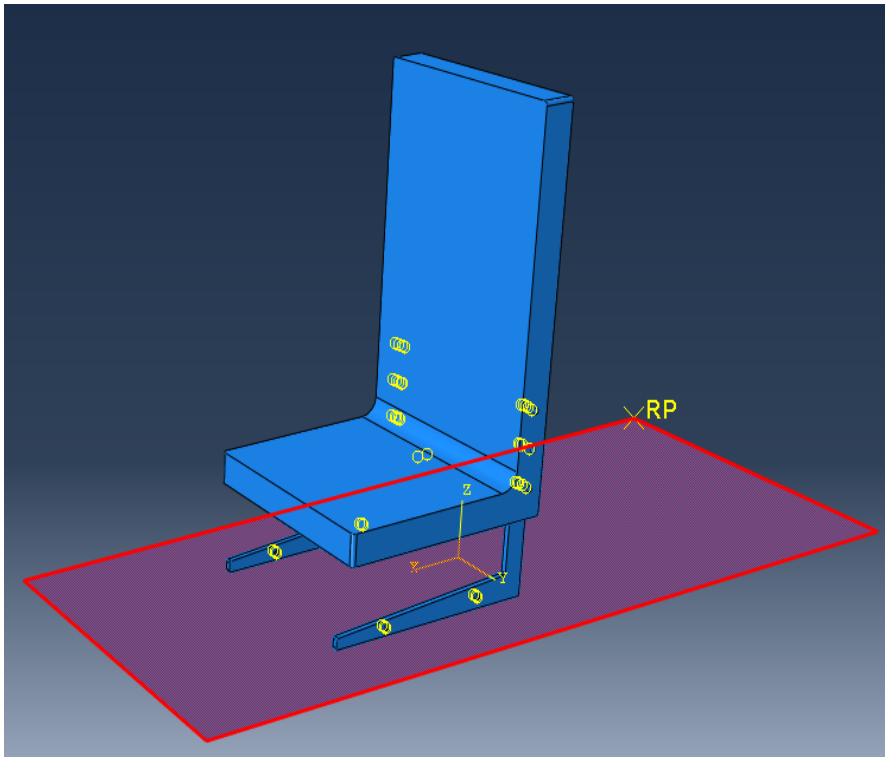

Figure 36: Reference point of rigid wall

As an initial condition definition of the crash simulation, predefined field section is used in order to define the impact velocity of the seat. In the analyses performed, impact simulation starts with an initial forward velocity of 4550 mm/s and downward velocity of -7880 mm/s which is defined in CS29.562. In this thesis study, the vertical acceleration is the main objective to investigate. For this reason, tracking of downward velocity will be done in order to study the vertical acceleration. Figure 37 shows the initial downward and forward velocity vectors given to whole seat body.

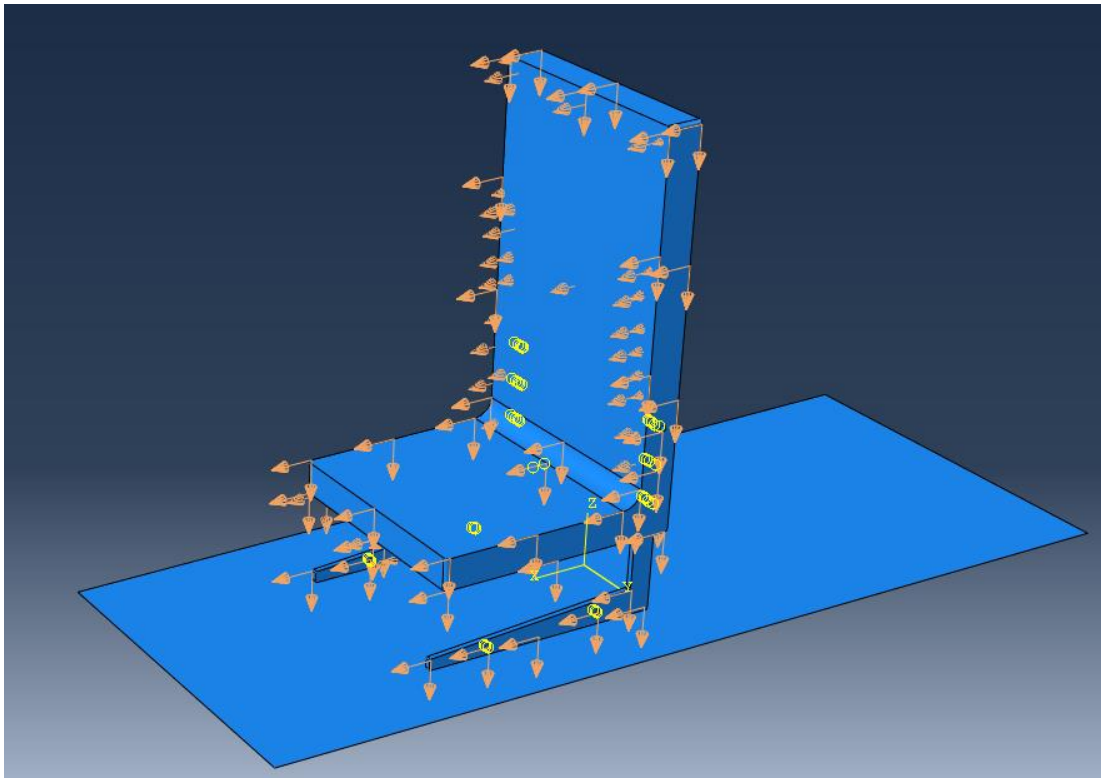

Figure 37: Initial velocity given to whole seat body

Finally, the passenger mass, which is specified as 77 kg by EASA, is assigned to a single RP as a concentrated mass and this RP is also coupled to the seat surface where the passenger sits as shown in Figure 38. The force given to the RP is 755.37 N (0.077ton x 9810mm/s^2) in the -Z direction.

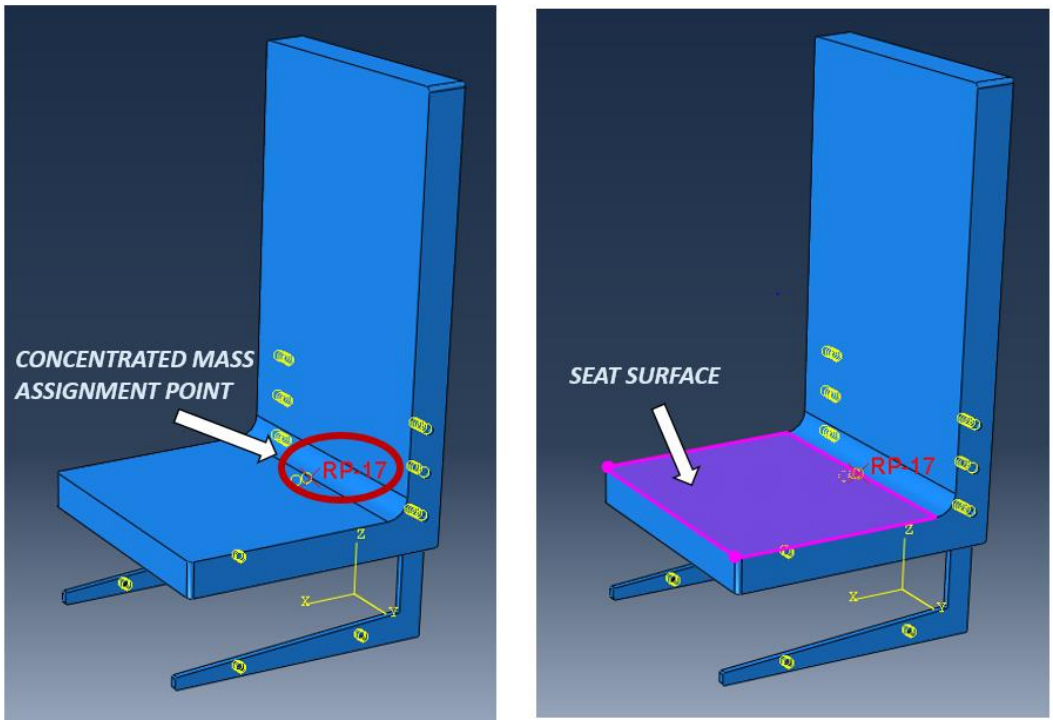

Figure 38: Reference point of concentrated mass

4.1.4 Finite Element Analyses

In ABAQUS, explicit dynamic analysis method is used for the crash simulation. ABAQUS explicit solver needs time step definition and frequency for the output collection from the model. History output is used to collect energy related values from the system; whereas field output is used to collect force, acceleration, velocity and strain related values.

Furthermore, mass scaling is used to speed up the analysis time. Mass scaling is commonly used method for computational efficiency in dynamic analyses. Explicit dynamic models contain a few very small elements that force the explicit analysis to use a small time increment to integrate the entire model, including these small elements, in time. By scaling the masses of these controlling elements, the size of the critical time-step, stable time increment, increases without affecting the dynamic response. For this crash simulation, the optimum stable time step is taken as 10^{-7} seconds. If this criterion is not satisfied, model automatically scales the system in order to have a stable time period of minimum 10^{-7} seconds.

After the definition of the constraints, loads, boundary conditions and crash parameters, finite element analyses are performed for two separate seat models in order to see the different between the resulting g loads of two seat designs. In addition, the crash simulation is repeated with the removal of damping mechanisms of two seat design in order to see the effect of the load-limiter on the crash load reduction.

4.2 Results

4.2.1 Acceleration Results

Acceleration pulse behavior of the helicopter seats that are used in the field are expected to fit the graph given in related regulations for the downward crash that defines the pass/fail criterion. One of those regulations is CS 29 as mentioned in chapter 2.3.1 Civil Regulations, gives a crash behavior graph as shown in Figure 10, which is given in 2.2.1 Design Criteria and Crash Physics chapter.

For this study, there is no aimed specific g load target taken from any regulations. Purpose of this thesis is to show how the absorber mechanisms work effectively by reducing the crash load independent from any target g load.

In the aim of comparison between the seat verification requirements and the simulation results, field output is used to collect acceleration, displacement and velocity values. The node location where the displacement field output is tracked is shown in Figure 39. This node is at the location where the occupant’s pelvis is and the loads are transferred to the lumbar area which is also a critical location of the occupant.

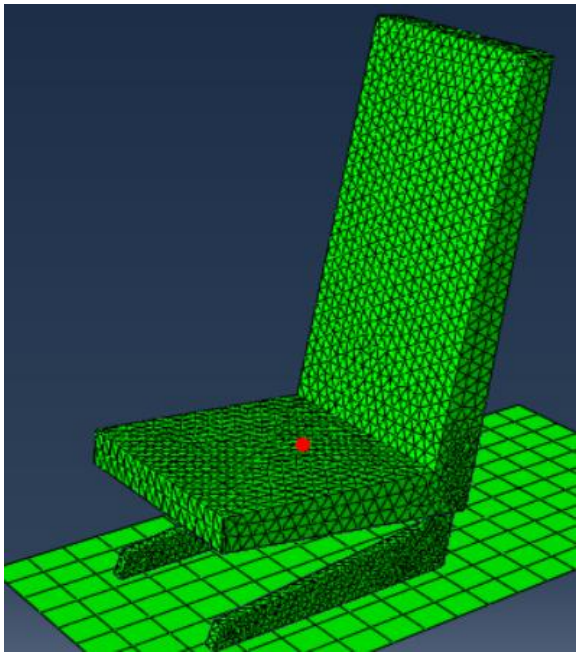

Figure 39: Seat field output location

The acceleration output graph is expected look like the ones given in
Figure 40 and Figure 41 which show the acceleration time histories of a fighter airplane recorded in a crash test.

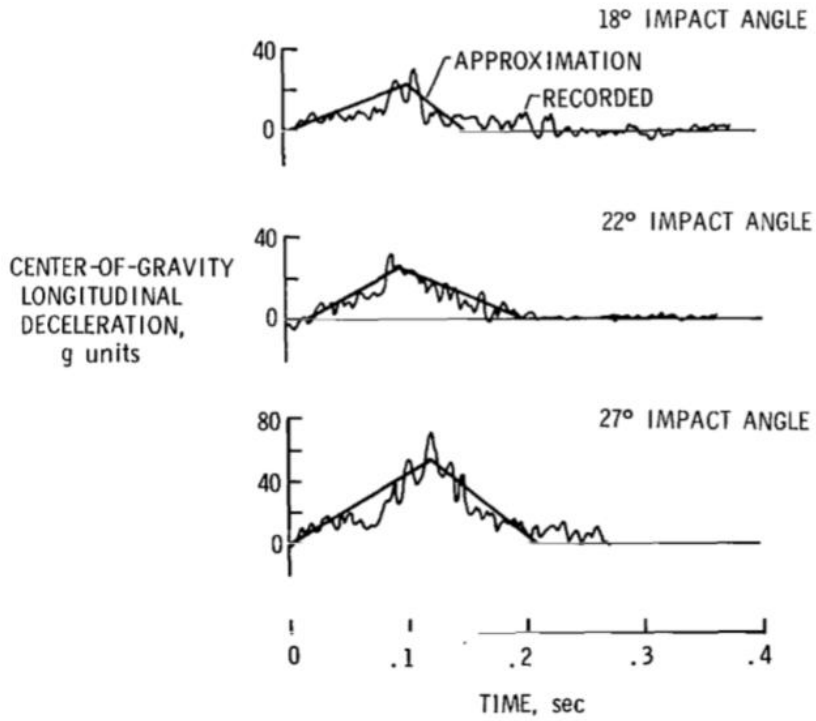

Figure 40: Time histories of decelerations of fighter airplane [24]

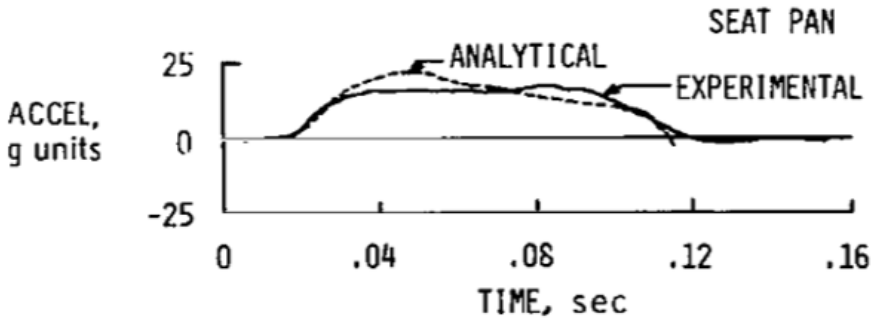

Figure 41: Time history of deceleration of fighter airplane seat pan [24]

Figure 42 shows the finite element mesh at the beginning moment of the crash event. Figure 43, Figure 44 and Figure 45 show how the steel damping part proceeds in time and gets into contact with the aluminum seat leg part during the crash event. This is how the plastic deformation occurs in the aluminum leg protrusion and the crash load on the seat pan reduces.

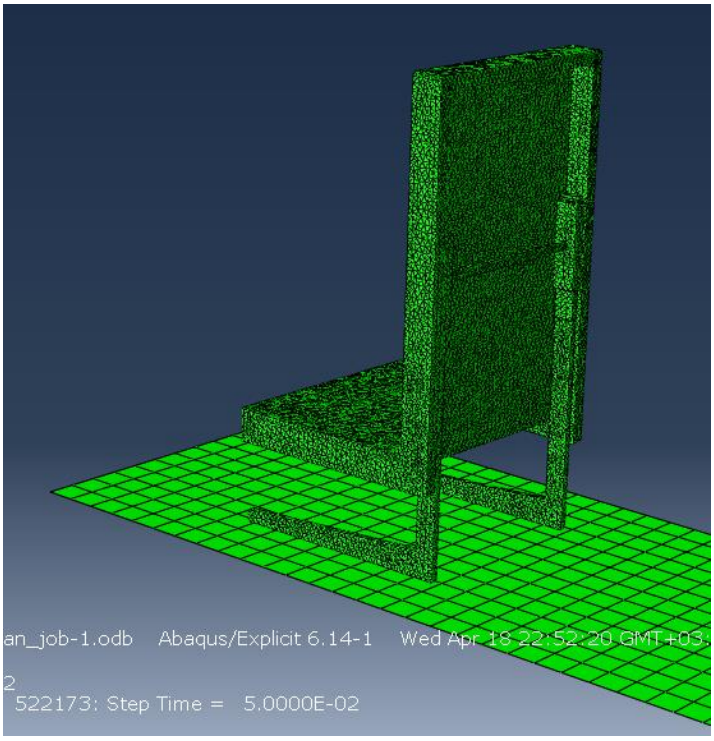

Figure 42: Finite element mesh at the beginning moment of the crash event (Time=0.00 second)

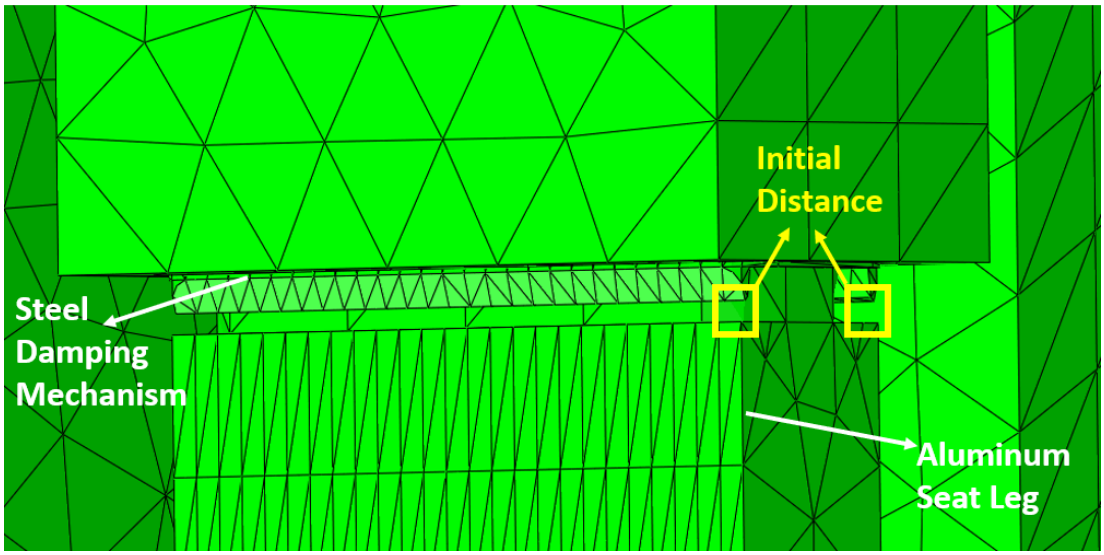

Figure 43: Distance between the damping part and the leg protrusion (Time=0.00 sec)

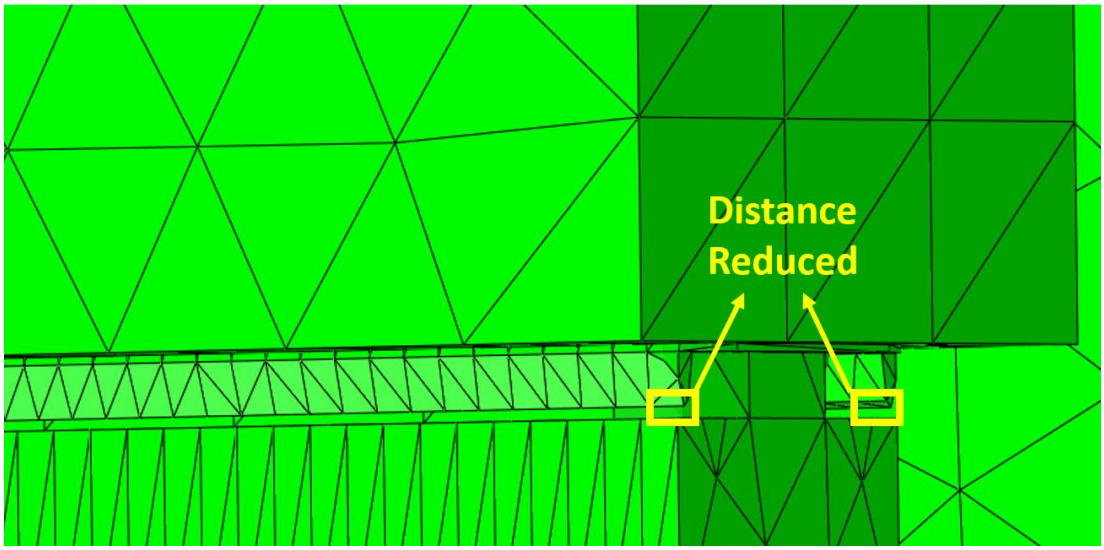

Figure 44: Distance between the damping part and the leg protrusion (Time=0.0009 sec)

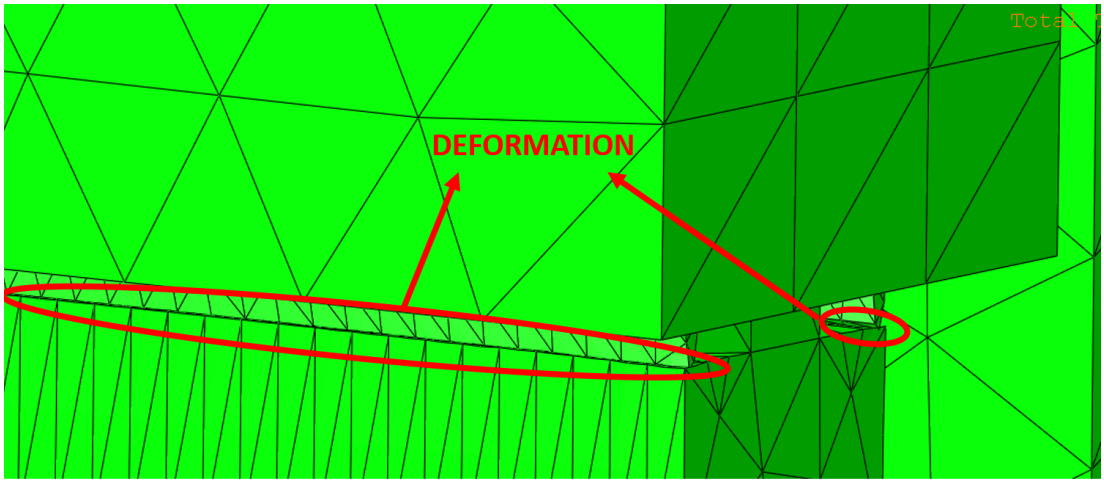

Figure 45: Distance between the damping part and the leg protrusion (Time=0.0011 sec)

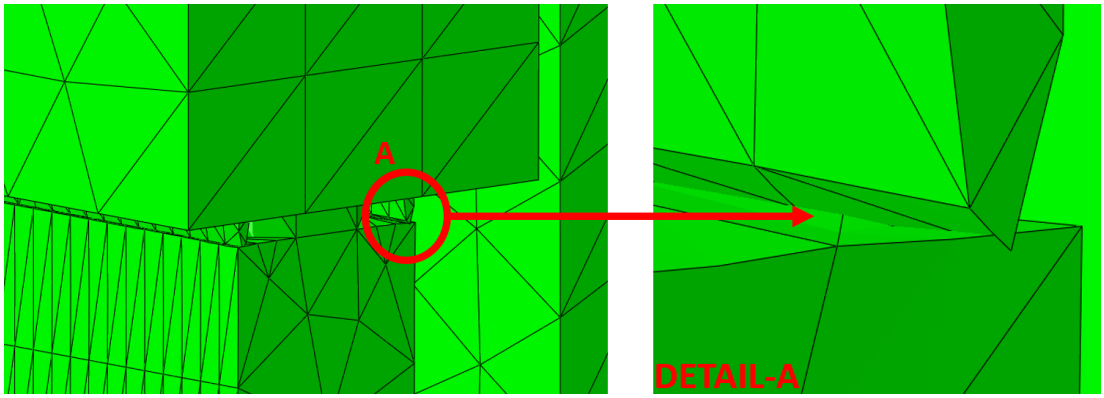

Figure 46: Detailed view of the plastic deformation

Figure 46 shows how the plastic deformation occurs in a close look. As the steel part gets into contact with the aluminum leg, with the crash velocity it deforms the legs and absorbs the crash energy.

To compare the crash load and accelerations, time histories are plotted and the results are examined. In the acceleration time-histories, because of high frequency content is seen, acceleration signals are usually filtered using a low-pass digital filter as mentioned in 3.3 Low-pass Digital Filtering chapter.

In this study, the acceleration output is taken from the seat pan and for the seat pan acceleration and output data is filtered with channel frequency class of 60 as compatible with the SAE J211 standard.

Investigating an actual test results of a rotorcraft seat will be useful to understand the outcome of the present thesis study. The seat subjected to the crash test has a rolling and flattening tube damping mechanism. Rolling and flattening tube logic is to give a form to a tube by rollers as shown in the Figure 47. In the seat absorber design, on the other hand, rollers are used to deform the tube by crushing it during the crash impact. In the damping mechanism, reels proceed on the tube-shaped legs by plastically deforming and crushing the aluminum legs.

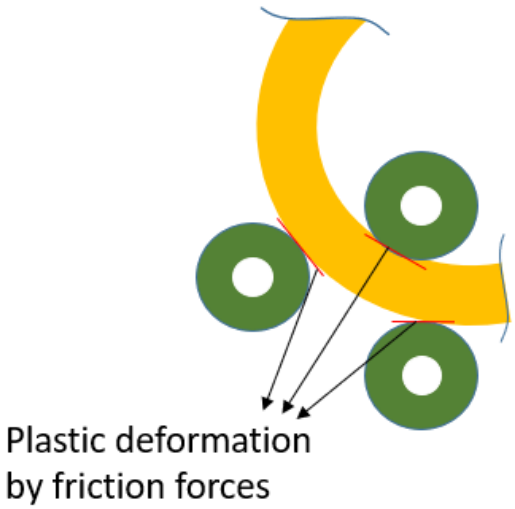

Figure 47: Rolling and flattening a tube

Test conditions are same with the conditions given in MIL-S-85510 military standard as seen in Figure 48. Standard defines the seat and seat leg positions with angles besides defining the maximum g load in a specific time range. To be successful in the test, acceleration results should be compatible with the Figure 17 that defines maximum acceptable vertical pulse acceleration and duration in MIL-S-85510 standard.

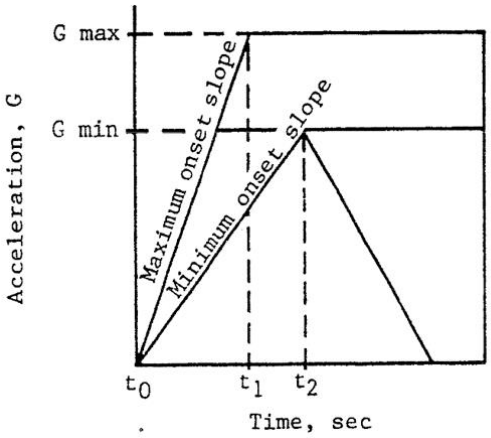

Parameter	Cabin seats	
	Qualification	R&D
t_1 sec	0.059	0.034
t_2 sec	0.087	0.087
G min	32	32
G max	37	37
Δv min, ft/sec	50	50

Test	Configuration 1/
1	Dummy inertial load 30° 10°

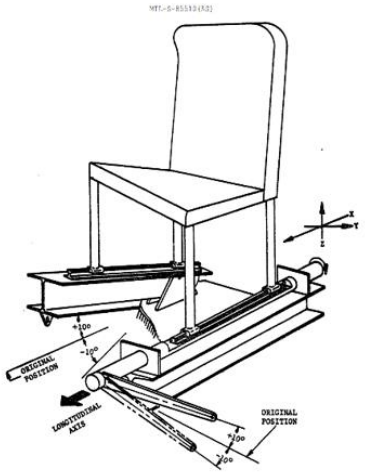

Figure 48: MIL-S-85510 test conditions [17]

In order to read the acceleration and force results of the seat with the damping mechanism, a hybrid dummy is used on which accelerometers and load cells are placed.

Figure 49 shows the location of the accelerometers and the load cells, which give the acceleration and load results during the crash event.

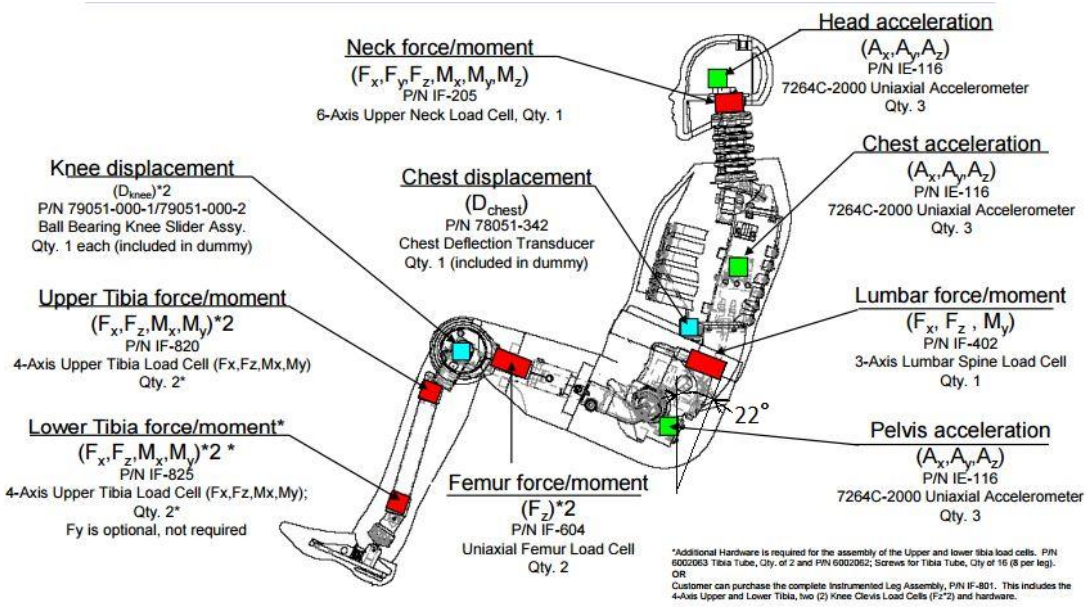

Figure 49: Accelerometer and load cell positions on Hybrid III test dummy

Besides test dummy, text fixture and the seat itself are also equipped with accelerometers. Figure 50 shows the acceleration time history of the test fixture and Figure 51 shows the seat pan acceleration time history.

In the test results, given in Figure 50 and Figure 51, Channel Frequency Class (CFC) filtering is also used as described in the SAE J211-1 specification. Figure 50 and Figure 51 figures give the filtered result as it is done in this study.

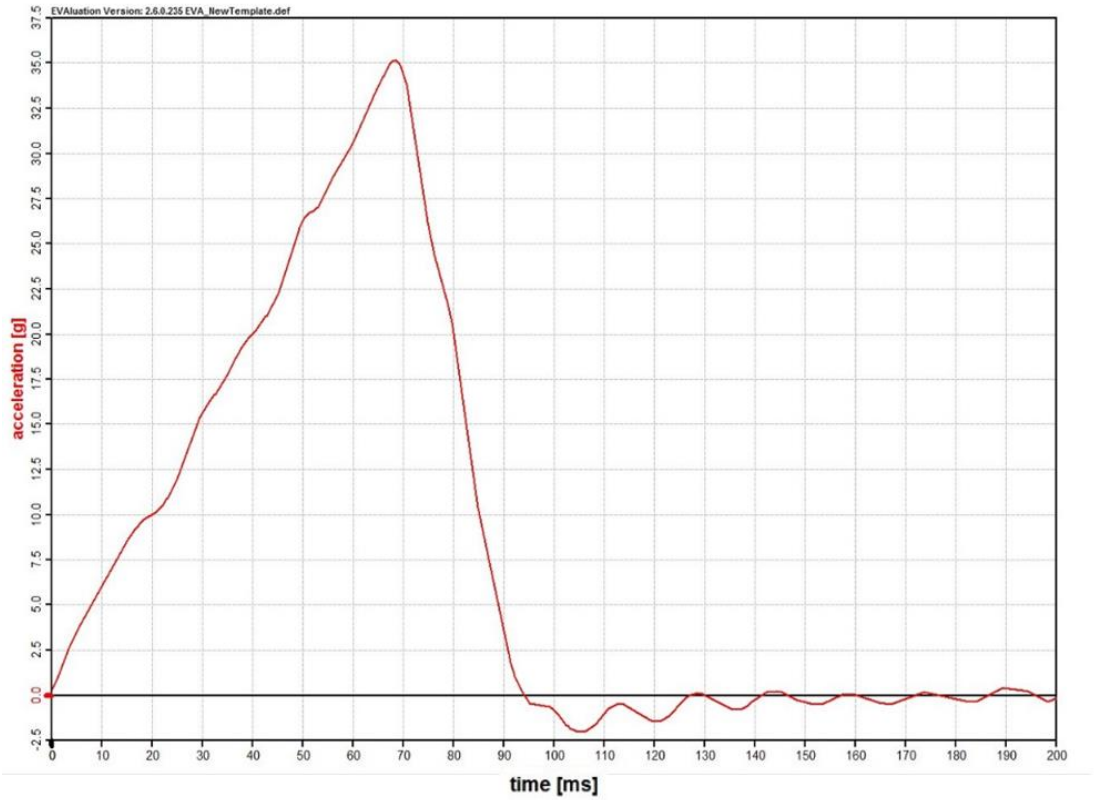

Figure 50: Acceleration time history of test fixture

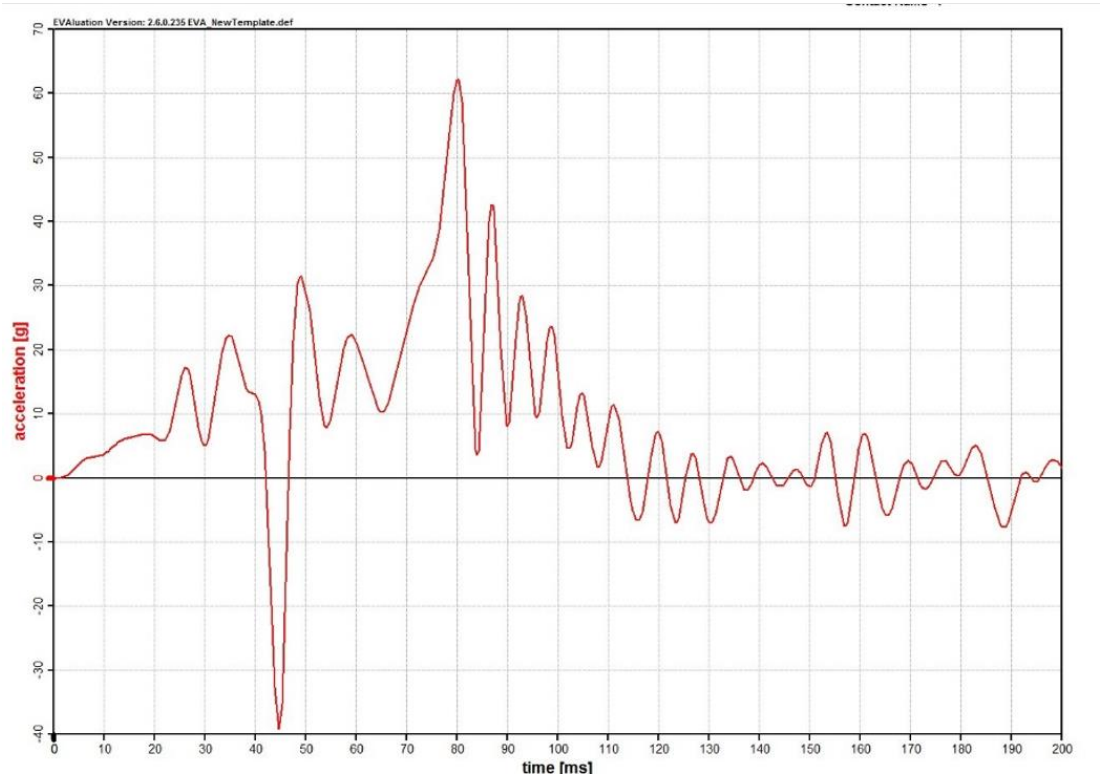

Figure 51: Acceleration time history of seat pan

In this study, the acceleration time histories are taken from the field output location and plotted. Acceleration data is gathered at the output location shown in Figure 52 below.

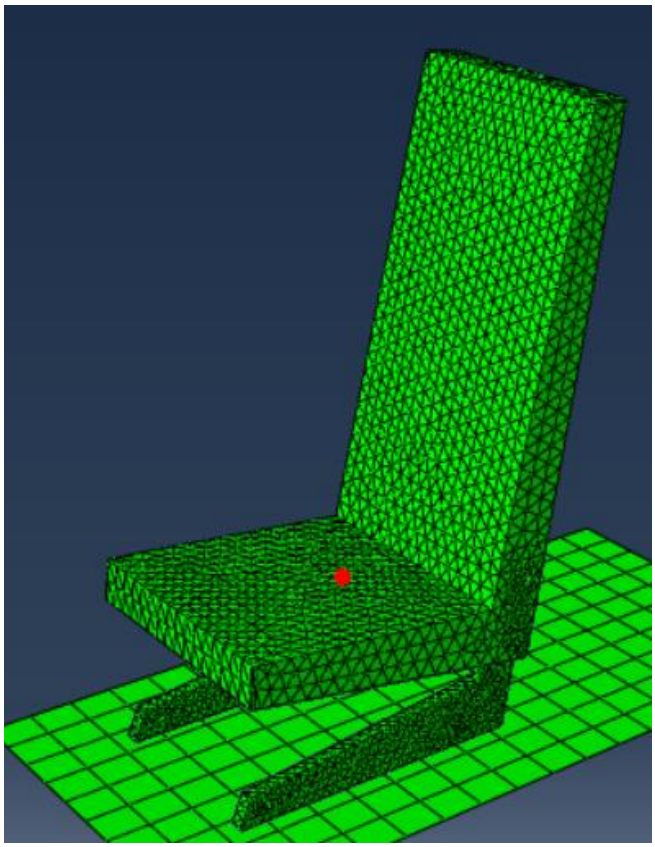

Figure 52: Seat Field Output Location

Figure 53 and Figure 54, given below, show the velocity versus time plot for the seat model-1 and the seat model-2 respectively.

Both graphs follow the same path and oscillate around zero after a specific time interval. Graphs show that the initial value is -7880 mm/s at the initial phase of the simulation, which is the input value that is given to ABAQUS as the initial condition of the downward velocity.

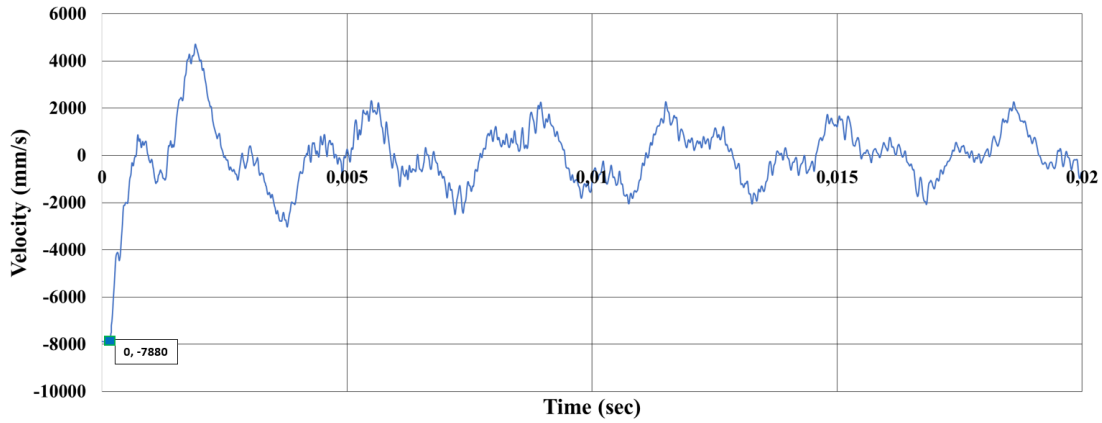

Figure 53: Velocity time history of the seat model-1

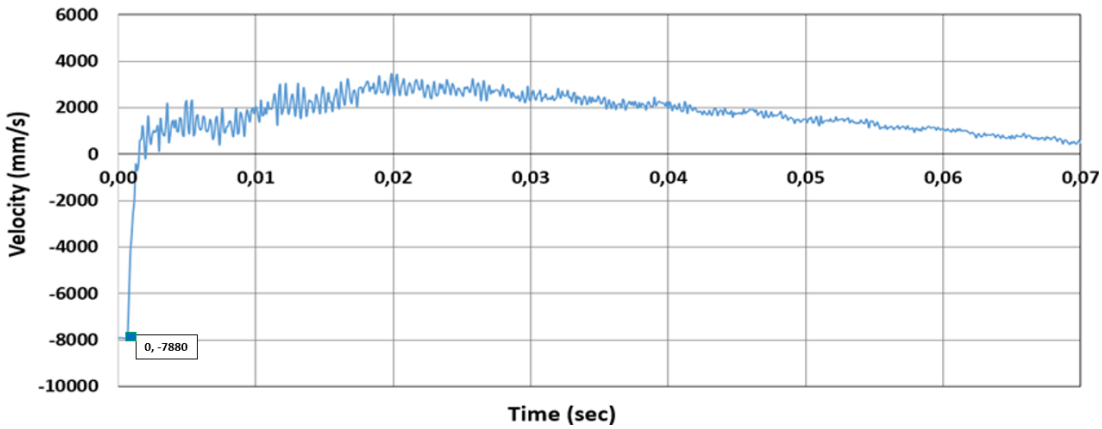

Figure 54: Velocity time history of the seat model-2

As seen in Figure 53 and Figure 54, velocity behaviors of two seat models are very alike but the seat model-2 starts to tend to zero in a higher time interval. This difference is mainly because that the seat weights are different and the seat model-1 does not have a damping system, while the seat model-2 has a damping mechanism. Due to the weight difference and the damping mechanism causes heavy seat, the seat model-2, slows down in a longer time interval compared to the seat model-1.

Figure 55, gives the unfiltered spatial acceleration time history for the seat model-1.

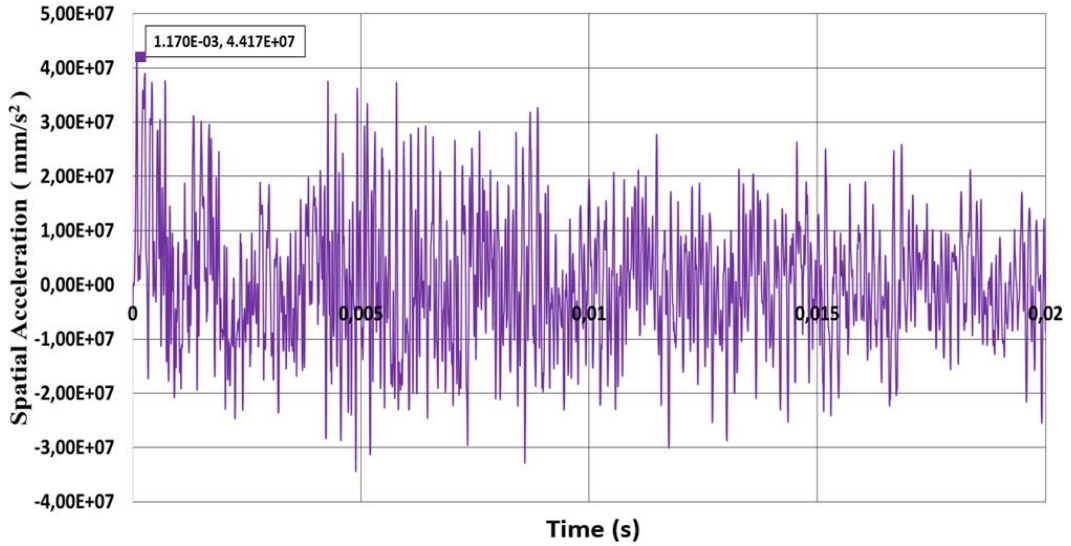

Figure 55: Unfiltered spatial acceleration time history of the seat model-1

The data presented in Figure 55 is filtered with CFC 60 to clean the phase shifts and noisy data. The filtered spatial acceleration versus time plot for the seat model-1 is presented in Figure 56 below.

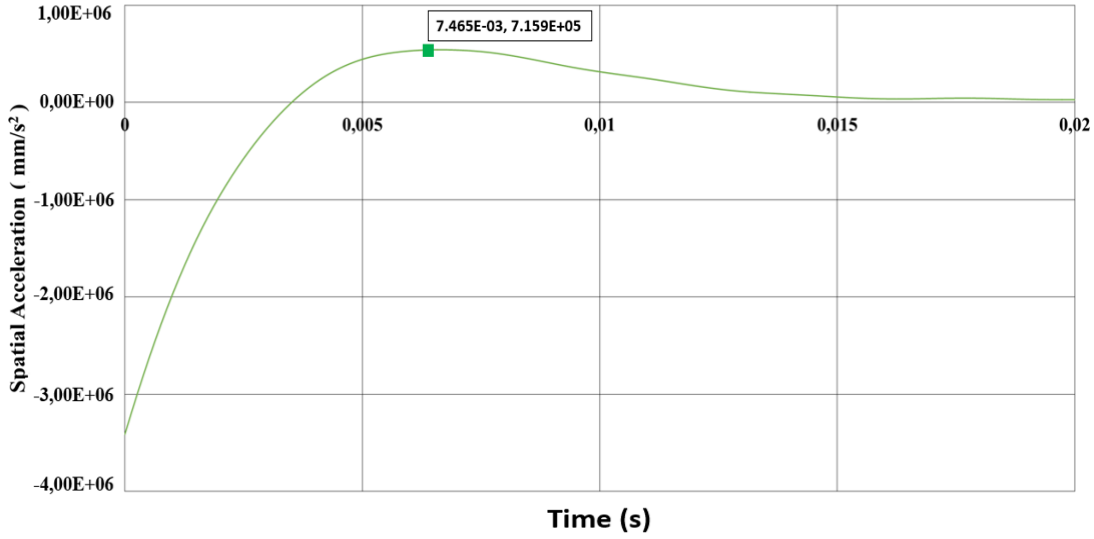

Figure 56: Filtered spatial acceleration time history of the seat model-1

Similarly, Figure 57 and Figure 58 give the unfiltered and filtered spatial acceleration versus time plots for the seat model-2 which includes an energy absorption mechanism based on plastic deformation of the aluminum legs of the seat.

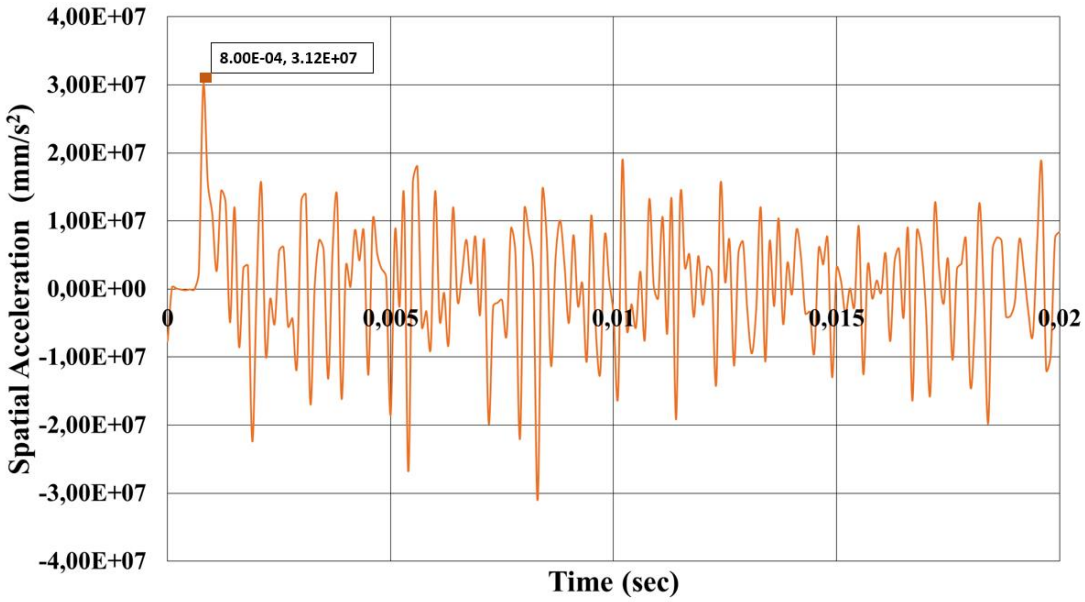

Figure 57: Unfiltered spatial acceleration time history of the seat model-2

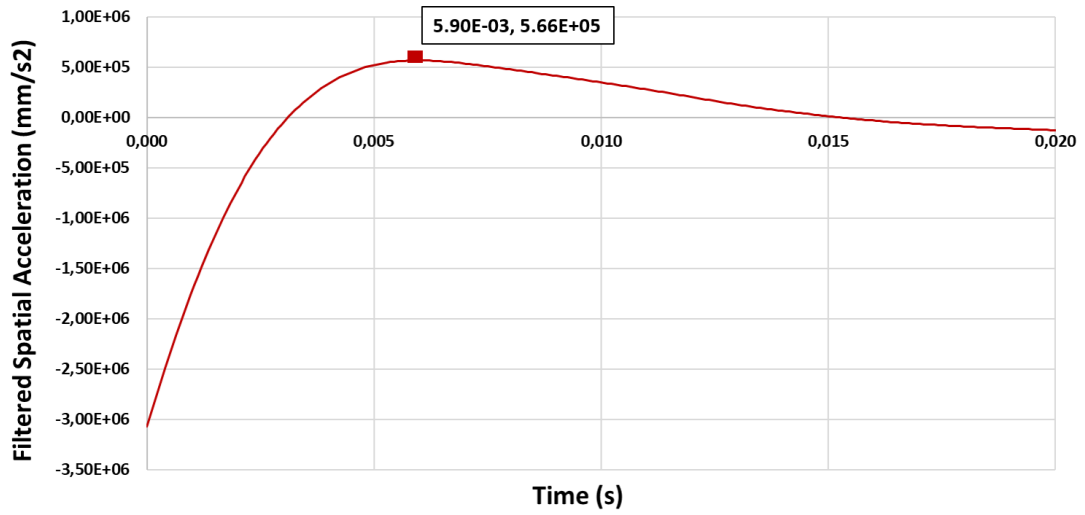

Figure 58: Filtered spatial acceleration time history of the seat model-2

It should be also noted that in order to compare accelerations in terms of g, the acceleration results given in the ordinates of Figure 55, Figure 56, Figure 57, Figure 58 and

Figure 59 should be divided by 9810 mm/s^2.

Figure 55 shows that the peak spatial acceleration of the seat model 1 is around $4.417x10^7$ mm/s^2 which is approximately 4502 g. For the seat model 2, on the other hand, peak spatial acceleration value is seen on Figure 57 as around $3.120x10^7$ mm/s^2 which is approximately 3180 g, which means an approximately 29% g reduction occurs with the damping mechanism.

In the same logic, comparison of model 1 and model 2 results can be done on the data gathered with CFC filter by looking at Figure 56 and Figure 58. Figure 56 shows that the peak filtered spatial acceleration of the seat model 1 is around $7.159x10^5$ mm/s^2 which is approximately 73 g. For the seat model 2, on the other hand, the peak filtered spatial acceleration value is seen on Figure 58 as around $5.66x10^5$ mm/s^2 which is approximately 60 g. It is seen that there is nearly %20 decrease in the peak g levels with only plastic deformation mechanism employed in the damping system of the helicopter seat.

In order to deeply understand the effect of energy absorber system, the same type acceleration comparison can be done by looking directly to
Figure 59 which shows the spatial accelerations of seat model 1 and model 2. Figure shows that that the seat model-2 design, the one which has a damping system, has lower peak acceleration compared to the seat model-1 design. By the virtue of the plastic deformation of the aluminum legs, it has been possible to absorb some portion of the crash energy in the seat model-2.

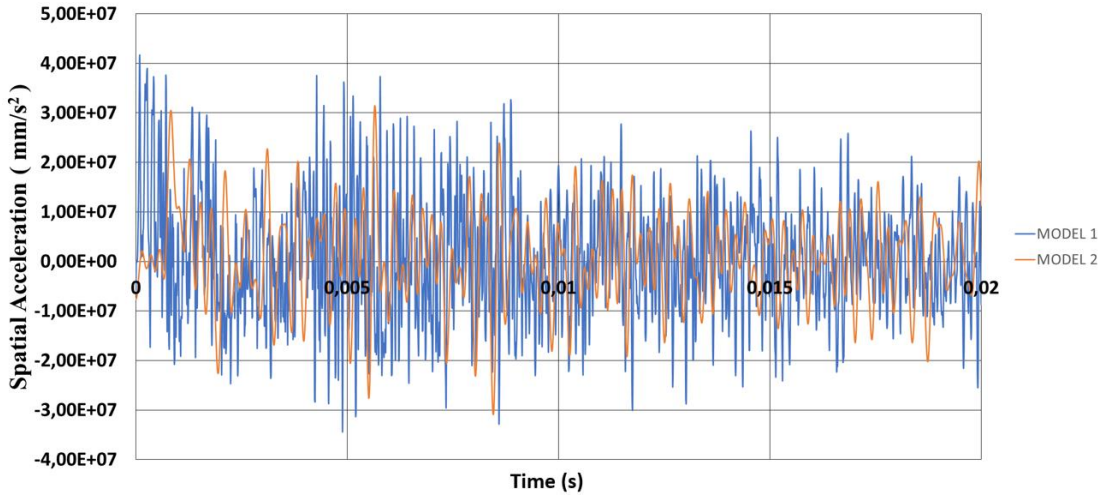

Figure 59: Comparison of the spatial acceleration time histories of the seat model-1 and the seat model-2

It should be noted that in the present analysis the floor where the seat is connected is modeled as rigid wall whereas in real case, helicopter floor is elastic and hence deformable.

As seen on the above graphs, acceleration time histories of the crash simulation have a parallel trend line. Furthermore, the both acceleration data of seat model 2, having load limiter, is similar with the actual test results given in Figure 50 and Figure 51, which makes the simulation results more reliable.

For the survivability of the occupants inside a helicopter at the instant of crash, the g levels and its duration are important. For the seat model-1, the one without the damping system, finite element analysis gives a result around of 73 g spatial acceleration in 0.007456 seconds. On the other hand, for the seat model-2, finite element analysis gives a result around of 60 g spatial acceleration in 0.0059 seconds.

CS 29 requirements [7] state that peak floor deceleration must occur in not more than 0.031 seconds after the impact and must reach a minimum of 30 g. For both seat models, higher g levels are reached in less time according to the CS 29 requirements. However, when two seat model results are compared given in Figure 56 and Figure 58, it is seen that there is nearly %20 decrease in the peak g levels with only plastic deformation mechanism employed in the damping system of the helicopter seat.

To make a comparison between a seat regulation requirements and seat analysis results, Figure 60, given below, taken from MIL-S-85510 can be used which gives the maximum acceptable duration-magnitude of uniform acceleration curve. In Figure 60 for the 42.5 g level acceptable duration of uniform acceleration is nearly 0.0043 seconds. Which means, according to military seat regulation requirement, if 42.5 g acceleration level is reached less than 0.0043 seconds, seat satisfies the area of injury criteria.

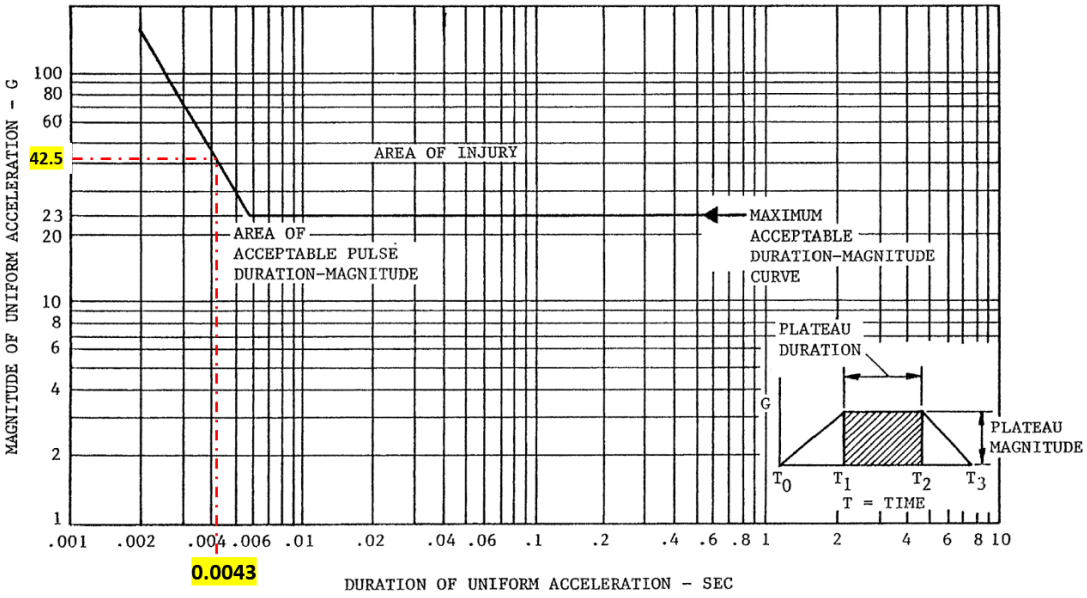

Figure 60: Maximum acceptable vertical pulse acceleration and duration values [17]

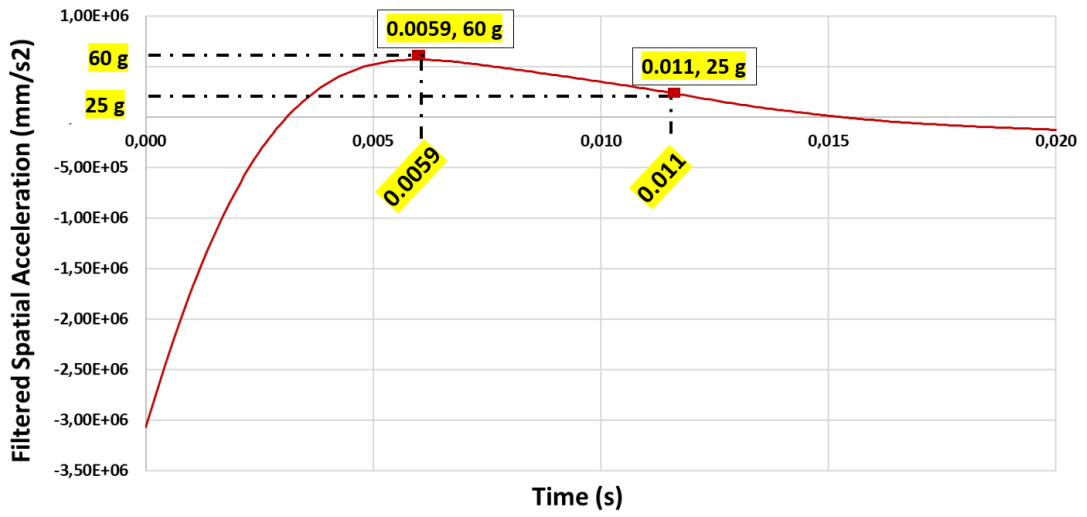

Figure 61: Duration of filtered spatial acceleration exposure of the seat model-2

Figure 61 given above, on the other hand, shows that for the seat model-2, the one with the damping mechanism, 60 g level is reached in 0.0059 seconds and 25 g level is reached in 0.011 seconds from the start of the impact event. Since the acceleration versus time curve is nearly linear beyond the peak acceleration level, one can assume that the sustained acceleration level is almost the average of 60 g and 25 g which is nearly equal to 42.5 g. As can be seen in Figure 61, according to the finite element

analysis results, the duration between 60 g and 25 g is approximately 0.0051 seconds. This result shows that the sustained acceleration duration at 42.5 g is in the area of injury and the seat model-2 does not satisfy the area of injury criteria. Because according to Figure 60, for the 42.5 g level acceptable duration of uniform acceleration is 0.0043 seconds.

However, if the sustained acceleration level is again taken as the average of 60 g and 0 g, as the same method used above, then one can see from Figure 60 that the acceptable duration for 30 g is 0.005 seconds. If one looks at the start of the impact event 60 g level from 0 g level is reached in 0.0029 seconds, and this result shows that the seat is not in the area of injury. Considering all these, it can be concluded that the present seat design with the damping mechanism needs to be improved to keep the sustained acceleration durations in the acceptable range based on the data provided in MIL-S-85510.

It should be noted that this study, it is intended to check the effectiveness of the damping mechanism based on the plastic deformation of the aluminum legs of the seat in the event of a crash. By using more than one damping mechanism both in the floor and the landing gear, g levels and sustained durations can be reduced even further to comply with MIL-S-85510.

It should also be noted that the acceleration graph result of the crash test given in Figure 50 and Figure 51 is alike with the acceleration time history graphs obtained as a result of finite element analysis performed in this study. It is thus shown that the finite element analysis is a reliable method to verify the capability of the energy absorbing system. Analysis of complex systems by numerical simulations is more efficient than the actual full-scale testing. Since the repetition of test is inevitable in case of failure, actual tests cause time and money loss during the certification. Finite element analysis, on the other hand, gives the chance of repetition by changing parameters in order to see the effect of any parameter individually without cost and time loss.

4.2.2 Energy Results

In order to see how the energy changes during the crash simulation, different energy types are taken as the analysis outcome. In addition, to make a comparison between the seat model-1 and the seat model-2, energy behavior curves are shown in the same graph.

Firstly, kinetic energy curves are drawn to see how it changes with time. Figure 62 shows the kinetic energy time histories of the seat model-1 and the seat model-2 together. It is expected from the seat models that, until the crash moment, velocity increases under the action of the gravitational and occupant weight loads. Then, after the impact, velocity has to decrease and then oscillate until the seat stops. This kind of behavior of velocity is seen on kinetic energy time history graphs of the seat model-1 and the seat model-2. When Figure 62 investigated, it is seen that the kinetic energy behavior of both seat models is very similar. While kinetic energy is increases at the beginning, after the crash, it starts to decrease and oscillate, which is an expected behavior. It can be seen also from the Figure 62 that the seat model-2 has a higher kinetic energy than the seat model-1, since it is heavier with steel damping mechanism installed on it. This weight difference between the seat model-1 and seat model-2 is also the reason of the difference between the beginning values of the kinetic energies seen on Figure 62.

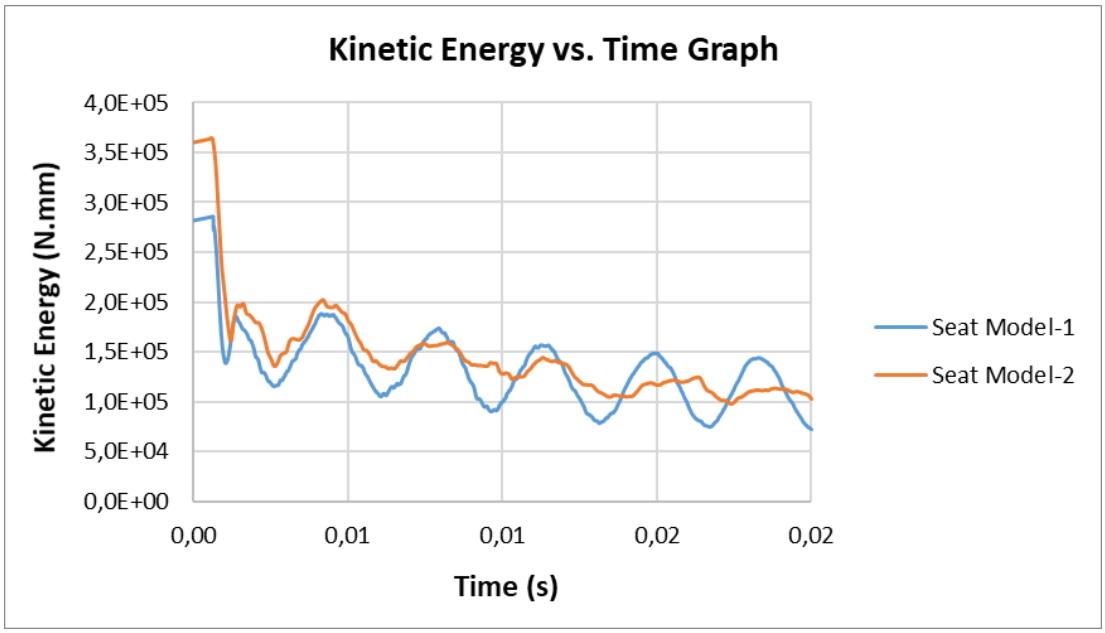

Figure 62: Kinetic energy time histories of the seat model-1 the seat model-2

The internal energy of a system is the energy contained within the system, excluding the kinetic energy of the system and the potential energy of the system. It keeps account of the gains and losses of energy of the system that are due to the changes in its internal state. Figure 63 shows the internal energy behavior of the seat model-1 and the seat model-2. Since the seat model-2 has a damping mechanism which is installed with the aim of energy absorption, it is expected to have a higher internal energy compared to the seat model-1. Figure 63 shows that this expectation is true and the seat model-2 has a higher internal energy than the seat model-1.

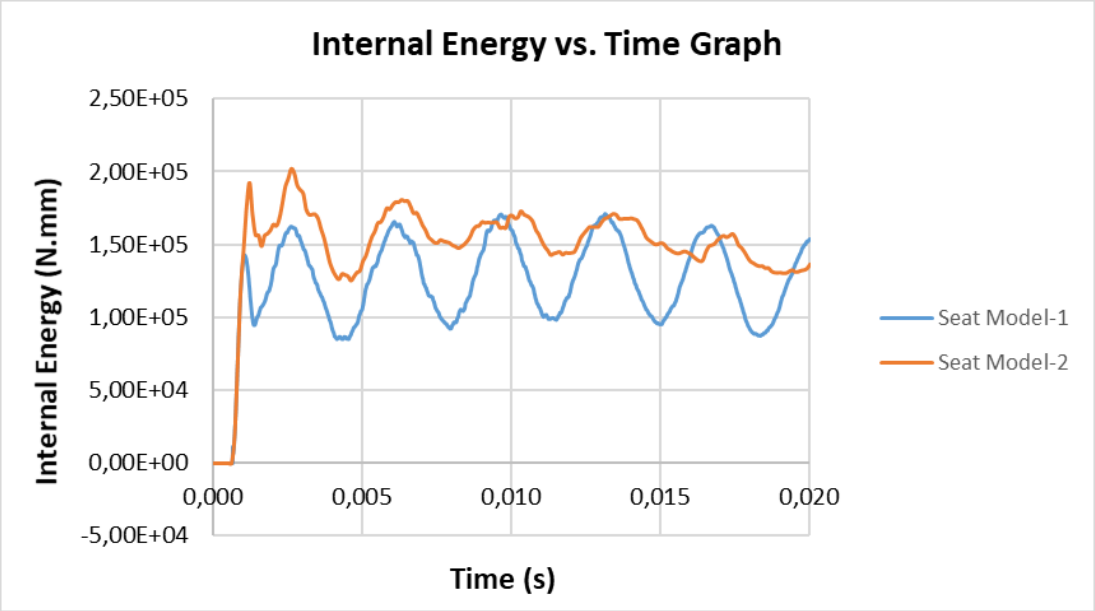

Figure 63: Internal energy time histories of the seat model-1 and the seat model-2

In the homogenized finite element procedure, plastic dissipation in the interfaces between the adjoining elements can occur as a combination of in-plane actions, bending moment, torsion and out-of-plane shear. In this thesis study, plastic dissipation is allowed only at the interfaces of the aluminum leg structure. The aim was to deform the aluminum leg plastically to decrease crash load.

Seat model-2 is designed with a steel damping mechanism, which accelerates and crushes the aluminum leg during the impact. For this reason, it is expected to see higher values in the plastic dissipation time history curve of the seat model-2

compared to the plastic dissipation time history curve of the seat model-1. This comparison is shown in Figure 64 which shows that the plastic dissipation energy of the seat model-2 is higher than the plastic dissipation energy of the seat model-2.

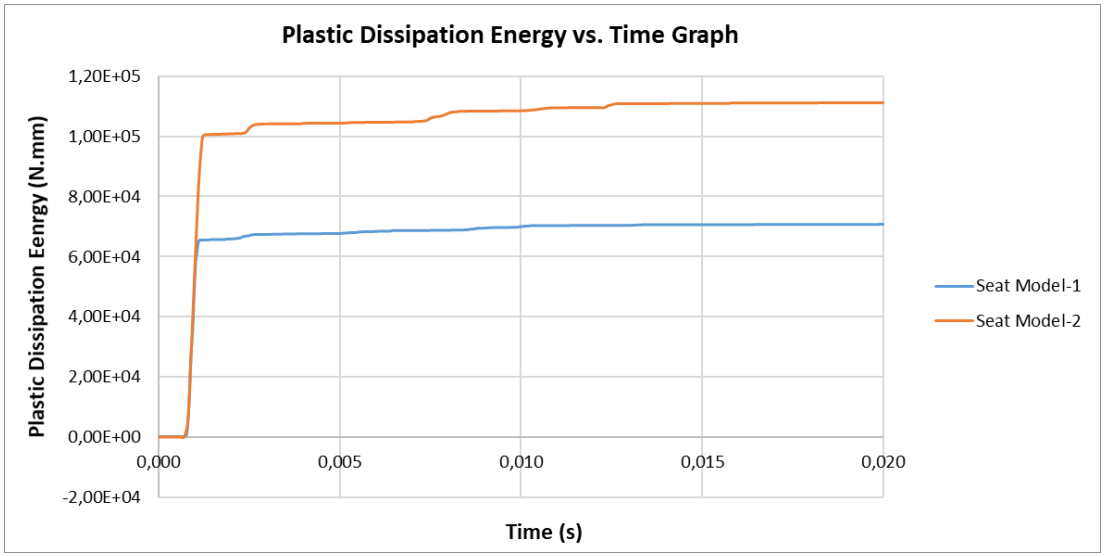

Figure 64: Plastic dissipation time histories of the seat model-1 and the seat model-2

4.2.3 Stress Results

In this section, Von Mises stress results are given by the captures of specific step time moments. Figure 65 shows the initial state of the seat model-2 where the simulation has not started yet and stress values are zero as seen on the color bar placed on upper left corner of the figure.

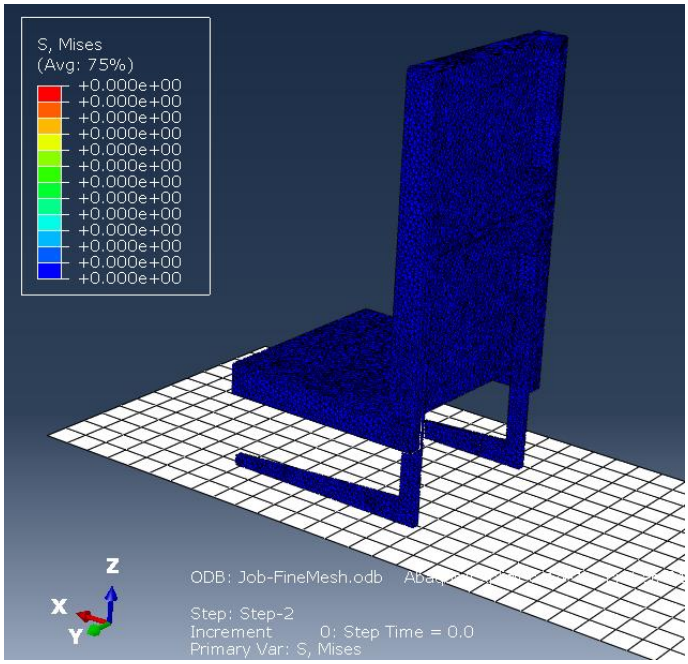

Figure 65: Initial state of the seat model-2 at time=0.00 sec, Unit: MPa

Figure 66 and Figure 67 show the stress state of the seat model-2 at 0.0007 and 0.0008 seconds of the analysis respectively. As it can be seen on the figures, when the seat gets in contact with the rigid wall, the stress on the legs increases as expected.

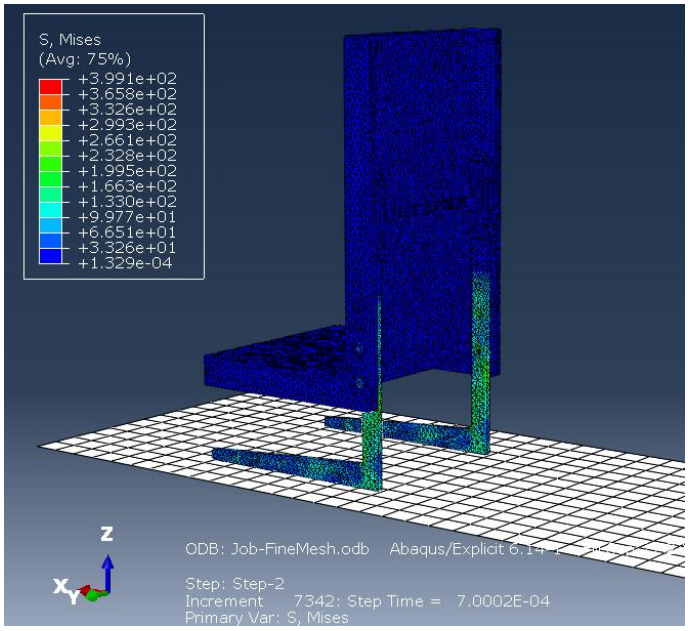

Figure 66: State of the seat model-2 at time=0.0007 sec, Unit: MPa

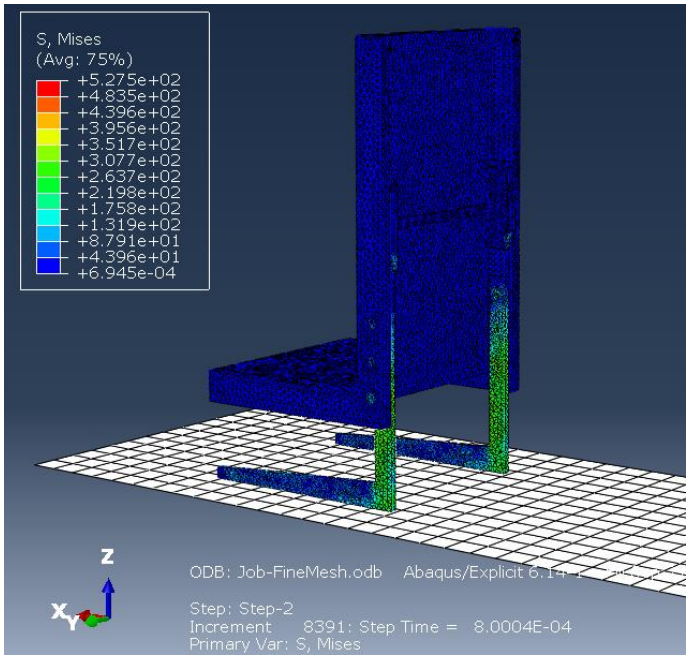

Figure 67: State of the seat model-2 at time=0.0008 sec, Unit: MPa

Figure 68, shows the stress state of the seat model-2 at 0.0009 seconds of the simulation. At this state, stress level on the legs decreased since the initial crash moment passed and stress spread. At this moment of the simulation the seat bucket and the seat damping parts are moving down.

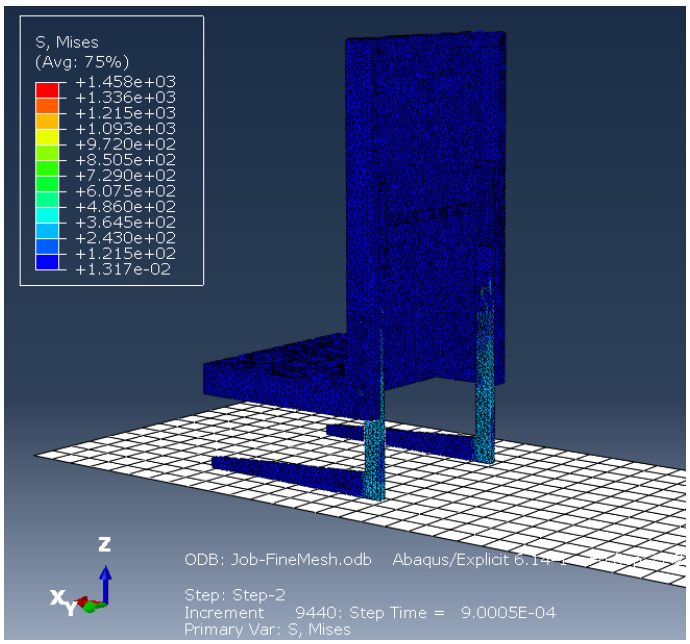

Figure 68: State of the seat model-2 at time=0.0009 sec, Unit: MPa

Figure 69 shows the stress state of the seat model-2 at 0.0012 seconds of the simulation, when the protrusion on the upper steel damping part gets in contact with the lower aluminum leg part of the seat model-2.

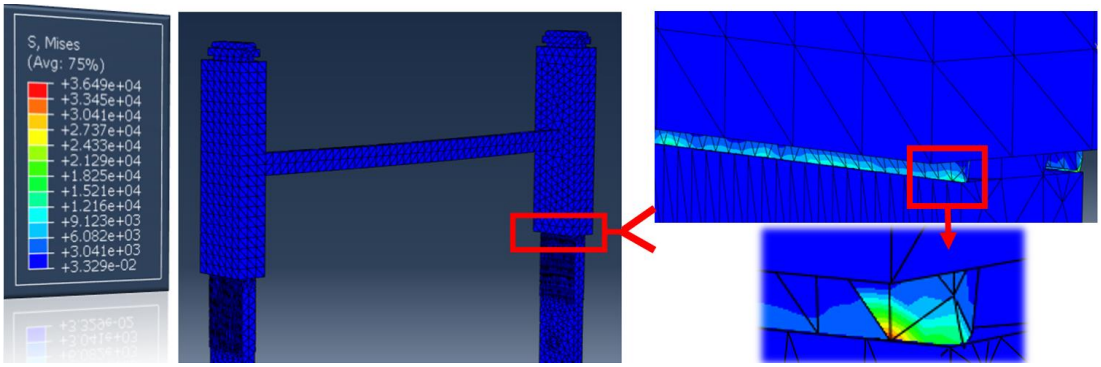

Figure 69: State of the seat model-2 at time=0.0012 sec, Unit: MPa

Since there is a hard contact between the upper steel damping part and the leg, it is expected to have a higher stress level at the contact region.

After the hard contact of the upper steel damping part and the leg, stress is distributed to the H-shaped damping mechanism connection part as seen in Figure 70, and this connection part goes under deformation. In addition, Figure 70 also demonstrates that after the contact of the protrusion and the lower leg part, stress level on the lower aluminum leg part is increased by the effect of crash load.

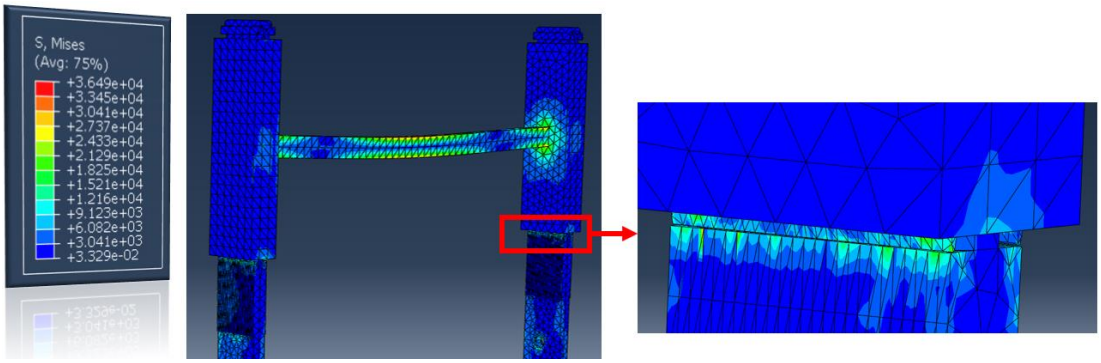

Figure 70: State of the seat model-2 at time=0.0015 sec, Unit: MPa

Finally, Figure 71 shows the ending of the finite element analysis at time 0.002 seconds at which the legs separated from the rigid wall and the seat bounces with the effect of crash.

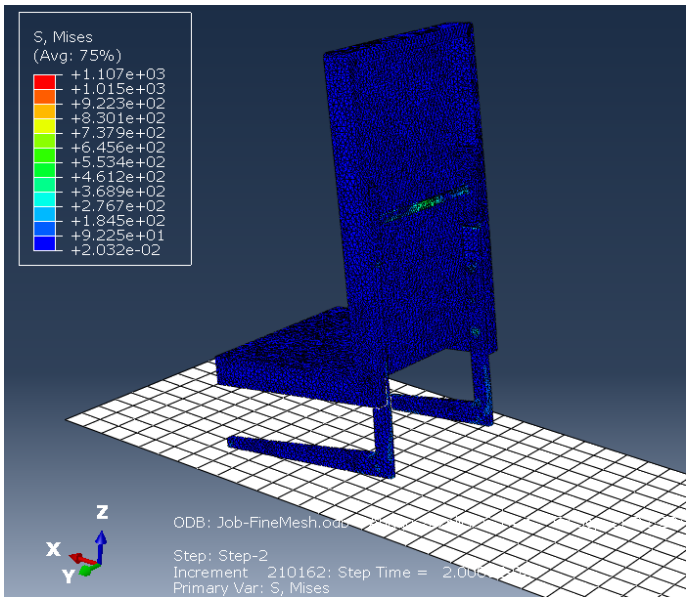

Figure 71: Final state of the seat model-at time=0.02 sec, Unit: MPa

4.2.4 Effect of Occupant Weight on the Acceleration Results

77 kg occupant weight was chosen first in the analyses to represent an occupant as described in the civil certification requirement. In order to see the occupant weight effect on the acceleration and energy behaviors, besides the 77 kg occupant weight defined in civil regulations, a higher weight is also used in the crash analysis and results are compared.

As a higher weight, 107 kg is chosen since it represents a heavy male occupant as seen in Table 5, which is given in Appendix-B of MIL-STD-1472, a human engineering standard [25]. MIL-STD-1472 standard is widely used in helicopter design stages by engineers when designing the cockpit and cabin environments to see, for example, if the pilots can reach the controls or to see whether the passenger knee distances are appropriate or not.

Table 5: Standing body dimensions of Air Force Pilots [25]

	Percentile values in cm (in)			
	5th percentile		95th percentile	
	Male	Female	Male	Female
Weight, kg (lbs)	64.89 (143.3)	52.83 (116.5)	107.12 (23.2)	81.21 (179.1)
1. Stature	168.1 (66.1)	160.1 (62.9)	190.1 (74.7)	174.4 (68.5)
2. Eye height (standing)	N/A	N/A	N/A	N/A
3. Shoulder (acromiale) height	135.7 (53.4)	131.6 (51.8)	154.8 (60.9)	143.9 (56.7)
4. Chest (nipple) height 1/	120.8 (47.6)	117.5 (46.3)	138.1 (54.4)	130.4 (51.3)
5. Elbow (radiale) height	104.8 (41.3)	N/A	120 (47.2)	N/A
6. Fingertip (dactylion) height	61.5 (24.2)	N/A	73.2 (28.8)	N/A
7a. Waist (iliocristale) height	101.3 (39.9)	N/A	117.2 (46.1)	N/A
7b. Waist (omphalion) height	99.9 (39.3)	95.7 (37.6)	116.1 (45.6)	107.2 (42.1)
7c. Waist (natural indentation) height	106 (41.7)	102.4 (40.2)	121.9 (47.9)	113 (44.4)
8. Crotch height	71.5 (28.1)	71.7 (28.2)	87.3 (34.3)	80.8 (31.8)
9. Gluteal furrow height	74.6 (29.4)	70.4 (27.7)	87.9 (34.6)	81.5 (32.1)
10. Knee (mid-patella) height	45.7 (18)	N/A	53.9 (21.2)	N/A
11. Calf height	32 (12.6)	N/A	39.3 (15.5)	N/A
12. Functional (thumbtip) reach	74.83 (29.4)	69.9 (27.5)	87.3 (34.3)	80.3 (31.6)
13. Functional reach, extended	82.3 (32.4)	79.8 (31.4)	97.3 (38.3)	94 (37.0)

FOOTNOTE:

1/ Bustpoint height for women.

NOTE:

1. N/A = Not available.

The finite element seat crash analysis is done with two different occupant weights as explained above to see the occupant weight effect on the peak acceleration values and on the crash load reduction. This parameter study is done with seat model-2, which has the energy absorber mechanism.

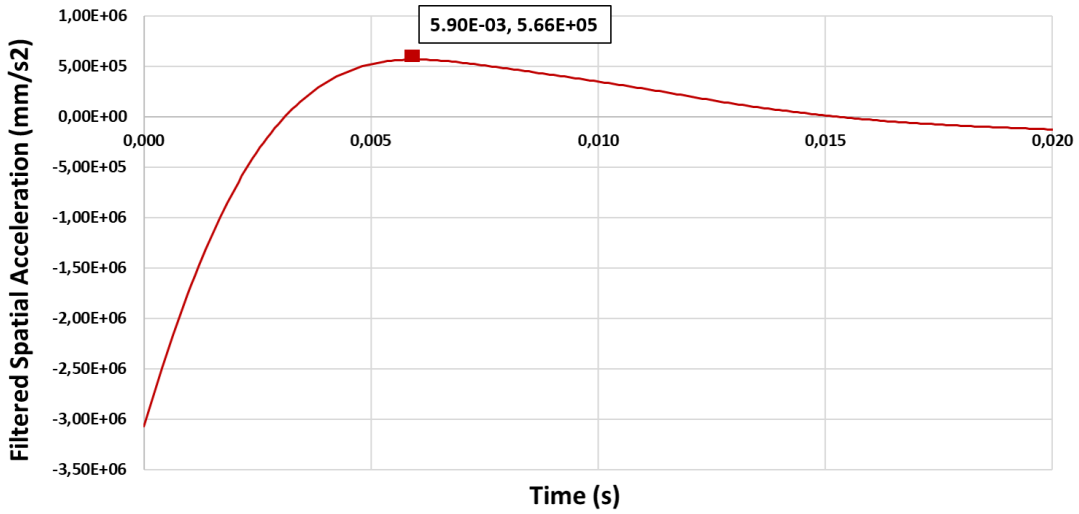

Figure 72: Filtered spatial acceleration time history of the seat model-2 simulated with 77 kg occupant weight

Figure 72 demonstrates the filtered spatial acceleration time history of the seat model-2 simulated with 77 kg occupant weight. As stated and deeply investigated in Section 4.2.1 Acceleration Results, the peak acceleration outcome of this analysis is around 50 g. The seat crash analysis performed with a 107 kg occupant weight, on the other hand, gives 76 g peak acceleration value as shown in Figure 73.

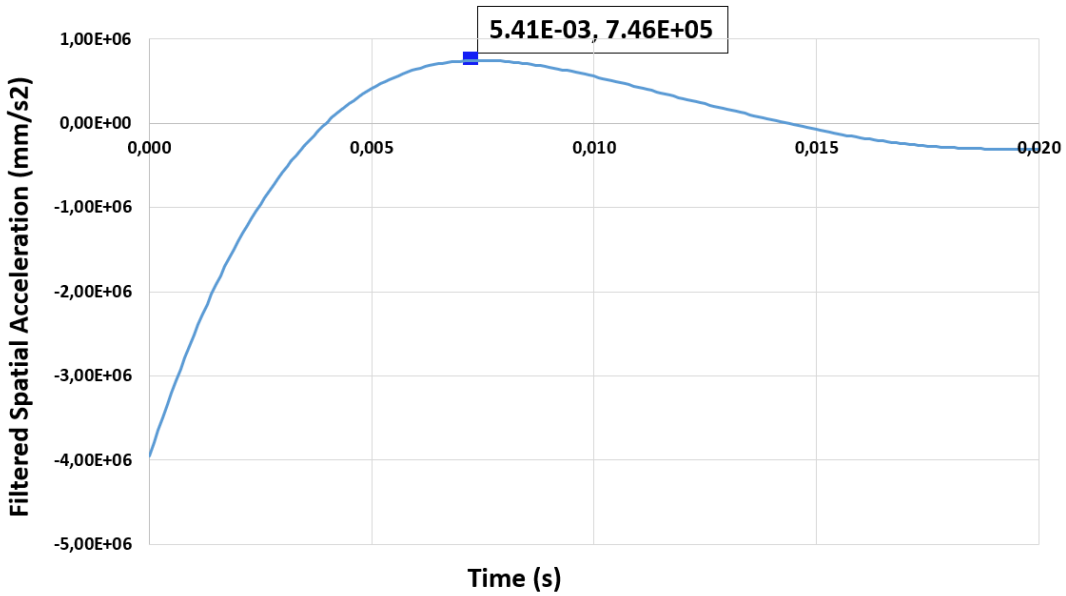

Figure 73: Filtered spatial acceleration time history of the seat model-2 simulated with 107 kg occupant weight

A conclusion may be drawn by examining Figure 72 and Figure 73, which are the figures showing the filtered spatial acceleration time history of the seat model-2

simulated with 77 kg and 107 kg occupant weight respectively. As demonstrated in these figures, the heavier occupant experiences higher g levels. This is mainly because, increasing weight ends with increasing crash loads and crash energy. However, it should be stated that, with a more effective damping mechanism, heavy occupant may be used as an advantage in the plastic deformation.

A more efficient damping mechanism can be designed to minimize the occupant weight effect because different types of human bodies are using the rotorcrafts and they all should be protected from a crash event.

4.2.5 Effect of Material on Acceleration Results

In this thesis study, the material of the upper damping part, as shown in Figure 74, is used for another parameter study.

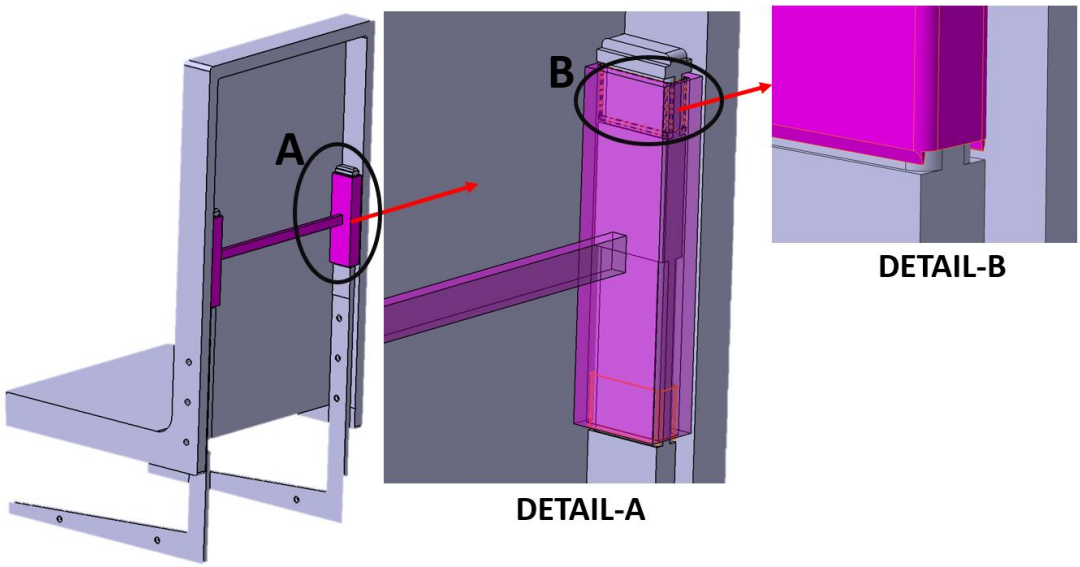

Figure 74: Upper damping part of the seat model-2

Figure 75 and Figure 76 show the peak acceleration values of the seat model-2 having steel and aluminum damping parts, respectively.

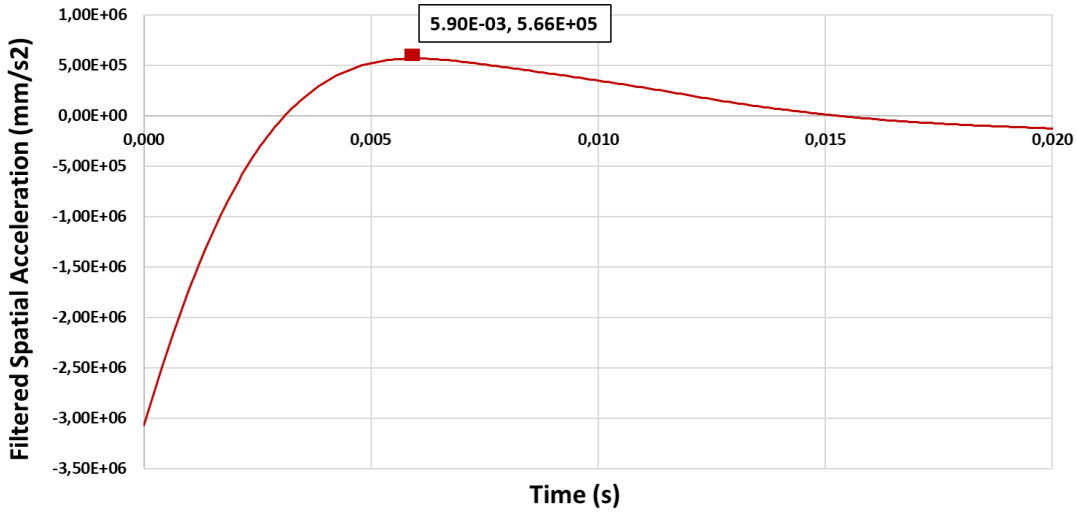

Figure 75: Filtered spatial acceleration time history of the seat model-2 simulated with steel upper damping part

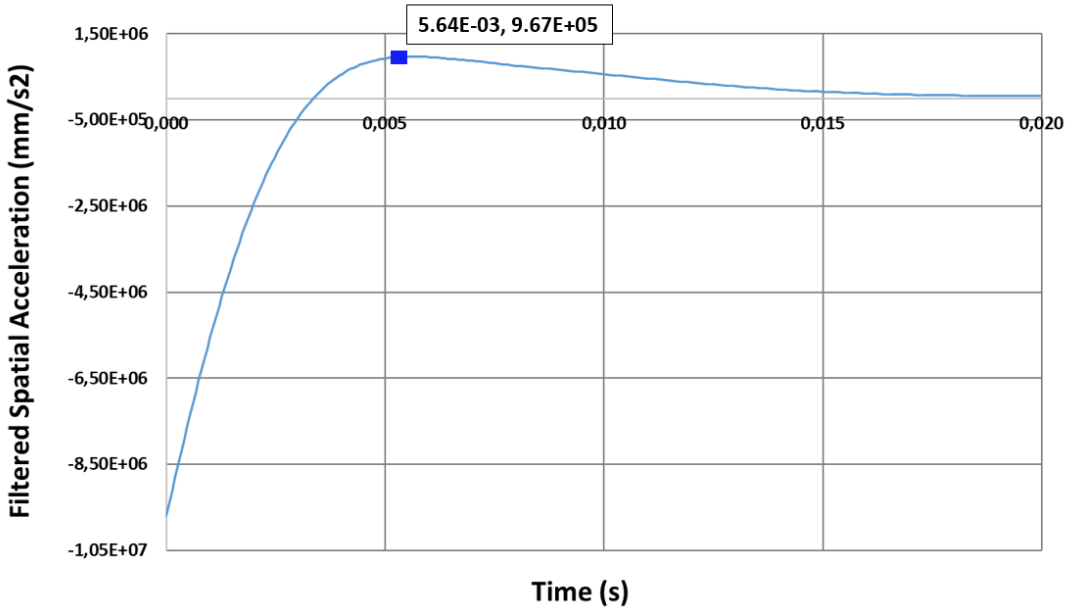

Figure 76: Filtered spatial acceleration time history of the seat model-2 simulated with aluminum upper damping part

The acceleration behavior of the seat model-2 crash simulation performed with different damping mechanism material is shown in Figure 75 and Figure 76. By looking at these two figures, it is concluded that the material has an important effect on peak acceleration values. While the steel damping part reaches a 60 g peak acceleration in 0,0059 seconds, the aluminum damping part reaches approximately

97 g peak acceleration in 0,00564 seconds. These results are expected because the steel damping mechanism is heavier than the aluminum part and accelerates quickly which means an increase in plastic deformation.

CHAPTER 5

CONCLUSION

5.1 General Conclusions

If a seat is to be installed on an aircraft platform, it should be certified with the regulation that is applicable for that specific aircraft platform. These regulations include dynamic requirements written to ensure the occupant safety in case of a crash. Dynamic requirements define the maximum crash load, in terms of g levels, and its time interval, which should be satisfied by the seat mechanism used for absorbing the crash energy. If the seat satisfies these test conditions, it is called as "Crashworthy Seat". Crashworthy seat design mainly depends on verification of the energy absorption system, which absorbs the crash energy to reduce the load on passenger's pelvis, head, neck and lumbar, which are the critical locations in the human body for the survival.

In this study, by the dynamic explicit analysis, the performance of the energy absorption mechanism of a helicopter seat was analyzed by examining the loads on the seat that the occupant receives.

A seat model is designed such that seat structure includes a seat bucket, two seat legs and an energy absorber mechanism. The energy absorbing mechanism works on the principle of plastic deformation of the aluminum legs of the seat. There is a protrusion on the upper damping part of the seat leg. In the crash moment, upper damping part accelerates and with its velocity, lower damping part is deformed and crushed. By this way, the crash pulses are reduced. The plastic deformation is the most important mechanism for the success of the absorbing system of the seat model such that it has to be effective in the load reduction that the occupant receives.

In order to investigate the effectiveness of the energy absorption mechanism, two separate seats, one which includes the damping system and the one without the damping system are exposed to the same crash condition. Results of the explicit finite element analysis show that the damping mechanism, which is based on the plastic deformation of the aluminum legs of the seat structure, absorbs some of the crash energy and decrease the load that the occupant receives.

Seat models that will be analyzed, are created in CATIA software and then, in step format, it is transferred to the ABAQUS analysis program, in which crash simulation analysis will be performed. ABAQUS is a general-purpose finite element program capable of simulating complex problems. The code's origins lie in highly nonlinear, transient dynamic finite element analysis using explicit time integration. This is why ABAQUS program is chosen for crash analysis.

The finite element modeling procedure starts with the cleaning up the geometry and prepare it for meshing. Cleaning the geometry means that the complex geometries and sharp edges are removed from the model in order to simplify the finite element model and to reduce the analysis time. Other important parameter of the reducing the analysis time is the finding the optimum mesh element size. In this aspect, mesh refinement is done and the optimum element size is determined, which is 7 mm in this study.

Furthermore, mass scaling is used to speed up the analysis time. Mass scaling is commonly used method for computational efficiency in dynamic analyses. Explicit dynamic models contain a few very small elements that force the explicit analysis to use a small time increment to integrate the entire model, including these small elements, in time. The size of the critical time-step, stable time increment, increases without affecting the dynamic response by scaling the masses of these controlling elements. For this crash simulation, the optimum stable time step is taken as 10^{-7} seconds. If this criterion is not satisfied, model automatically scales the system in order to have a stable time period of minimum 10^{-7} seconds.

While preparing the simulation model, for the crash analysis, materials and their characteristics should be defined as analysis parameters. These parameters include

stress-strain relation, density, elastic modulus, Poisson's ratio and the frictional coefficient. Elastic modulus and Poisson's ratio define the elastic properties of the material. Stress-strain numbers, on the other hand, define the plastic properties of the material.

The materials used in the analysis are aluminum, steel and aluminum is for the seat leg structure and steel is used for the damping mechanism in order to plastically deform the aluminum legs. For the seat bucket, on the other hand, a user defined material is defined with the same elastic behavior as aluminum but with different density.

Following the material definition, boundary conditions are defined for the finite element analysis model. To simulate the crash event, 2D discrete rigid planar shell geometry is used to represent the rigid wall. The boundary condition is used to define the fixed non-deformable rigid wall. While modeling the wall, a single reference point (RP) is created at the corner of the surface in order to define the rigid wall boundary condition. As an initial condition definition of the crash simulation, an initial forward velocity of 4550 mm/s and downward velocity of -7880 mm/s is defined as stated in CS29.562. Furthermore, the passenger mass is assigned to a single RP as a concentrated mass of 77 kg, and this RP is also coupled to the seat surface where the passenger sits. The force given to the RP is 755.37 N (0.077ton x 9810mm/s^2) in the -Z direction. With those definitions, crash analysis is performed for both seat model 1 and seat model 2.

In order to evaluate the crash simulation and make a comparison between the aviation seat regulation requirements and the analysis results, acceleration and velocity output is taken in vertical z-direction.

Results of the explicit finite element analysis show that the damping mechanism, which is based on the plastic deformation of the aluminum legs of the seat structure, absorbs some of the crash energy and decrease the load that the occupant receives. It is shown that with only plastic deformation, damping system decreases approximately 20 % of the peak g level that the seat transmits to the occupant.

As it is shown in Figure 58, the seat model 2 damping mechanism reaches 60 g level in 0.0059 seconds and 25 g level in 0.011 seconds from the start of the impact event. The average of 60 g and 25 g which is nearly equal to 42.5 g and the duration between 60 g and 25 g is approximately 0.0051 seconds. In Figure 17, the figure that gives the maximum acceptable acceleration and duration values, for the 42.5 g level acceptable duration of uniform acceleration is 0.0043 seconds, which means that according to the finite element analysis results, by the sustained acceleration duration at 42.5 g, the seat model-2 does not satisfy the area of injury criteria of MIL-S-85510 military standard. However, if the sustained acceleration level is again taken as the average of 60 g and 0 g, as the same method used above, then one can see from Figure 60 that the acceptable duration for 30 g is 0.005 seconds. If one looks at the start of the impact event 60 g level from 0 g level is reached in 0.0029 seconds, and this result shows that the seat model-2 is not in the area of injury. Considering all these, it can be concluded that the present seat design with the damping mechanism needs to be improved to keep the sustained acceleration durations in the acceptable range based on the data provided in MIL-S-85510.

Besides making a comparison between analysis and the seat regulations, parameter studies are also carried out in this thesis study. Two different analysis are studied with changing parameters of occupant weight and damping mechanism material in order to see how these parameters affects the peak acceleration value.

Following statements are concluded at the end of the parameter study;

- As the occupant weight increase, the crash load is also increase.
- The energy absorber design used in this thesis study, highly depends on the upper damping part behavior since the basic principle is based on this behavior by the means of plastic deformation. Because of this dependency, material of this damping part highly affects the crash load.

It is further concluded that the present seat design with the damping mechanism needs to be improved also to keep the sustained acceleration durations in the acceptable range based on the data provided in CS-29 civil standard. It should be noted in this study it is intended to check the effectiveness of the damping

mechanism based on the plastic deformation of the aluminum legs of the seat in the event of a crash. By using more than one damping mechanism, g levels can be reduced even further. Generally, in helicopter structures crash energy is taken by the landing gear, fuselage and the seat before the occupant is affected from the crash event. In this study it has been shown that the energy absorption mechanism in the seat solely reduces the peak acceleration by %20. It has been also observed that the sustained durations of accelerations slightly overpass the limits given by MIL-S-85510. However, in a more realistic application, considering that the landing gear and the fuselage structure will absorb significant portions of impact energy, it is deemed that the energy absorbing mechanism which works on the principle of plastic deformation of the aluminum legs of the seat is sufficient for the purpose.

5.2 Recommendations for Future Works

The following studies are suggested as the future work that can be conducted as future work.

- A test can be done to see the correlation between the actual test results and the simulation results.
- Simulations can be done with including pitch and roll effects on the seat legs as described in the civil regulation.
- Simulations can be performed with new materials to see the material effect on crash dynamics.

REFERENCES

1. Renner, M. (2013) *Global Air Transport Continues to Expand*, Worldwatch Institute (New York: W.W. Norton & Co.), December 2013.
2. LS-DYNA, Livermore Software Technology Corporation (2015), http://www.lstc.com.
3. DYTRAN, MacNeal-Schwendler Corporation (MSC) Software (2013), http://www.mscsoftware.com/.
4. PAMCRASH, ESI Group (1985), https://www.esi-group.com/.
5. ABAQUS, ABAQUS Inc. (1978), https://www.simulia.com.
6. Rapaport M., Forster E., Schoenbeck A., *Spinal Injury Criterion for Military Seats*, Naval Air Warfare Center, Aircraft Division, Patuxent River, MD.
7. European Aviation Safety Agency (2012) *Certification Specifications CS-29: Large Rotorcrafts*, December 2012.
8. Desjardins S. P. (2003), *The Evolution of Energy Absorption Systems For Crashworthy Helicopter Seats*, PRESIDENT SAFE, INC TEMPE, ARIZONA
9. Bhonge, P. (2008) *A Methodology for Aircraft Seat Certification by Dynamic Finite Element Analysis*, Doctoral dissertation, Wichita State University, USA, Dec 2008.
10. Simitcioglu G. & Dogan V. (2013), *Dynamic Finite Element Analysis of an Aircraft Seat*, Ankara International Aerospace Conference, Turkey, September 2013.
11. Dhole N. (2010), *Development and Validation of a Finite Element Model of a Transport Aircraft Seat Under Part 25.562 Dynamic Test Conditions*, Master thesis, Wichita State University, USA, May 2010.
12. Annett, M. S. and Polanco, M., *LS-DYNA Analysis of Full-Scale Helicopter Crash Test*, 11th International LS-DYNA Users Conference - Dearborn, MI, USA - June 6-8, 2010.

13. Peherstorfer B., Bohn B., Garcke J. Iza-Teran R., Paprotny A., Schepsmeier U. and Thole C., *Analysis of Car Crash Simulation Data with Nonlinear Machine Learning Methods*, International Conference on Computational Science- Barcelona, Spain - June 5-7, 2013.
14. Pawlus W., Nielsen J. E., Karimi H. R. and Robbersmyr K. G., *Mathematical Modeling and Analysis of a Vehicle Crash*, 4th European Computing Conference - Bucharest, Romania - April 20-22, 2010.
15. Kim B. S., Park K. and Song Y., *Finite Element Frontal Crash Analysis of Nev Vehicle's Platform with Upper and Sub Frame Body*, 28th International Symposium on Automation and Robotics in Construction – Seoul, Korea, June 29 - July 2, 2011.
16. Engleder A., Markmiller J. & Mueller R., «*The Evolution of Airbus Helicopters Crashworthy Composite Airframes for Transport Helicopters»,* 41st European Rotorcraft Forum 2015
17. MIL-S-85510 Military Specification, *Seats, Helicopter Cabin, Crashworthy, General Specification,* MIL-S-85510, November 1981.
18. Eriksen J. H., Nona R. A., *Helicopter Design Criteria for Crew Crash Protection and Anthropometric Accommodation,* North Atlantic Treaty Organization, STANAG No. 3950.
19. SAE Aerospace (2005), *Performance Standard for Seats in Civil Rotorcraft, Transport Aircraft and General Aviation Aircraft, 2005.*
20. CATIA, Dassault Systems (1981), https://www.3ds.com/products/catia/
21. Fasanella E. L. & Jackson K. E., *Best Practices for Crash Modeling and Simulation,* U.S. Army Research Laboratory Vehicle Technology Directorate Langley Research Center, October 2012, Hampton, Virginia
22. Society of Automotive Engineers, Recommended Practice: Instrumentation for Impact Test – Part 1, Electronic Instrumentation, SAE J211/1, March 1995
23. Johnson, G.R. and Holmquist, T.J., *Test data and computational strength and fracture model constants for 23 materials subjected to large strains, high strain rates, and high temperatures,* LA-11463-MS, Los Alamos National Laboratory, 1989

24. Thomson R. G., Garden H. D., Hayduk R. J., *Survey of NASA Research on Crash Dynamics*, NASA Technical Paper 2298, 1984, Langley Research Center, Hampton, Virginia.
25. MIL-STD-1472G Military Specification, *Human Engineering*, Department of Defense Design Criteria Standard, January 2012.